

AD-777 268

ENERGY SPECTRA FOR FREQUENCY-SHIFT-
KEYED SIGNALS TRANSMITTED BY SYN-
CHRONOUSLY RESONATED, VERY LOW
FREQUENCY ANTENNAS

Tee R. Hadley, III

Air Force Institute of Technology
Wright-Patterson Air Force Base, Ohio

December 1973

DISTRIBUTED BY:

NTIS

National Technical Information Service
U. S. DEPARTMENT OF COMMERCE
5285 Port Royal Road, Springfield Va. 22151

ENERGY SPECTRA FOR FREQUENCY-SHIFT-KEYED
SIGNALS TRANSMITTED BY SYNCHRONOUSLY
RESONATED, VERY LOW FREQUENCY ANTENNAS
THESIS

GE/EL/73A-10

Tee R. Hadley III
Captain USAF

Approved for public release; distribution unlimited.

i

Unclassified

Security Classification

DOCUMENT CONTROL DATA - R & D

(Security Classification of title, body of abstract and index information must be entered when the overall report is classified)

ORIGINATING ACTIVITY (Company, factory)

Air Force Institute of Technology (AFIT-EN)
Wright-Patterson AFB, Ohio 45433

REPORT SECURITY CLASSIFICATION

Unclassified

REPORT GROUP

3. REPORT TITLE

Energy Spectra for Frequency-Shift-Keyed
Signals Transmitted by Synchronously
Resonated, Very Low Frequency Antennas

4. DESCRIPTIVE NOTES (Type of report and inclusive dates)

AFIT Thesis

5. AUTHOR(S) (First name, middle initial, last name)

Tee R. Hadley III
Captain USAF

6. REPORT DATE

December 1973

7a. TOTAL NO. OF PAGES

100

7b. NO. OF REFS

8

8a. CONTRACT OR GRANT NO

b. PROJECT NO

c.

d.

9a. ORIGINATOR'S REPORT NUMBER(S)

GE/EE/73A-10

9b. OTHER REPORT NO(S) (Any other numbers that may be assigned this report)

10. DISTRIBUTION STATEMENT

Approved for public release; distribution unlimited.

11. SUPPLEMENTARY NOTES

Approved for public release; IAW AFR 100-17.

JERRY C. HIX, Captain, USAF
Director of Information

12. SPONSORING MILITARY ACTIVITY

Rome Air Development Center
Communication and Navigation Div.
Griffiss AFB, New York 13441

13. ABSTRACT

Electronic broadbanding is a technique whereby very low frequency (VLF) antennas can be resonated (retuned) synchronously with a frequency shift-keyed (FSK) signal for transmission of binary data at rates well over 1000 baud. The purpose of this thesis is to investigate the transmitted energy density spectrum for an electronically broadbanded VLF antenna system in which a frequency shift can occur only at the instant of an antenna-current zero-crossing with positive slope. A computer solution shows that the transmitted spectrum is approximately equivalent to the spectrum of an ideal, constant amplitude, FSK signal.

A further investigation, again by computer program, shows that if the total frequency shift between the marking and spacing frequencies occurs over a finite period, rather than instantaneously, then the spectrum's sidelobes will be reduced significantly. The spectrum for a 27,000 Hz center-frequency VLF antenna transmitting at 1600 baud by means of electronic broadbanding can be reduced from 3 to 18 dB in the first five sidelobes. No evaluation is made on the detectability of the signal with the non-instantaneous frequency shift. Numerous plots of the computer-generated spectra are included.

Reproduced by
NATIONAL TECHNICAL
INFORMATION SERVICE
U S Department of Commerce
Springfield VA 22151

DD FORM 1473
1 NOV 65

ia

Unclassified

Security Classification

il

ENERGY SPECTRA FOR FREQUENCY-SHIFT-KEYED
SIGNALS TRANSMITTED BY SYNCHRONOUSLY
RESONATED, VERY LOW FREQUENCY ANTENNAS

THESIS

Presented to the Faculty of the School of Engineering
of the Air Force Institute of Technology

Air University

in Partial Fulfillment of the
Requirements for the Degree of
Master of Science

by

Tee R. Hadley III, B.S.E.E.

Captain

USAF

Graduate Electrical Engineering

December 1973

Approved for public release; distribution unlimited.

ic

Preface

For the readers, wherever you are, I appreciate your interest in this paper and I hope that it may be of some benefit to you. In its final form, this thesis is not an exceedingly complex scholastic work, but the path to its solution was frequently obscured. The most pleasing result of this paper is that the conclusions are very useful.

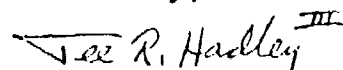
I wish to thank my thesis advisor, Professor Robert Reinman, for his continuous encouragement throughout this effort, and I especially want to express my appreciation to Mr. John Gamble of Rome Air Development Center who took the time to make this thesis topic available to AFIT. In addition, I want to thank Profs. John D'Azzo and Thomas Owen who provided important editing comments.

Most of all, I want to express my gratitude to my wife, Donna, for her understanding and patience in the eighteen months that I have spent in pursuit of a Master's Degree. In addition, when our young daughter Catherine Melissa can read this preface, I want her to know that she made part of each day happier.

As a final acknowledgment, I wish to thank the American taxpayers who financed this thesis. I hope that this work will add strength to their defense.

This thesis is dedicated to my parents, who encourage excellence in all endeavors, and whose lives exemplify enduring perseverance to overcome all adversity.

Sincerely,



Tee R. Hadley III

Contents

	Page
Preface	ii
List of Figures	v
Abstract	vii
I. Introduction	1
II. Background	3
A VLF Antenna Model	4
Energy Relationships for Synchronous Resonance	6
A General Switched-L Circuit for FSK Transmission	11
An Antenna Modulator for Synchronous Resonance	13
Implications	15
III. Current Analysis for Synchronously Resonated Antennas	16
Antenna Transient Analysis	16
Error Fraction Calculations	19
IV. Spectral Analysis for Synchronously Resonated Antennas	22
Examination of the Signal	22
The Stochastic Process	26
Solution Method: A Finite-Time Power Spectrum	28
Relations Between the Circuit Parameters	31
Generation and Compilation of Spectra	32
V. Frequency Modulation for Spectrum Shaping	44
What Type of Modulation?	44
Modification of the Program	46
VI. Comparisons	59
The Single-Step Cases	59
The Multi-Step Cases	60

Contents

	Page
VII. Conclusions and Recommendations	71
Conclusions	71
Single-Step Cases	71
Multi-Step Cases	72
Recommendations	73
Bibliography	75
Appendix A: Computer Programs	76
Appendix B: Ideal Spectra for $M = 1/2$	88
Vica	90

List of Figures

<u>Figure</u>	<u>Page</u>
1 Very-Low-Frequency Antenna Model	4
2 Switched-Reactance Circuits	8
3 Steady-State Current Relations	10
4 Switched-L Synchronous Resonator	12
5 An Inductively-Coupled Synchronous Resonator	13
6 General Error-Fraction Time Relations	20
7 Antenna Current Envelope	24
8 Downshift and Upshift Antenna Current Relations	25
9 Spectra for 125 Baud, $M = 1/2$	35
10 Spectra for 540 Baud, $M = 1/2$	36
11 Spectra for 800 Baud, $M = 1/2$	37
12 Spectra for 1200 Baud, $M = 1/2$	38
13 Spectra for 1600 Baud, $M = 1/2$	39
14 Spectra for 2000 Baud, $M = 1/2$	40
15 Spectra for 540 Baud, $M = 1.0$	41
16 Spectra for 540 Baud, $M = 2.0$	42
17 Spectra for 540 Baud, $M = 3.0$	43
18 Multi-Step Switching for FSK Signals	46
19 Low-Band Spectra for Steps = 1	48
20 Low-Band Spectra for Steps = 5	49
21 Low-Band Spectra for Steps = 10	50
22 Low-Band Spectra for Steps = 15	51
23 Mid-Band Spectra for Steps = 5	52

<u>Figure</u>	<u>Page</u>
24 Mid-Band Spectra for Steps = 10	53
25 Mid-Band Spectra for Steps = 15	54
26 High-Band Spectra for Steps = 1	55
27 High-Band Spectra for Steps = 5	56
28 High-Band Spectra for Steps = 10	57
29 High-Band Spectra for Steps = 15	58
30 Low-Band Comparison for Steps = 5	62
31 Low-Band Comparison for Steps = 10	63
32 Low-Band Comparison for Steps = 15	64
33 Mid-Band Comparison for Steps = 5	65
34 Mid-Band Comparison for Steps = 10	66
35 Mid-Band Comparison for Steps = 15	67
36 High-Band Comparison for Steps = 5	68
37 High-Band Comparison for Steps = 10	69
38 High-Band Comparison for Steps = 15	70

Abstract

Electronic broadbanding is a technique whereby very low frequency (VLF) antennas can be resonated (retuned) synchronously with a frequency-shift-keyed (FSK) signal for transmission of binary data at rates well over 1000 baud. The purpose of this thesis is to investigate the transmitted energy density spectrum for an electronically broadbanded VLF antenna system in which a frequency shift can occur only at the instant of an antenna-current zero-crossing with positive slope. A computer solution shows that the transmitted spectrum is approximately equivalent to the spectrum of an ideal, constant amplitude, FSK signal.

A further investigation, again by computer program, shows that if the total frequency shift between the marking and spacing frequencies occurs over a finite period, rather than instantaneously, then the spectrum's sidelobes will be reduced significantly. The spectrum for a 27,000 Hz center-frequency VLF antenna transmitting at 1600 baud by means of electronic broadbanding can be reduced from 3 to 18 dB in the first five sidelobes. No evaluation is made on the detectability of the signal with the non-instantaneous frequency shift. Numerous plots of the computer-generated spectra are included.

I. Introduction

The United States Air Force's Survivable Low Frequency Communication System uses the very low frequency (VLF) portion of the spectrum to achieve reliable long-range communications. This thesis is an examination of the energy spectrum of a specific FSK modulation scheme that could be used for VLF communications. In this thesis, frequency-shift keying is defined as a form of binary frequency modulation in which a specific frequency is transmitted for a digital zero, and a different frequency is transmitted for a digital one.

In 1972, Rome Air Development Center sponsored a development contract for the purpose of building a prototype mechanism that could be used to broaden the apparent bandwidth of conventional VLF antennas so that frequency-shift-keyed (FSK) signals could be transmitted at higher rates than those previously possible. The mechanism was named the Experimental Transmitting Antenna Modulator (ETAM) and its design was made possible by the use of newly-developed, high-speed, silicon-controlled rectifiers (SCR). The ETAM is a realization of a synchronous-resonance broadbanding technique wherein the antenna is resonated (retuned) in accordance with the frequency of the FSK signal being transmitted. In addition, each frequency change can occur only at the instant of an antenna-current zero-crossing with

positive slope (Ref 4.1-15). The purpose of this thesis is to determine the frequency spectrum for FSK signals transmitted from a VLF antenna system which uses an electronic broadbanding device such as the ETAM.

The study is limited to VLF transmitting systems in which there is no amplitude modulation of the transmitter voltage envelope. However, in contrast to FSK signals whose entire frequency shift occurs instantaneously, this study includes an analysis of electronically broadbanded systems whose frequency transitions are non-instantaneous.

II. Background

One method of modulating radio signals for transmission of digital data is frequency-shift keying, wherein a specific frequency is transmitted for a mark (a digital one) and a different frequency is transmitted to signify a space (a digital zero). Transmission rates for FSK signals in the VLF range (10 - 100 kHz) are severely limited by the bandwidth of conventional VLF antennas. Because of the extremely long wave lengths (up to 30 km), VLF antennas are electrically very short, and in order to achieve efficient power transmission, the antenna/transmitter system must be tuned to form a high-Q resonant circuit. The result is that typical VLF antennas may have a 3 dB bandwidth of 100 Hz or less (Ref 8:38). The bandwidth limitation restricts the FSK transmission rate to approximately 50 baud, or to a total of 50 marks and spaces per second, because of the phase distortion and amplitude transients which would occur at higher transmission rates (Ref 4:555).

Numerous methods have been investigated to increase VLF transmitting system bandwidths, but the most successful technique is to retune the antenna system in synchronization with the FSK signal by either capacitance modulation or by inductance modulation (Ref 4:555). The method of synchronous retuning, or synchronous resonance, can be described in terms of a mathematical model.

A VLF Antenna Model

VLF antennas can be modeled as series RLC circuits, and a generally accepted model is shown in Fig. 1. The model is valid for frequencies well below the uncompensated resonance frequency of the antenna. Due to the effects of the electromagnetic fields, the antenna's apparent inductance varies with frequency. For frequencies which are within the VLF range and that are less than half the uncompensated resonance frequency of the antenna (approximately 100 kHz), the apparent inductance changes by less than 5% and is considered as a constant (Ref 7:19,645).

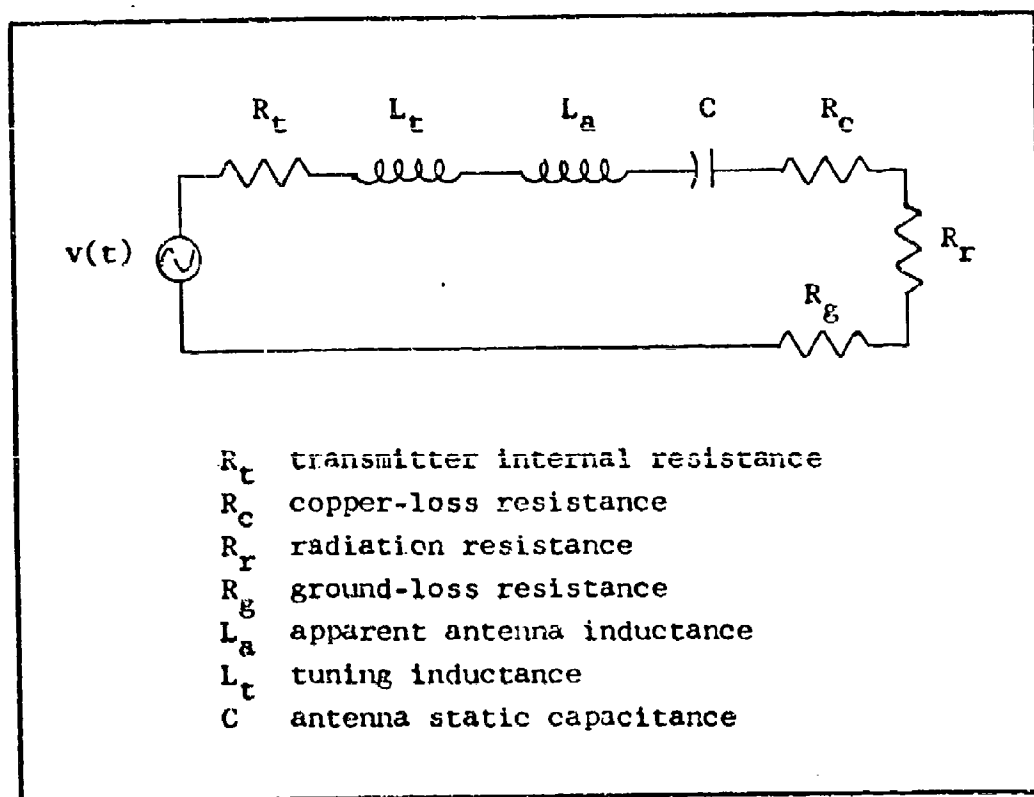


Fig. 1. Very-Low-Frequency Antenna Model

The average total power (P_t) transmitted from a VLF antenna can be expressed as

$$P_t = 40 \pi^2 I_o^2 (h/\lambda)^2 \quad \text{watts} \quad (1)$$

where I_o is the antenna current peak value, h is the effective height of the antenna, and λ is the transmitted wavelength. From Eq (1), a radiation resistance (R_r) may be defined as the resistance which would dissipate P_t watts when a sinusoidal current with peak value I_o flows through it (Ref 7:645). Hence,

$$R_r = (2P_t)/I_o^2 = 80 \pi^2 (h/\lambda)^2 \quad \text{ohms} \quad (2)$$

The radiation resistance for installed VLF antennas is normally between 0.05 and 0.3 ohms, while the total of all the other circuit resistances (R_{tot}) is between 0.1 and 0.7 ohms. The result is that the transmission efficiency (R_r/R_{tot}) is in the 0.25-to-0.65 range. However, one modern VLF antenna has a transmission efficiency of 0.88 (Ref 8:142).

The tuning inductance, L_t , is added to the circuit in order to lower the system resonant frequency from its uncompensated one to the desired frequency in the VLF range. Such inductors carry large currents and have been conventionally constructed as air-core coils.

Since the circuit is a familiar RLC circuit, the system 3 dB Bandwidth is the ratio of the resonant frequency to the system Q. The system Q is the ratio of the

circuit reactance to the total resistance. The equation for the bandwidth is

$$\text{Bandwidth}_{(3\text{dB})} = 2\pi f^2 C R_{\text{tot}} \quad \text{Hz} \quad (3)$$

References to bandwidth are to be made with caution, since it must be explicitly stated whether the bandwidth referred to is the system bandwidth, or that of the antenna alone. The system bandwidth is twice the antenna bandwidth, due to the transmitter being matched to the antenna, which appears as a resistance at the system resonant frequency. In this paper, the system bandwidth will be used unless otherwise stated.

The narrow bandwidth implies that for FSK modulation, the mark and space frequencies must both be well inside the 3 dB bandwidth limits, and that the baud rate must be low enough so that the transmitted signal amplitude and phase are not unduly distorted by transients. Such transient distortion reduces radiated power and receiver detection efficiency (Ref 4:556). One method for increasing the apparent bandwidth, and thereby increasing the potential baud rate, is that of synchronous resonance.

Energy Relationships for Synchronous Resonance

Higher transmission rates and wider apparent bandwidths may be achieved for pulsed transmission circuits, such as for FSK modulation, by a variation of the following concept. When it is possible to insert or to remove a portion of one

type of reactive element with the appropriate amount of stored energy at instants when the other type of reactive element in a resonant circuit has dissipated all of its stored energy, then an instantaneous steady-state oscillation is achievable. Such a technique permits instantaneous switching between a quiescent condition and a steady-state response. Further, it enables a change in resonant frequency of an oscillating circuit as often as once each cycle. In the application to FSK transmission, the transmitter frequency and the circuit's resonant frequency may be simultaneously changed without exciting large transients, by inserting or removing a portion of the reactive element whose stored energy is at a minimum. The result is that the steady-state response is obtained almost immediately (Ref 2: 375). The physics of such a switching operation is apparent when viewed in a set of differential equations.

A circuit model from which the circuit differential equation can be derived is shown in Fig. 2. Each circuit has a switchable DC source (V or I) for establishing initial conditions, but both circuits have the same differential equation when their respective switches are in position 2. The equation is

$$v(t) = L \frac{di}{dt} + i R + \frac{1}{C} \int_{-\infty}^t (i) dt \quad (4a)$$

or,

$$v(t) = L \ddot{q} + R \dot{q} + \frac{1}{C} (q_0 + q) \quad (4b)$$

where i is the time-dependent current and q is the time-

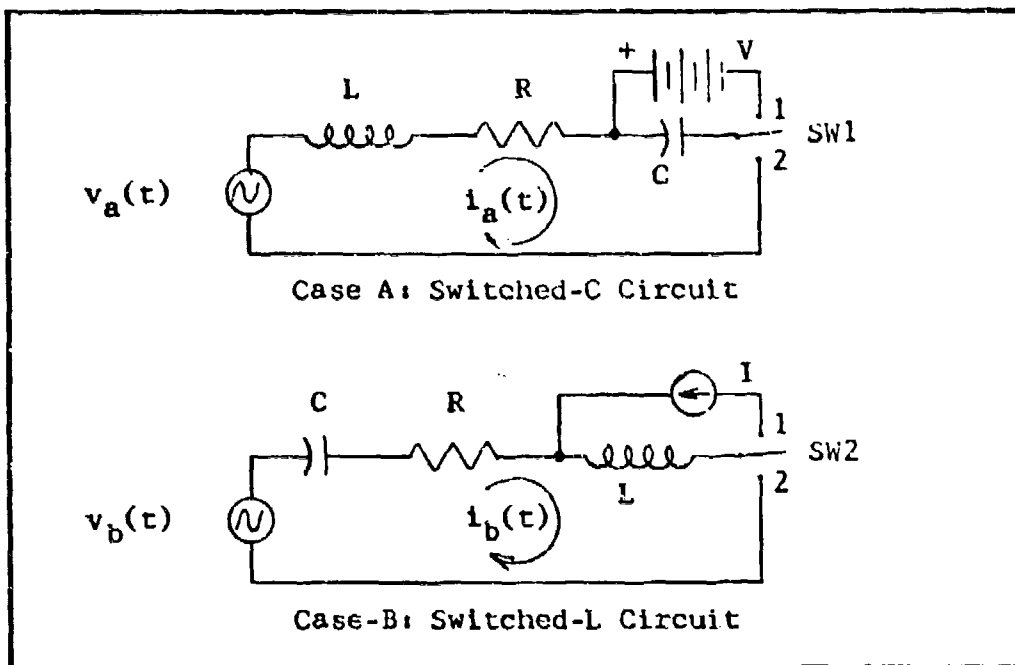


Fig. 2. Switched-Reactance Circuits

dependent capacitor charge. If i or q is assumed to exhibit a zero-transient response, then the required initial conditions can be determined from Eqs (4a) and (4b).

Assume for Case A, the switched-C circuit of Fig. 2, that the steady-state current is $i_a(t) = I_o \sin(\omega t)$ and that the switch $SW1$ is moved from position 1 to position 2 at time $t = 0$. For Case B, the switched-L circuit of Fig. 2, assume the steady-state current is $i_b(t) = I_o \cos(\omega t)$, and that the switching is the same as for the switched-C circuit.

The result for Case A is

$$v_a(t) = \omega L I_o \cos(\omega t) + R I_o \sin(\omega t) + \frac{I_o}{\omega C} (1 - \cos(\omega t)) + \frac{1}{C} \int_{-\infty}^0 i_a(t) dt \quad (5)$$

and the result for Case B is

$$v_b(t) = -\omega L I_0 \sin(\omega t) + R I_0 \cos(\omega t) + \frac{I_0}{\omega C} \sin(\omega t) + \frac{1}{C} \int_{-\infty}^0 i_b(t) dt \quad (6)$$

For a resonant circuit, $\omega L = \frac{1}{\omega C}$, which enables cancellation of two terms in each of Eqs (5) and (6). The results are

$$v_a(t) = R I_0 \sin(\omega t) + \frac{I_0}{\omega C} + \frac{1}{C} \int_{-\infty}^0 i_a(t) dt \quad (7)$$

and

$$v_b(t) = R I_0 \cos(\omega t) + \frac{1}{C} \int_{-\infty}^0 i_b(t) dt \quad (8)$$

for Cases A and B, respectively. The integral terms of Eqs (7) and (8) are the initial voltages on the capacitors. If the voltage generator V for Case A equaled

$$V = \frac{1}{C} \int_{-\infty}^0 i_a(t) dt = -\frac{I_0}{\omega C} \quad (9)$$

and if the initial current $i_a(0) = 0$, or if the capacitor voltage for Case B was

$$\frac{1}{C} \int_{-\infty}^0 i_b(t) dt = 0 \quad (10)$$

and the current source $I = i_b(0) = I_0$, then $i_a(t)$ and $i_b(t)$ would be zero-transient sinusoids. If different assumptions had been made, such as $i_a(t) = I_0 \cos(\omega t)$ or $i_b(t) = I_0 \sin(\omega t)$, then the exact initial conditions $I = i_a(0) = I_0$ (for the switched-C case) and $V = -\frac{I_0}{\omega C}$ (for the switched-L case) required for a zero-transient response could not be obtained.

The application of the above principle to a circuit operating at resonance can result in a frequency-change current transient that is a small fraction of the steady-state current amplitude. Fig. 3 depicts the relations which yield such a shift. To make a transient-less frequency change to $I_0 \sin(\omega t)$, the current must be zero and the capacitor voltage must be $-\frac{I_0}{\omega C}$. Such constraints on the current are satisfied every 2π radians, but the capacitor

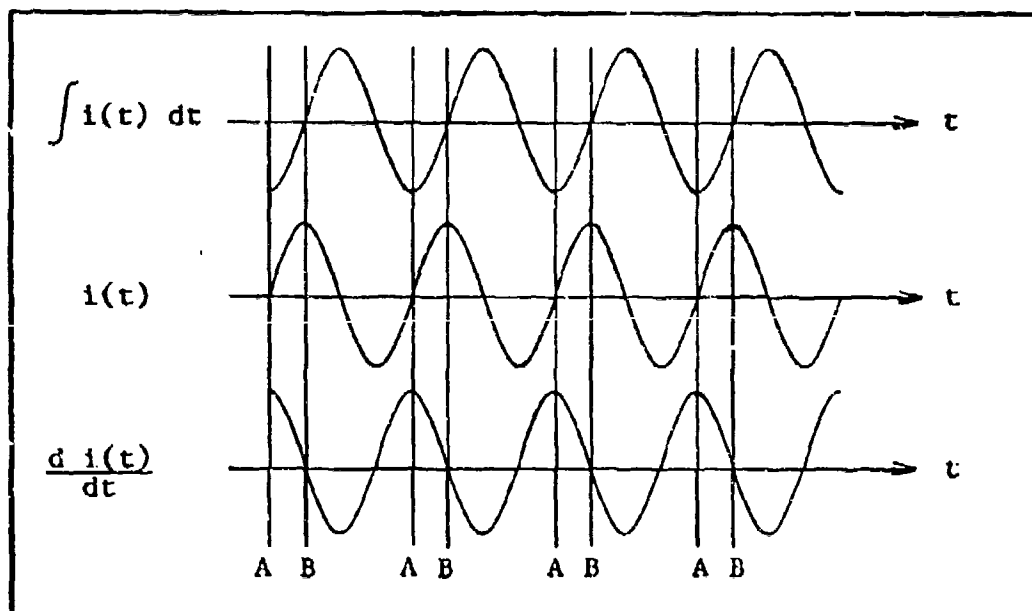


Fig. 3. Steady-State Current Relations

voltage constraint is not met exactly. The capacitor is charged to $-I_0/(\omega_0 C)$, where ω_0 is the radian frequency prior to the change, and such points are designated by "A" on Fig. 3. To make a change to $I_0 \cos(\omega t)$, the capacitor voltage must be zero and the current must be at a maximum. Such

time points are designated as "B" on Fig. 3. A change to $I_0 \cos(\omega t)$ would have no transient because the current peak is independent of the resonant frequency. Therefore, an ideal frequency change can be made by modulating the capacitor when its voltage is zero, or a near-ideal frequency change can be made by adjusting the inductor when the current is zero and the capacitor voltage is at a negative peak (a minimum). For the two cases discussed in this paragraph, the capacitor energy ($CV^2/2$) and the inductor energy ($LI^2/2$) are at mutually exclusive maxima, that is, one or the other has all the stored energy at the time of the change (Ref 2:376).

Synchronous resonance schemes have been attempted both through capacitor modulation and through inductor modulation (Ref 2:377). The inductor modulation case exhibits an almost negligible transient if the frequency shift is small in comparison to the resonant frequency. The system whose spectrum is sought uses induction modulation; however, it can achieve frequency shifts which are significant in comparison to the resonant frequency.

A General Switched-L Circuit for FSK Transmission

The circuit of Fig. 4 is capable of a zero-transient frequency shift for the $\cos(\omega t)$ form, or those denoted by "B" on Fig. 3. For the $\sin(\omega t)$ -type frequency shift, or those which are denoted by "A", a transient response will occur. For the type-B ($\cos(\omega t)$) shifts, the initial condition generator must create a current, I_0 , in the

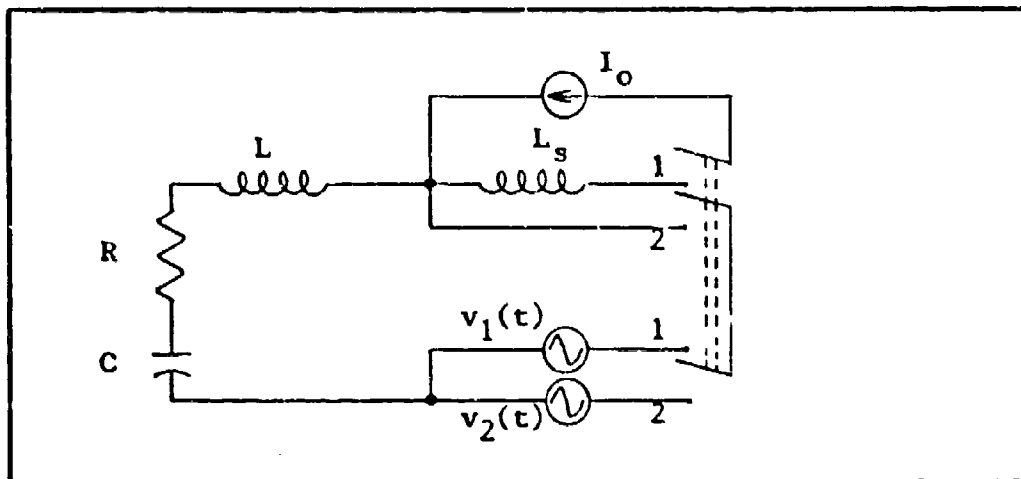


Fig. 4. Switched-L Synchronous Resonator

switching inductor, L_s , and the voltage sources must be changed simultaneously with the L_s switches. The addition of L_s will lower the resonant frequency. To return to the original frequency, the ganged switches must be placed to their original position when the current is at a positive maximum. However, the type-A ($\sin(\omega t)$) shifts can be achieved if the current source is a short circuit, and if the frequency transition occurs at an antenna-current zero-crossing with positive slope. The addition of L_s will again lower the resonant frequency, and the transient is caused by the mismatch in the capacitor voltage. The capacitor is charged to a maximum energy level at one frequency; however, the frequency change corresponds to a different capacitive reactance and therefore to different voltage and energy levels from those which are necessary for a zero-transient response.

In both the example cases, the voltage sources are assumed to have phase continuity. That is, at the time of each frequency change, there is no instantaneous jump in the voltage phase. Such a constraint implies a special synchronization between the sources, as well as between the circuit current and the switching time of L_g . Appropriate synchronization and control circuits were developed for the ETAM (Ref 4:7).

An Antenna Modulator for Synchronous Resonance

A model of a synchronously resonated antenna modulator for FSK transmission is shown in Fig. 5. The model is a variation of the circuit in Fig. 4, in that the effective primary inductance is L_1 if the switch is open, and the inductance changes to approximately $L_1 - (M^2/L_2)$, with R_2 very small, when the switch is closed. Not shown in Fig. 5 is a

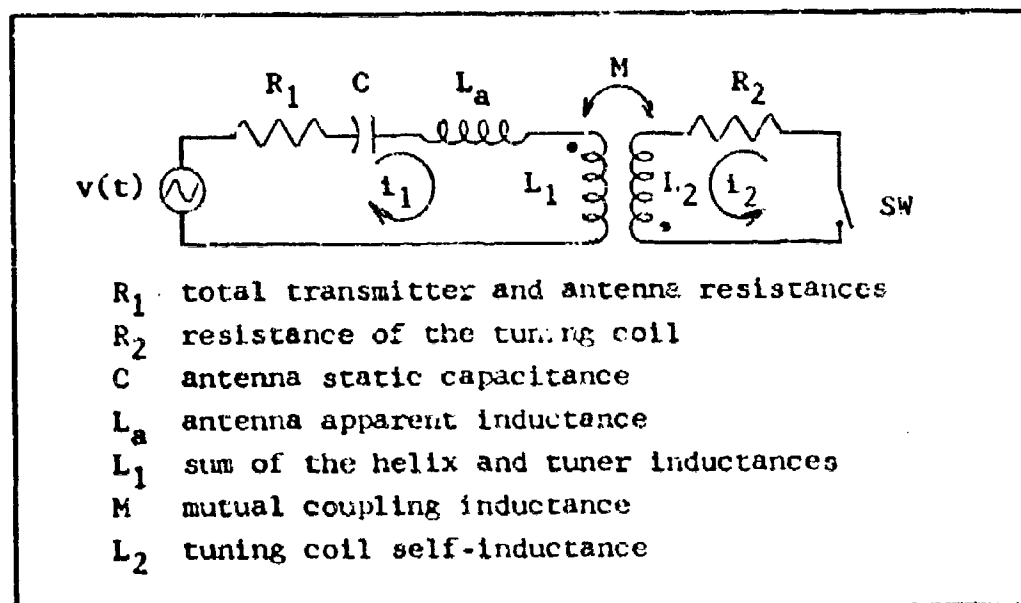


Fig. 5. An Inductively-Coupled Synchronous Resonator

timing circuit which enables the switch to open or to close and which changes the frequency of the source at the instant of an antenna-current zero-crossing.

Operational, synchronously resonated FSK systems use a saturable reactor or an electronically switched inductive shorting ring technique to achieve broadbanding. Either technique can be modeled as the circuit of Fig. 5. Such broadbanding methods are, however, limited by the large inherent saturable-reactor time-constant, or they are limited by the speed of the solid state switches. The two time delays cause an error in the switching instant and a prominent phase transient occurs for transmission rates higher than 50 baud (Ref 3:555).

The ETAM has demonstrated that VLF antennas can be synchronously resonated for broadbanding by inductors which are magnetically coupled to the antenna tuning inductance, and that are short- or open-circuited with newly-developed, high-speed, silicon-controlled rectifiers. The result is that the resonant frequency of the system instantaneously follows the frequency to be transmitted, although a transient does occur due to the capacitor voltage error. The high-current, high-voltage rectifiers are triggered so that in this switched-L configuration all changes in resonant frequency occur at the instant of an antenna-current zero-crossing.

Implications

The implications of electronic broadbanding are that VLF FSK transmissions can now be made at rates much higher than previously feasible, and in addition, the shift between the marking and spacing frequencies can be many times the system bandwidth. The energy spectrum for the synchronously resonated, FSK, antenna current at the higher baud rate will therefore be far wider than the bandwidth for an antenna without synchronous resonance.

III. Current Analysis for Synchronously Resonated Antennas

The preceding chapter contains a circuit diagram for an inductively-coupled antenna resonator for electronically-broadbanded FSK transmission. The purpose of Chapter III is to develop an expression for the antenna-current transient response of antennas which use the resonator, and to develop an expression for the capacitor voltage error.

Antenna Transient Analysis

If the antenna circuit is considered as an RLC circuit, then its differential equation is that of Eqs (4a) and (4b). Gamble (Ref 3:Appendix B) has shown that if the steady-state current is $v(t) = A \sin(\omega_0 t)$, then the steady-state capacitor charge is expressed by

$$= \frac{A}{R\omega_0} \cos(\omega_0 t) \quad (11)$$

if

$$\left(\frac{R}{2L}\right)^2 \ll \frac{1}{LC} \quad (12)$$

Fig. 4 indicates that an inductance, L_s , is added to or removed from the circuit at each frequency change. If Eq (4b) is expressed as

$$\ddot{q} + 2\alpha\dot{q} + \omega^2 q = \frac{1}{L} v(t) \quad (13)$$

where

$$\alpha = \frac{R}{2L} \quad (14a)$$

and

$$w^2 = \frac{1}{LC} \quad (14b)$$

and if an inductance, L_s , is added to the circuit, then Eqs (14a) and (14b) are changed to

$$\alpha_1 = \frac{R}{2(L+L_s)} \quad (15)$$

and

$$w_1^2 = \frac{1}{(L+L_s)C} \quad (16)$$

If the source is simultaneously set to $v(t) = A \sin(w_1 t)$, then Eq (13) is changed to

$$\ddot{q} + 2\alpha_1 \dot{q} + w_1^2 q = \frac{A}{L+L_s} \sin(w_1 t) \quad (17)$$

and the Laplace transform of Eq (17) is

$$s^2 Q(s) - sq(0) - \dot{q}(0) + 2\alpha_1 sQ(s) - 2\alpha_1 q(0) + w_1^2 Q(s) = \frac{A}{L+L_s} \frac{w_1}{s^2 + w_1^2} \quad (18)$$

The proper capacitor charge for a zero-transient response at radian-frequency w_1 is

$$\int_{-\infty}^0 \frac{A}{R} \sin(w_1 t) dt = q(0) = - \frac{A}{Rw_1} \quad (19)$$

in accordance with Eq (9). However, a voltage error does exist and departure from Gamble's analysis (Ref 3; Appendix B) allows the initial charge to be redefined as

$$q(0) = \frac{-A}{Rw_1} (1 + \gamma_1) \quad (20)$$

where γ_1 is the capacitor-charge error-fraction. The subscript 1 is for parameters at the shift to any general frequency w_1 . If Eq (15) is rewritten

$$\frac{2}{R} \frac{A}{(L+L_s)} \frac{R}{2} = \frac{2A}{R} \alpha_1 \quad (21)$$

then substitution of Eqs (20) and (21) into (18) yields

$$Q(s)[s^2 + 2\alpha_1 s + w_1^2] + \frac{A}{Rw_1}(1 + \gamma_1)[s + 2\alpha_1] = \frac{2A\alpha_1}{R} \frac{w_1}{s^2 + w_1^2} \quad (22)$$

where $\dot{q}(0) = i(0) = 0$ for an antenna-current zero-crossing.

Then

$$Q(s) = -\frac{A}{Rw_1} \left[\frac{s}{s^2 + w_1^2} + \gamma_1 \frac{(s + \alpha_1) + \alpha_1}{(s + \alpha_1)^2 - w_n^2} \right] \quad (23)$$

where

$$w_n^2 = w_1^2 - \alpha_1^2 \quad (24)$$

The inverse Laplace transform yields $q(t)$, and differentiation of $q(t)$ gives the current $i(t)$. Since, from Eq (12),

$$\alpha_1^2 \ll w_1^2 \quad (25)$$

then

$$w_n \approx w_1 \quad (26)$$

The complete response, $i(t)$, is

$$i(t) = \frac{A}{R_1} [1 + \gamma_1 \exp(-\alpha_1 t)] \sin(w_1 t) \quad (27)$$

where Eqs (15), (16) and (20) define the parameters.

A more meaningful form of Eq (27) is produced when the relation

$$BW = \text{Bandwidth}_{(3\text{dB})} = \frac{f_1}{Q} = \frac{\left(\frac{w_1}{2\pi}\right)}{\left(\frac{w_1 L}{R}\right)} = \frac{1}{\pi} \frac{R}{2L} = \frac{1}{\pi} \alpha_1 \quad (28)$$

is substituted into the exponential term of Eq (27). The result is

$$i(t) = \frac{A}{R_1} [1 + \gamma_1 \exp(-\pi BW t)] \sin(w_1 t) \quad (29)$$

Eq (29) emphasizes that the transient term decays more rapidly when the antenna bandwidth is increased.

The antenna current expressions, Eqs (27) and (29), are based upon having a knowledge of the error fraction, γ_1 , at the time of the frequency shift. Given such information, an error fraction can be calculated for a frequency shift which occurs at any ensuing antenna-current zero-crossing.

Error Fraction Calculations

The capacitor voltage at time t can be expressed as

$$v_c(t) = \frac{1}{C} \int_0^t i(\sigma) d\sigma + k \quad (30)$$

where k is the voltage at $t = 0$ and $i(t)$ is from Eq (27).

The constraints of Eqs (12) and (25), with the requirement that all error-fraction calculations need be made only at the instant of an antenna-current zero-crossing (that is, when an integer-multiple of cycles has been completed), yield

$$v_c \Big|_{t = \frac{2\pi n}{w_a}} = \gamma_a \frac{A}{CR_a w_a} \left[1 - \exp\left(-\frac{2\pi n \alpha_a}{w_a}\right) \right] + k_a \quad (31)$$

Fig. 6 depicts the time relations for Eqs (32) and (33) below. From Eq (20), the initial capacitor voltage at time $t = 0$ is

$$= \frac{A}{\omega_a R_a C} (1 + \gamma_a) \quad (32)$$

and the voltage at the instant of a later frequency change may be similarly expressed as

$$= \frac{A}{\omega_b R_b C} (1 + \gamma_b) \quad (33)$$

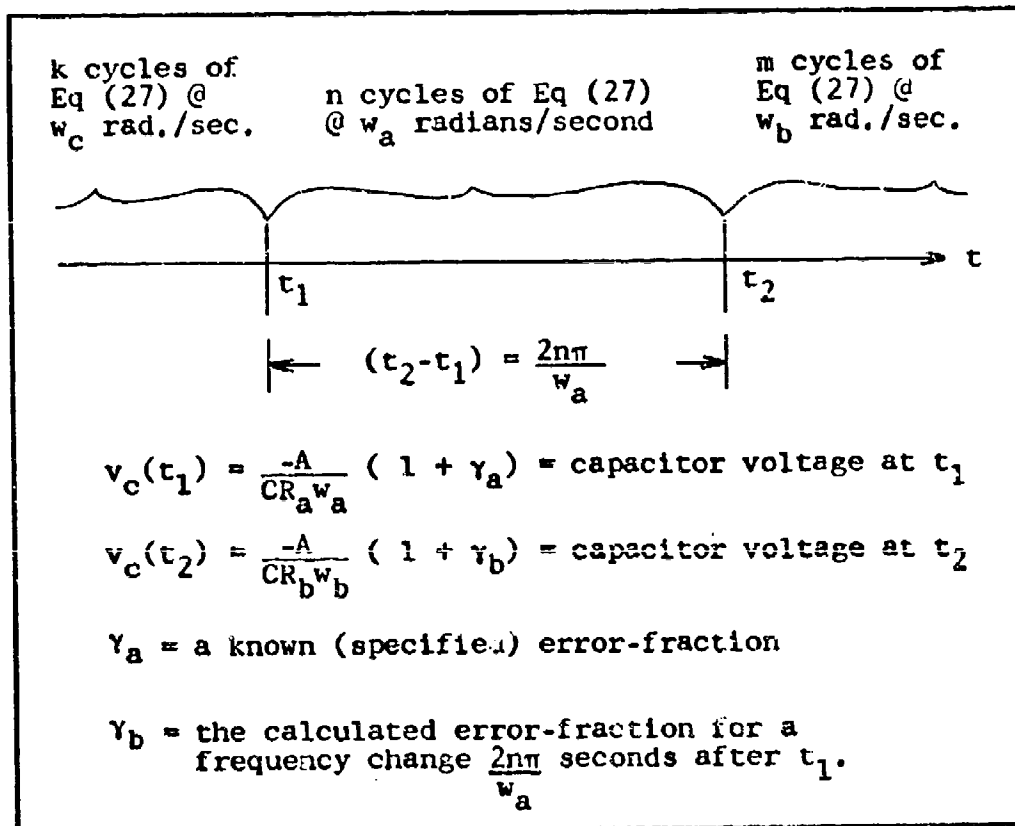


Fig. 6. General Error-Fraction Time Relations

Substitution of Eqs (32) and (33) into Eq (31) yields

$$\gamma_b = \frac{R_b w_b}{R_a w_a} \left[1 + \gamma_a \exp\left(-\frac{2\pi\alpha_a}{w_a}\right) \right] - 1 \quad (34)$$

from which the error fraction at the next frequency shift can be calculated. Eqs (27) and (34) provide a method of calculating the antenna current, given a specific FSK bit stream.

IV. Spectral Analysis for Synchronously Resonated Antennas

In Chapter III, expressions for the antenna current and for the capacitor voltage error were developed. In Chapter IV a method is developed for finding the energy spectrum of FSK signals which are transmitted through a synchronously resonated, VLF antenna that is retuned to the marking and spacing frequency at the instant of the antenna-current zero-crossing.

Examination of the Signal

The signal set which determines what is to be transmitted is a bit stream of marks and spaces, or ones and zeros. Such a binary bit stream is similar to the output from a teletype or from a binary encryption device. For this study the bit stream is assumed to be a series of independent, equiprobable ones and zeros.

By assuming that n (the number of cycles) is infinite for Eq (34), one can calculate the maximum error fraction at the instant of a frequency change which occurs after steady-state oscillation has been reached. Consider that for a change to the higher frequency Eq (34) gives the maximum error-fraction as $+0.1$, and for a change to the lower frequency Eq (34) gives the maximum error-fraction as -0.1 . However, for the transmission of a random bit-stream the error-fraction would not reach those maxima. The values

that the error-fractions assume are distributed in an unspecified manner between the two maxima. For example, if an antenna with a 3 dB static bandwidth of 65 Hz is synchronously resonated, then the time constant shown in Eq (29) for the decay of the transient would be $(1/(\pi EW)) \approx 0.005$ seconds. The transient would exist for approximately 0.025 seconds, and it would fully decay only for transmission rates less than 40 baud. The transient essentially never fully decays for high-baud systems such as are within the capability of the ETAM.

Comparison of Eqs (27) and (34) with Fig. 5 reveals the following constraints upon the system. At the time of change to a higher frequency, the switch SW is closed, thereby reducing the total inductance in the system. However, the switch and coil resistance, R_2 , is reflected back into the primary in accordance with the mutual coupling between the coils. The result is that the inductance is decreased by L_s and the resistance is increased by the reflected value of R_2 , so that the system bandwidth is increased. The converse happens when the lower frequency is switched, i.e., the system bandwidth is decreased. Examination of Eq (27) shows that the steady-state current for the higher frequency is smaller than that for the lower frequency, because the total circuit resistance is larger for the higher frequency signal and the peak source voltage, A , remains constant. As an illustration, assume for a specific transmitting system that the total resistance is increased by 15% for the higher

frequency and that the error fraction maxima are $+0.1$ and -0.1 . The resistance difference and the error fraction maxima have been used in Fig. 7 to depict the antenna current that results from transmission of a random bit stream. Only the envelope of the sinusoidal antenna current is shown in Fig. 7.

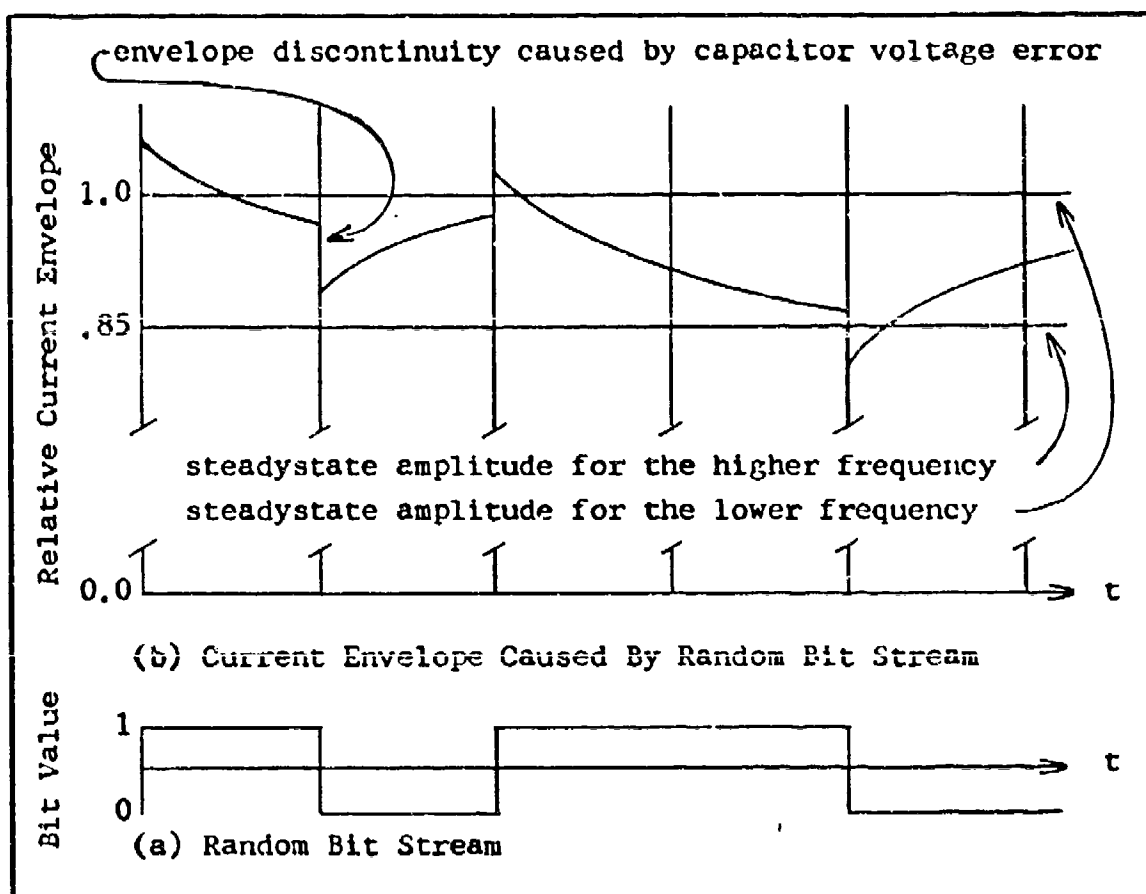


Fig. 7. Antenna Current Envelope

The data shown on Fig. 7 do not indicate that each frequency shift occurs only at the instant of an antenna-current zero-crossing. Fig. 8, however, illustrates the current/time relations near a key-shift point. The frequencies, decay rates, and steady-state current levels are for illustrative purposes only. The important feature of Fig. 8 is that the frequency shift must occur within one cycle of the frequency which existed prior to the key shift. The change could occur anywhere from the instant of the key shift up to one full cycle later, depending upon the phase of the antenna current at the instant of the key shift.

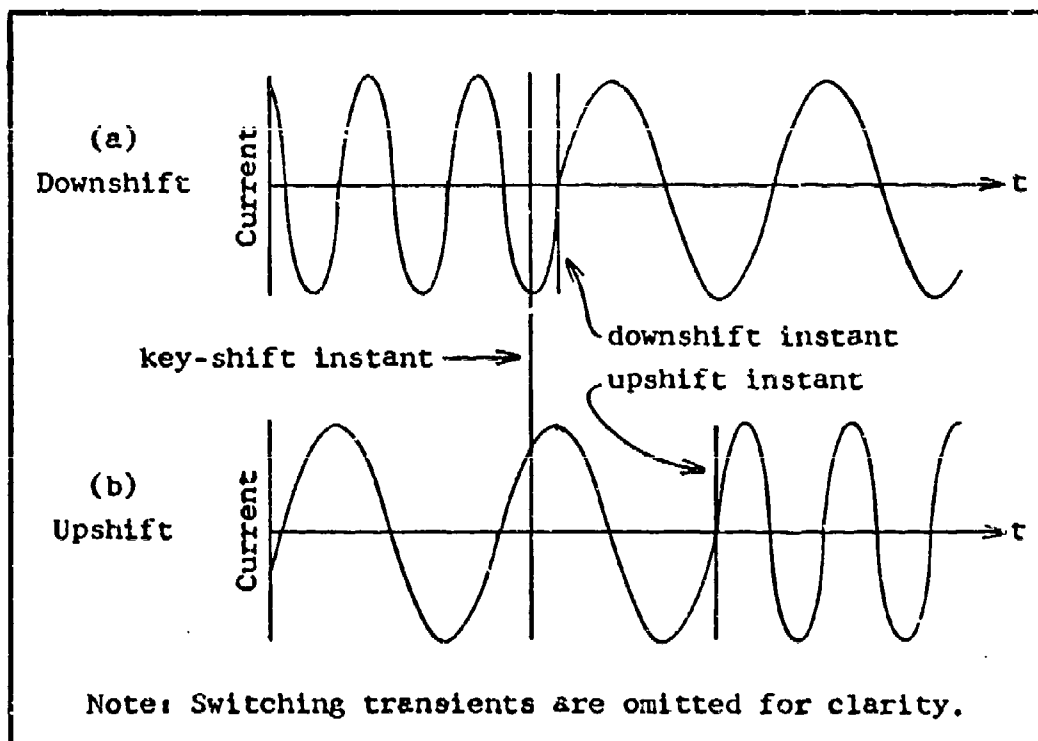


Fig. 8. Downshift and Upshift Antenna Current Relations

The Stochastic Process

If the expected value of a stochastic process is constant in time, and if the autocorrelation function of the process is a function only of the time difference ($t_1 - t_2$), then the process is wide-sense stationary and the power spectrum for the process is the Fourier transform of the autocorrelation function. Bennett and Rice (Ref 1:2355-2385) used those concepts to develop the power spectrum for a different type of FSK signal from that which has been described in this paper. The signal which Bennett and Rice used was phase-continuous (as is the ETAM signal), but the frequency changes occurred at the time of the key-shift; i.e., there was no delay due to the antenna-current zero-crossing. In addition, their signal did not include any transient analysis, but their simplifications and the postulation of a uniform density for the signal's phase at a frequency shift resulted in an analytic expression for the described power spectrum. One important result of Bennett and Rice's work is that the analytic expression showed that the power spectrum for a certain class of FSK signals decreases rapidly with respect to frequencies away from the transmitting system's center frequency. That class of FSK signals has a modulation index (M) that is 0.5, where

$$M = \frac{f_u - f_l}{\text{Baud Rate}} \quad (35)$$

and where f_u = upper transmitted frequency and f_l = lower transmitted frequency.

If Eq (27) is expressed in a form to show one segment of one realization of the antenna current's stochastic process, then

$$i(t) = \frac{A}{R} [1 + \gamma \exp(-\alpha t)] \sin(\omega t) \quad 0 \leq t \leq \frac{2\pi n}{\omega} \quad (36)$$

Where γ , α , n , ω , and R are realizations of random variables. However, probability densities may be assumed only for R , α , and ω because they are functions of the underlying random telegraph signal whose density function is known (R , α , and ω assume one of two values). The random variable n may have a binomial-type density function, but there is no definite data to confirm that. Finally, γ 's density function can only be described in terms of its range of values; i.e., the maxima described under the previous sub-heading. As a result, the mean and autocorrelation of the ETAM process cannot be calculated directly. As a hypothesis, however, the ETAM's power spectrum could be very similar to that for Bennett and Rice's work, because the range for γ is in general a small fraction, and the range of values for n can only be different by a fraction of a cycle when compared to Bennett and Rice's FSK process. Since that hypothesis is only an estimate, the author chose to develop a general-case, iterative method for describing the power spectrum for ETAM-produced signals for any general value of modulation index M .

Solution Method: A Finite-Time Power Spectrum

An expression relating the energy of a signal $v(t)$ to that signal's Fourier transform is

$$E = \int_{-\infty}^{+\infty} f^2(t) dt = \frac{1}{2\pi} \int_{-\infty}^{+\infty} |F(w)|^2 dw$$

$$= \int_{-\infty}^{+\infty} [(\text{Re}(f))^2 + (\text{Im}(f))^2] df \quad (37)$$

where E is defined as the energy dissipated by voltage $f(t)$ applied across a one-ohm resistor, or by a current $f(t)$ through a one-ohm resistor. Eq (37) states that the energy of a signal is given by the area under the $|F(w)|^2$ (the magnitude squared) curve, integrated with respect to the frequency variable $f = w/2\pi$ (Ref 6:127). The power spectrum can be interpreted as the energy per unit bandwidth (in Hz) contributed by frequency components at frequency f . The units of the energy density spectrum are joules per Hz.

The Fourier transform for a finite number of cycles of the antenna current (an n -cycle segment of one realization of the random process $i(t)$) can be expressed as

$$F(w) = \left(\frac{1-D}{E}\right) H w_1 + H \gamma_1 w_1 \frac{(B - A B D + A C G)}{B^2 + C^2}$$

$$+ j \frac{G H}{E} w_1 + j H \gamma_1 w_1 \frac{(A C D - C + A B G)}{B^2 + C^2} \quad (38)$$

where

$$A = \exp\left(-\frac{2\pi n a_1}{w_1}\right) \quad (38a)$$

$$B = \alpha_1^2 + w_1^2 - w^2 \quad (38b)$$

$$C = 2w\alpha_1 \quad (38c)$$

$$D = \cos\left(\frac{2\pi n w}{w_1}\right) \quad (38d)$$

$$E = w_1^2 - w^2 \quad (38e)$$

$$G = \sin\left(\frac{2\pi n w}{w_1}\right) \quad (38f)$$

$$H = \frac{A_1}{R_1} \quad (38g)$$

and where w_1 is the radian frequency for that specific segment. All the other subscripted parameters must be assigned appropriate values for the conditions at the beginning of the segment. The definitions of each of the values are as presented for those of Eq (27).

The transform of Eq (38) can be adapted to generate the power spectrum for a finite time-series of the waveforms of Eq (27) by application of the time-shift theorem. The time-shift theorem states that if a waveform is shifted in time, then the Fourier transform of the shifted wave can be found by multiplying the known transform by $\exp(-j\omega T_d)$, where T_d is the time to which the waveform is shifted. Hence, the Fourier transform for a finite number of sequential waveforms like Eq (27) can be found by adding the $\exp(-j\omega T_d)F(\omega)$ product for each segment. That is possible because the Fourier transform is linear and superposition holds.

A finite series of marks and spaces from the underlying random process gives rise to a finite sequence of antenna cur-

rent waveforms {Eq (27)}. Therefore Eq (38), along with the time-shift theorem, can be used to calculate the Fourier transform's real and imaginary values at specific frequencies. The value of the energy density spectrum at a specific frequency f_1 can then be calculated by

$$F(f_1)^2 = \left\{ \sum_{j=1}^m \text{Re}_j(f_1) \right\}^2 + \left\{ \sum_{j=1}^m \text{Im}_j(f_1) \right\}^2 \quad (39)$$

where $\text{Re}_j(f_1)$ and $\text{Im}_j(f_1)$ are the real and imaginary values of the Fourier transform of the j -th segment at frequency f_1 .

Eqs (38) and (39) are discontinuous at the frequency which is being transmitted. An expression (via L'Hospital's rule) that is valid at the discontinuities is

$$\begin{aligned} \lim_{w \rightarrow w_1} F(w) = & E \gamma_1 w_1 \frac{[\alpha^2 (1 - A)]}{\alpha^2 (\alpha^2 + 4w_1^2)} - \frac{j\pi n H}{w_1} \\ & - jH \gamma_1 w_1 \frac{[-C(1 - A)]}{\alpha^2 (\alpha^2 + 4w_1^2)} \quad (40) \end{aligned}$$

where the parameters are defined as for Eq (38).

In order to make the finite-time energy density spectrum meaningful for a comparative analysis, the spectral components must be normalized, and that is done by adjusting the spectral values at each frequency so that the area under the energy spectrum is one joule, when integrated across the entire frequency domain. One possible way to do that is to divide the energy density spectrum of Eq (39) by the total energy. The energy (E) of one segment {Eq (27)} of the antenna current is

$$E = H^2 \left\{ \frac{\pi n}{w_1} - \frac{4\gamma_1 w_1^2}{\alpha_1^3 + 4\alpha_1 w_1^2} (A-1) - \frac{\gamma_1^2 w_1^2}{4\alpha_1^3 + 4\alpha_1 w_1^2} (A^2-1) \right\} \quad (41)$$

where the parameters are as defined for Eq (38). The total energy is the sum of the energies for each segment of the series.

Relations Between the Circuit Parameters

The method outlined in the preceding paragraphs provides a way to generate the energy density spectrum for the antenna current resulting from a finite-length random telegraph signal. There does remain, however, a set of unspecified relations between the parameters of practically all the preceding equations. The parameters are R_a and R_b , the total circuit resistances for the case of the lower transmitted frequency (f_a) and the higher transmitted frequency (f_b), respectively. The 3 db bandwidth and the total inductance for the lower and higher transmitted frequencies have been designated BW_a , BW_b , L_a , and L_b , respectively. The first relationship between the parameters is

$$R_b = \left[1 + .015 \left(\frac{f_b - f_a}{BW_a} \right) \right] R_a \quad (42)$$

The relation for Eq (42) is entirely empirical in that it was formulated from the results of Hartley's work which included the resistance of the SCR switches (Ref 4:557). In addition to Eq (42), Eq (28) can be used to express the ratio of L_a and L_b as

$$\frac{L_b}{L_a} = \frac{f_a^2}{f_b^2} = \frac{R_b BW_a}{R_a BW_b} \quad (43)$$

from which

$$BW_b = \frac{f_b^2 R_b BW_a}{f_a^2 R_a} \quad (44)$$

The use of Eq (42), (43) and (44) provides a rational basis for selection of the parameters for Eqs (27), (34), (39), (40) and (41).

Generation and Compilation of Spectra

A computer program for calculating the energy density spectrum generated by the transmission of a finite-length random bit-stream through a synchronously resonated VLF antenna was written and used to provide data from which the spectra for various cases were plotted. The principle expressions used in the computer program were Eq (38), the Fourier transform; Eq (39), the power spectrum; Eq (41), the energy in one signal segment; and Eqs (42) - (44), the inter-parameter relations. The program is completely general in that the modulation index, bandwidth, baud rate and the marking and spacing frequencies are variables. Appendix A contains a listing of the fundamental portions of the program.

Since the program is completely general, a specific set of parameters representing those of a hypothetical VLF transmitting system were chosen to demonstrate the program's spectrum-generating capabilities. The hypothetical system

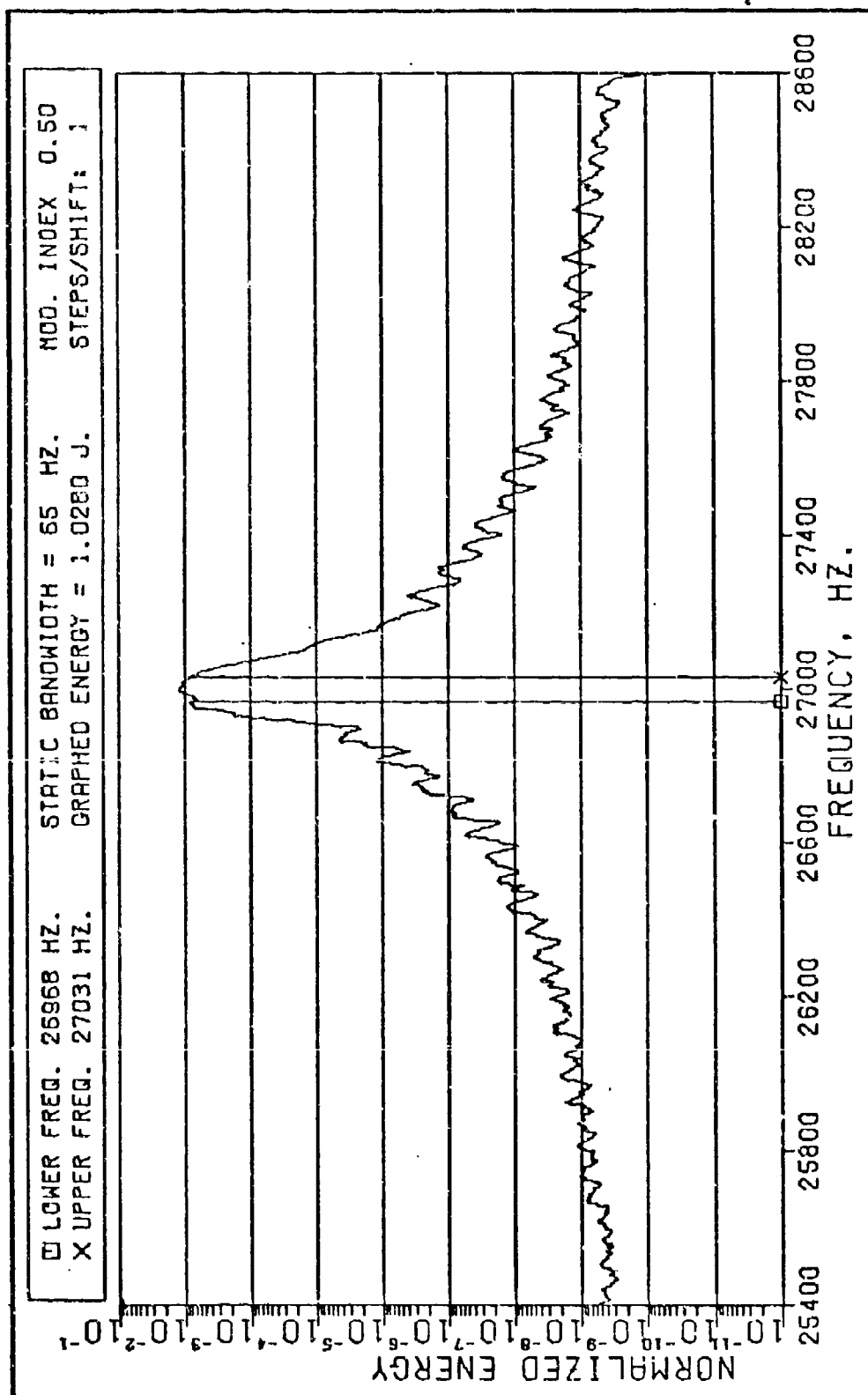
was designed to operate at 27000 Hz center frequency with a 3 dB bandwidth of 65 Hz. Given those constraints, Watt's work (Ref 8:125-140) was examined to determine a reasonable value for the antenna's static capacitance and the value of 0.05 microfarad was chosen. Eq (3) then gave 0.28 ohms as the total circuit resistance at the lower frequency. The remaining inter-parameter relations were determined in the program by use of Eqs (28), (42) and (44).

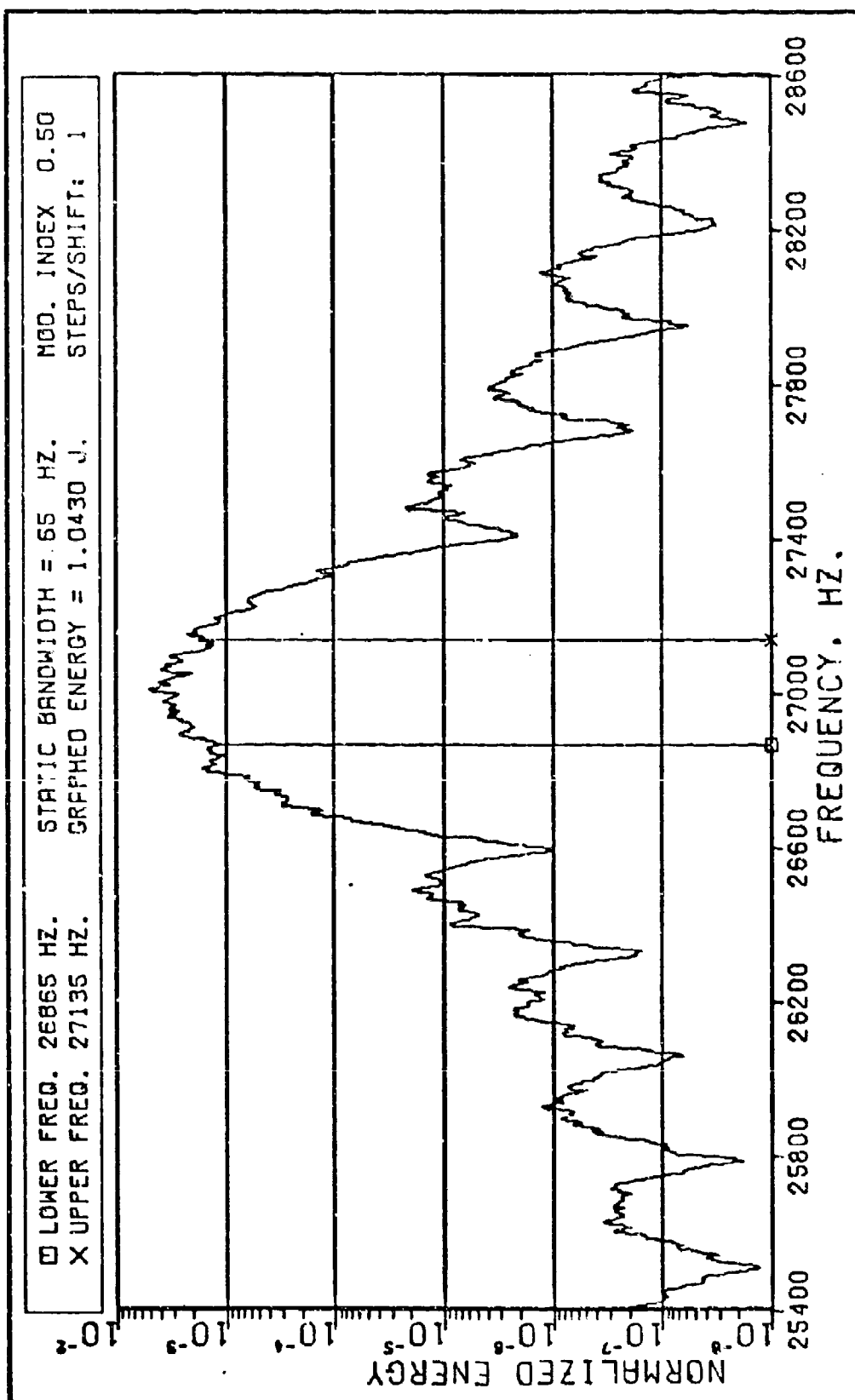
Trial program runs showed that the energy density spectrum for individual cases reached a definite pattern after as few as 200 random bits were read and processed. The specific cases that were run for this thesis all had an identical random bit stream which was 1000 bits long. That choice provided for a comparison between specific cases in which the baud rate and the modulation index {Eq (35)} were varied.

The energy density spectra were plotted by using a separate computer program, but the resulting plots were not well suited to comparative purposes because the spectrum line was jagged and greater than one inch wide. As a result, a smoothing routine was developed for the plotting program, and that particular set of Fortran instructions is listed in Appendix A. The entire plotting routine was not included because, while the Fortran language is general, the auxiliary plotters are certainly not. All of the plots shown in the remainder of this thesis have been smoothed by that routine.

The program was used to examine several cases for the above-specified antenna using an ETAM-like synchronous resonance system. For the first set of six plots, Figs. 9 - 14, the baud rate was varied from 125 to 2000 in order to examine how the main, or center, lobe of the energy density spectrum varied with the baud rate. The next three plots, Figs. 15 - 17, are for cases where the baud rate remains constant at 540, but the modulation index is varied.

Each of the plots mentioned above is a portion of a normalized energy density spectrum; i.e., the entire spectrum has one joule under the curve. The upper and lower transmitting frequencies are marked on the plots, and the normalized energy under the curve on each plot has been integrated and entered in the header at the top of the plots. Due to the finite length and the random nature of the bit stream, the integrated energy varies from 0.92 to 1.04 joules; hence, the number shown on the plots must be interpreted liberally. The "steps/shift = 1" entry indicates that the frequency shift for that plot was an instantaneous shift; i.e., the entire shift occurred in one step at the instant of the antenna-current zero-crossing.

Fig. 9. Spectra for 125 Baud, $M = 1/2$.

Fig. 10. Spectra for 540 Baud, $M = 1/2$.

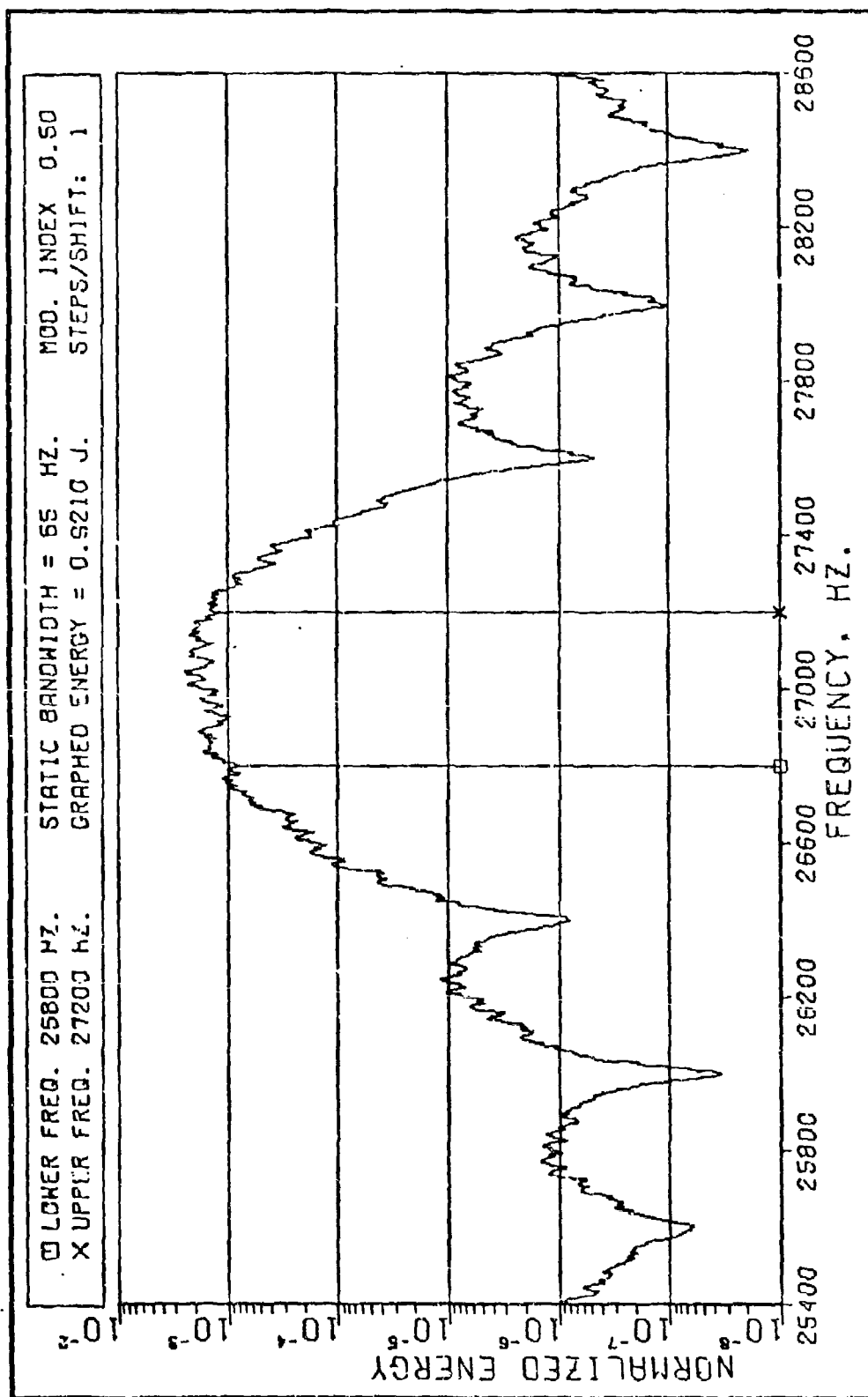
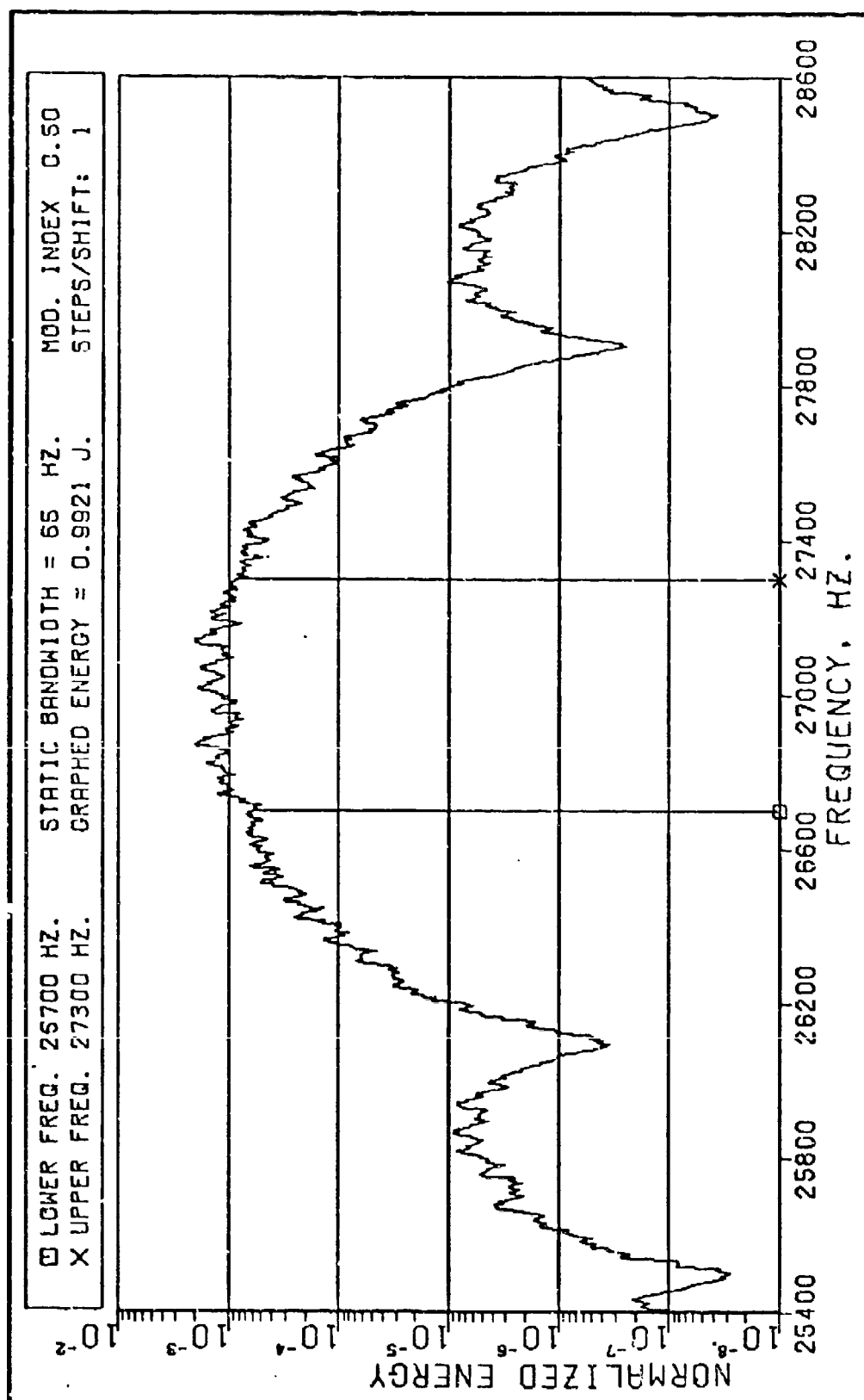
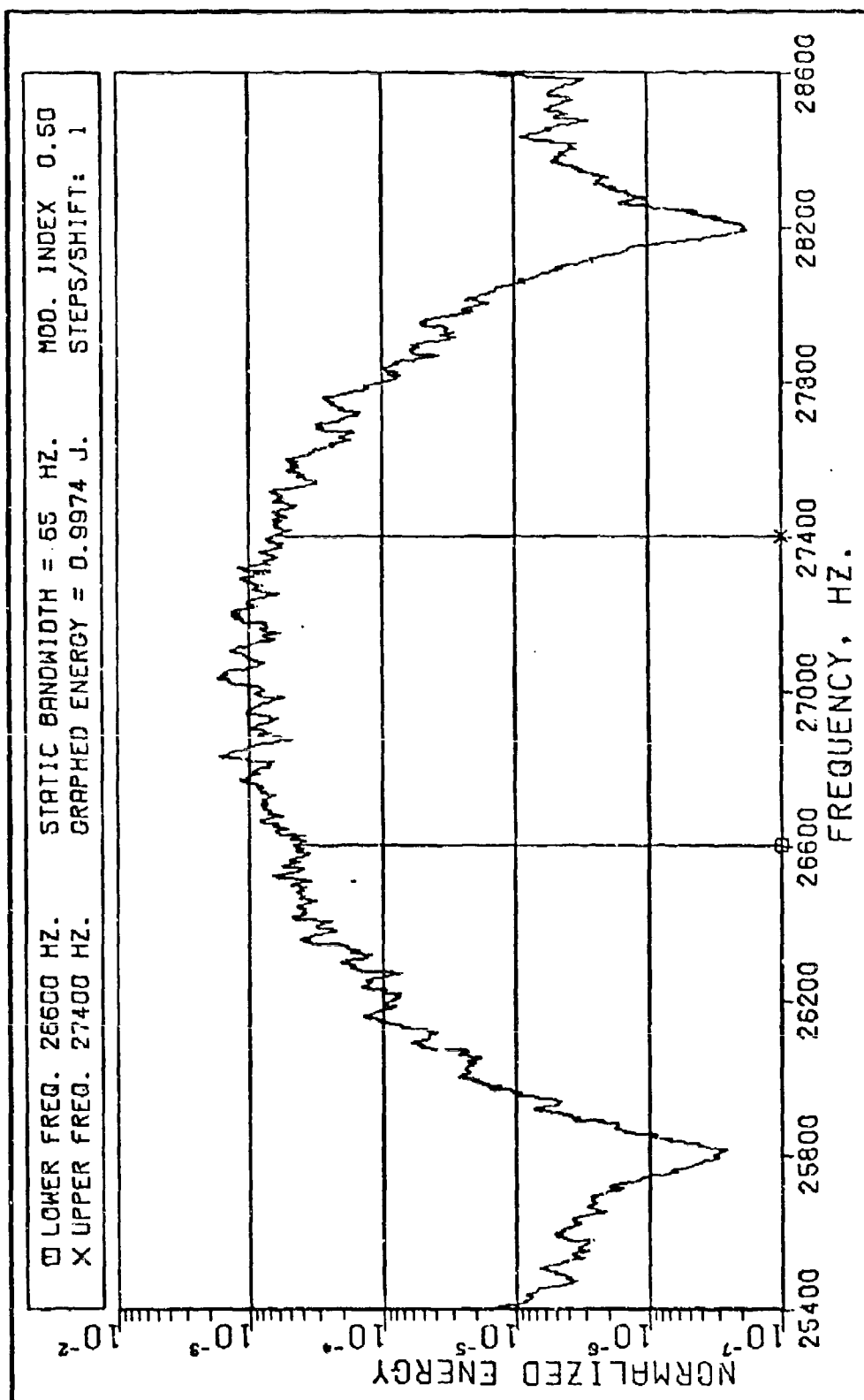
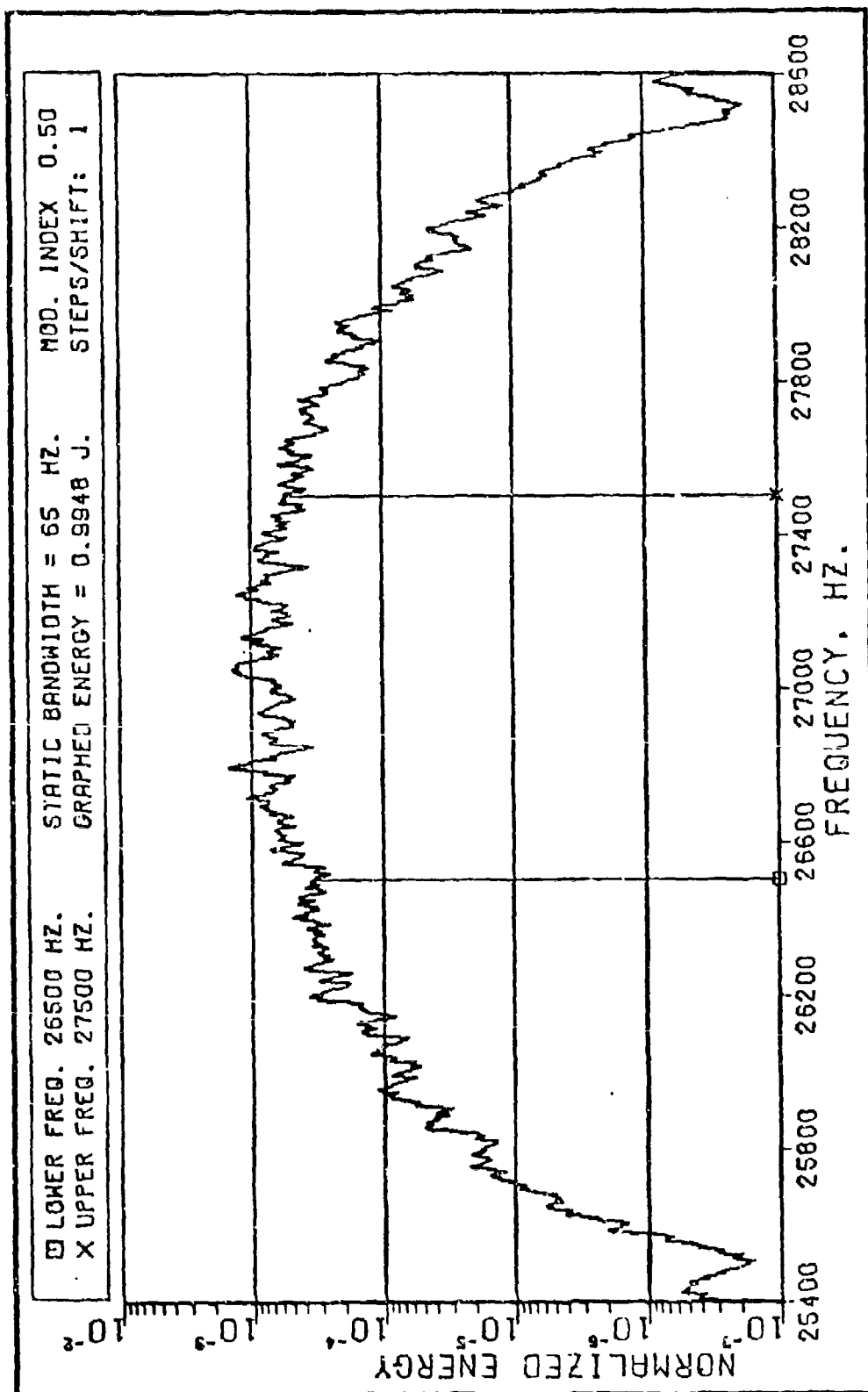


Fig. 11. Spectra for 800 Baud, M = 1/2.

Fig. 12. Spectra for 1200 Baud, $M = 1/2$.

Fig. 13. Spectra for 1600 Baud, $M = 1/2$.

Fig. 14. Spectra for 2000 Baud, $M = 1/2$.

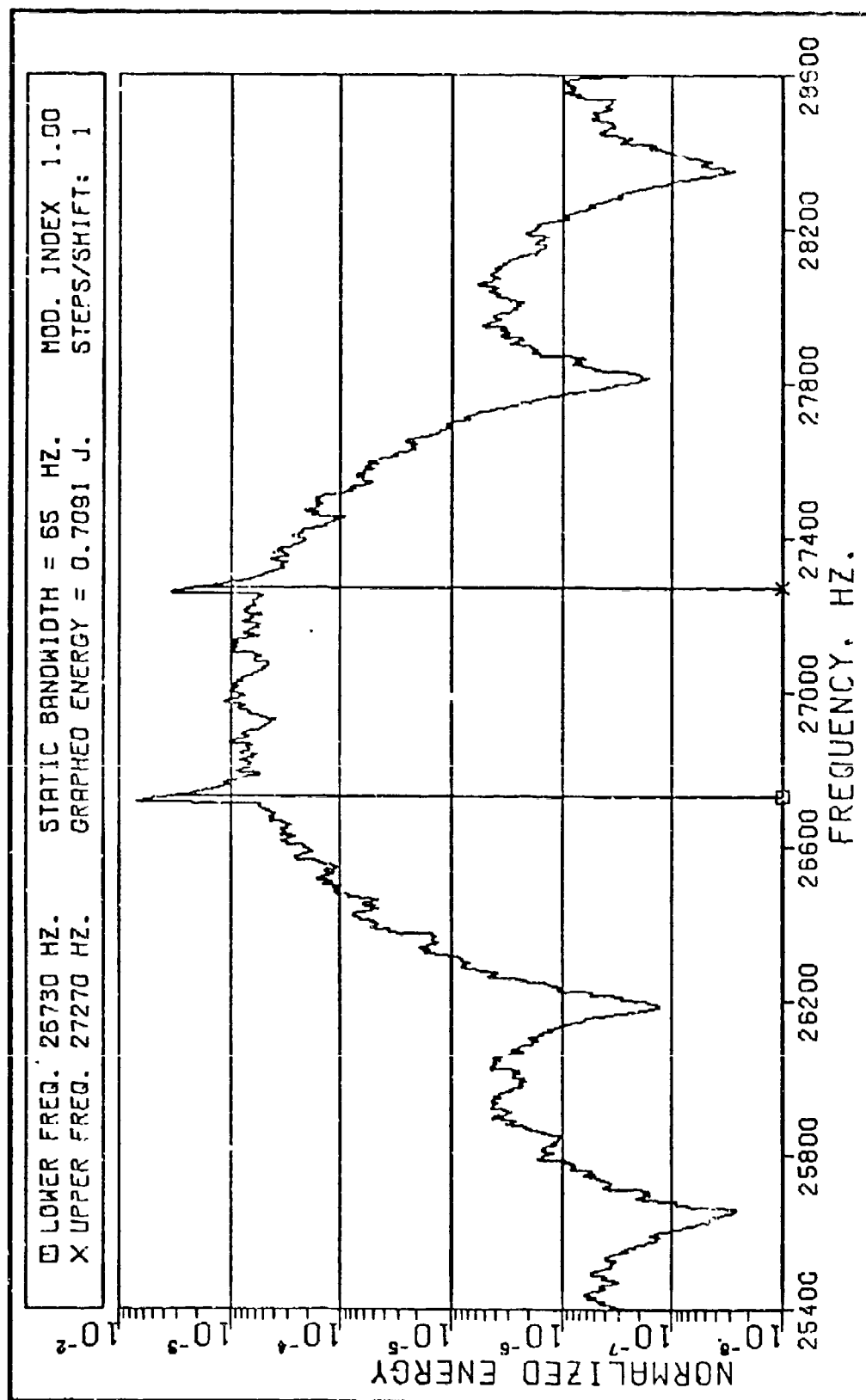


Fig. 15. Spectra for 540 Baud, M = 1.0.

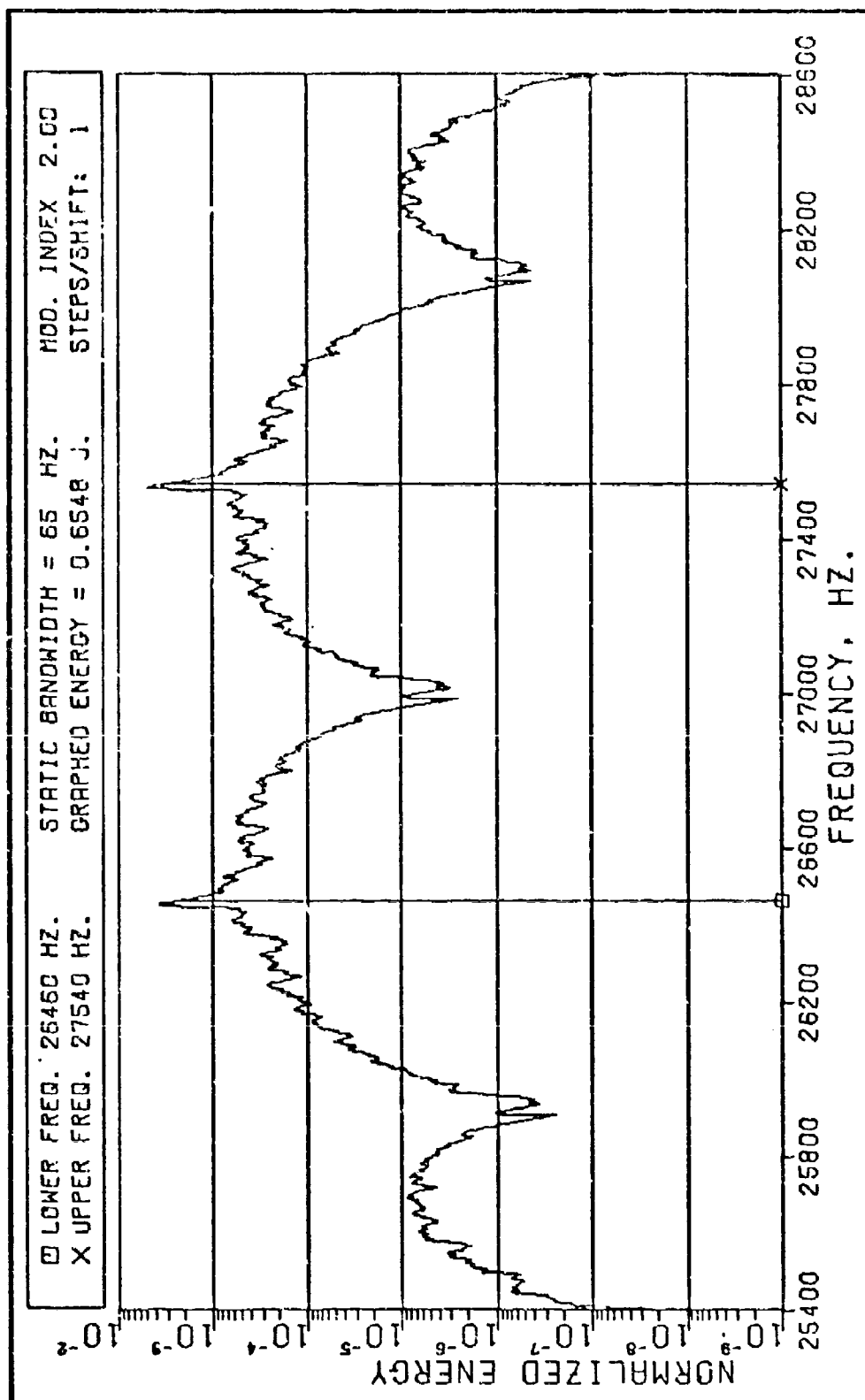


Fig. 16. Spectra for 540 Baud, M = 2.0.

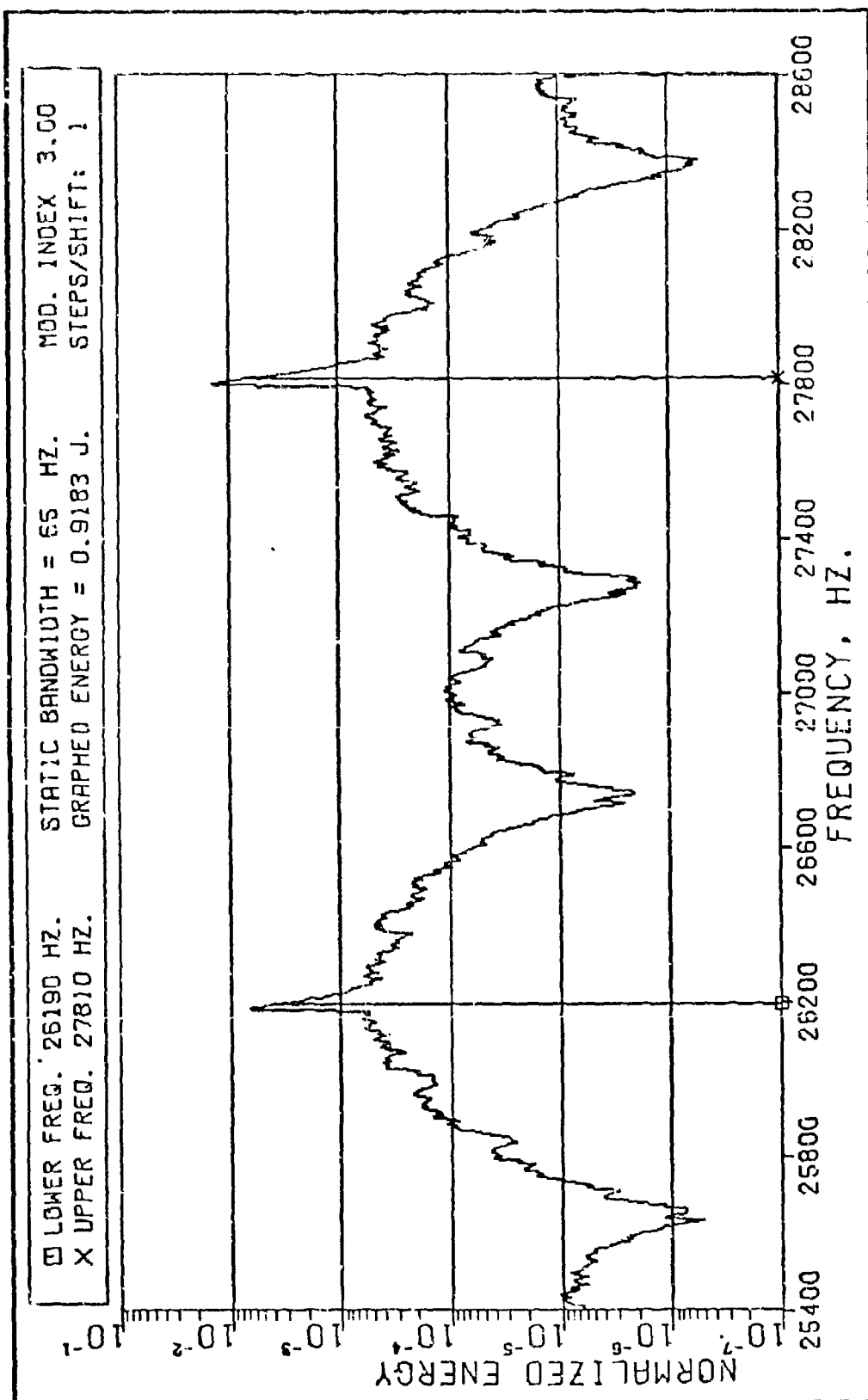


Fig. 17. Spectra for 540 Baud, M = 3.0.

V. Frequency Modulation for Spectrum Shaping

A method for determining the energy density spectrum for the transmission of FSK data through a synchronously resonated VLF antenna was shown in Chapter IV. The method was programmed in Fortran and the results of that program appear on computer-generated plots under the last sub-heading of Chapter IV. In Chapter V, an investigation is made to determine the effect of frequency modulation on reducing the width of the energy spectrum's main lobe and on reducing the spectrum's magnitude at frequencies far removed from the system's center-frequency.

What Type of Modulation?

The sponsor for this thesis, RADC, requested that the effects of making the frequency changes between f_a and f_b over a discrete time period (rather than the total shift occurring at the instant of the antenna-current zero-crossing) be investigated as a means of reducing out-of-band spectra. The frequencies f_a and f_b are the lower and higher transmitted signals.

As mentioned in Chapter II, synchronously resonated antennas could have a theoretical zero-transient frequency change once each cycle, at the next antenna-current zero-crossing. Changes that do not occur at the zero-crossing can cause significant current transients which reduce the signal's

detectability and potentially can cause damage to the SCR switches. Hence, a feasible and desirable method of frequency modulation for a synchronously resonated antenna is to approximate the desired frequency/time relationship with incremental frequency changes, each occurring at an antenna-current zero-crossing and each lasting at least one complete cycle.

There are limitations as to how much frequency modulation can occur for one specific key-shift, because for the higher key-shift rates at VLF, there are a small number of individual cycles for each individual baud. For example, a 1600 baud keying rate transmitted on a system with a center frequency of 27,000 Hz results in each mark or space having 16 or 17 cycles. The frequency modulation certainly cannot last beyond one baud, and the correlation and detection of the transmitted signal will be degraded in an unspecified manner as the time period for the shaping is increased. There is simply no time for elaborate frequency shaping schemes.

For this thesis, therefore, an approximation to linear frequency modulation is the only case investigated for spectra reduction. Fig. 18 shows a frequency/time chart for (1) a segment of an FSK signal, (2) the same signal with linear frequency modulation, and (3) the discrete step frequency modulation that is within the capabilities of a slightly modified ETAM circuit.

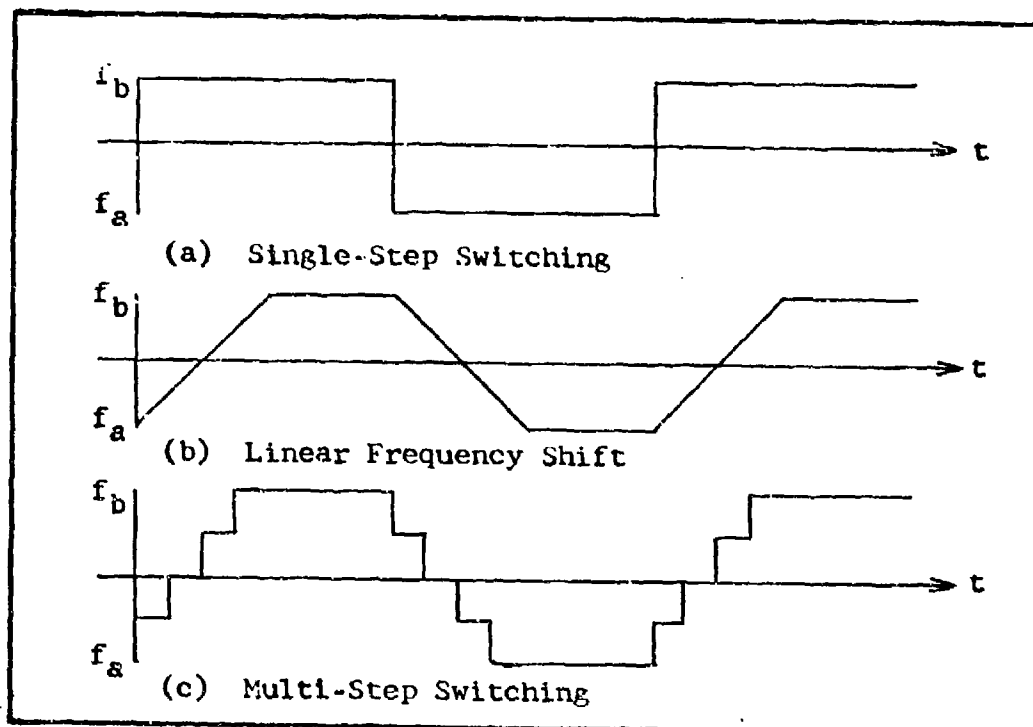


Fig. 18. Multi-Step Switching for FSK Signals

Modification of the Program

The program was modified so that the number of steps, or the number of discrete frequency changes for a single key-shift, could be specified by a data card. The result is that the finite-time spectrum for a random bit-stream could be calculated for an arbitrary amount of frequency modulation, or an arbitrary number of discrete steps. The transmitter frequency shift and the system resonant frequency shift was the same for each discrete step, as shown on Fig. 18.

The spectra for several cases is plotted on Figs. 19 through 29. In each case, the center frequency is 27,000 Hz, and the baud rate is 1600. The spectra were calculated

for the number of steps per shift being equal to 1, 5, 10, and 15. Three frequency bands were plotted for each of the four different cases, the bands being 0 - 32000 Hz (Low-Band), 25400 - 28600 Hz (Mid-Band), and 32000 - 64000 Hz (High-Band). The same 1000 bit data stream that was used on the single-step cases was used on the multi-step cases. In addition, the error fraction was calculated for each single cycle in the multi-step frequency transitions.

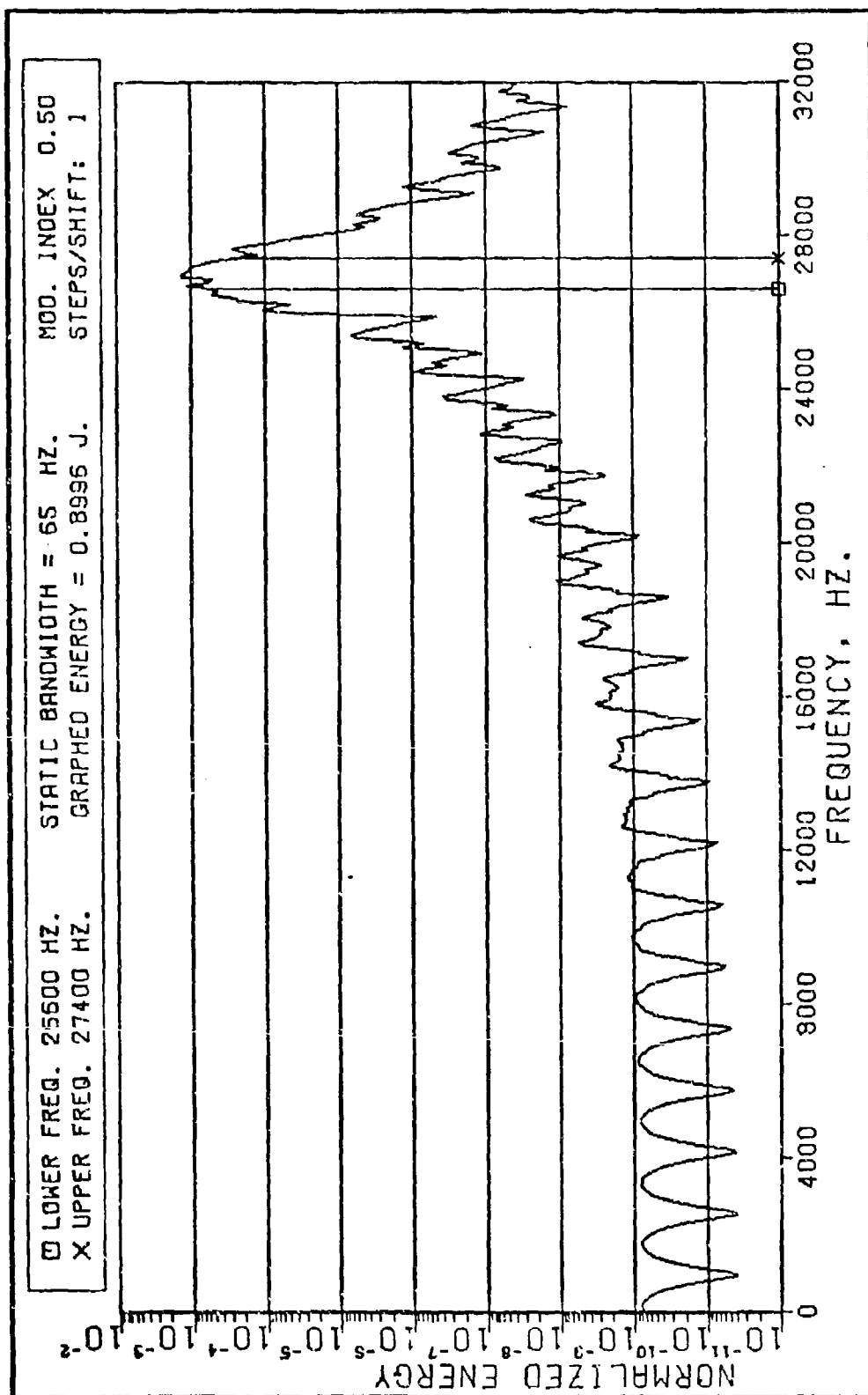


Fig. 19. Low-Band Spectra for Steps = 1.

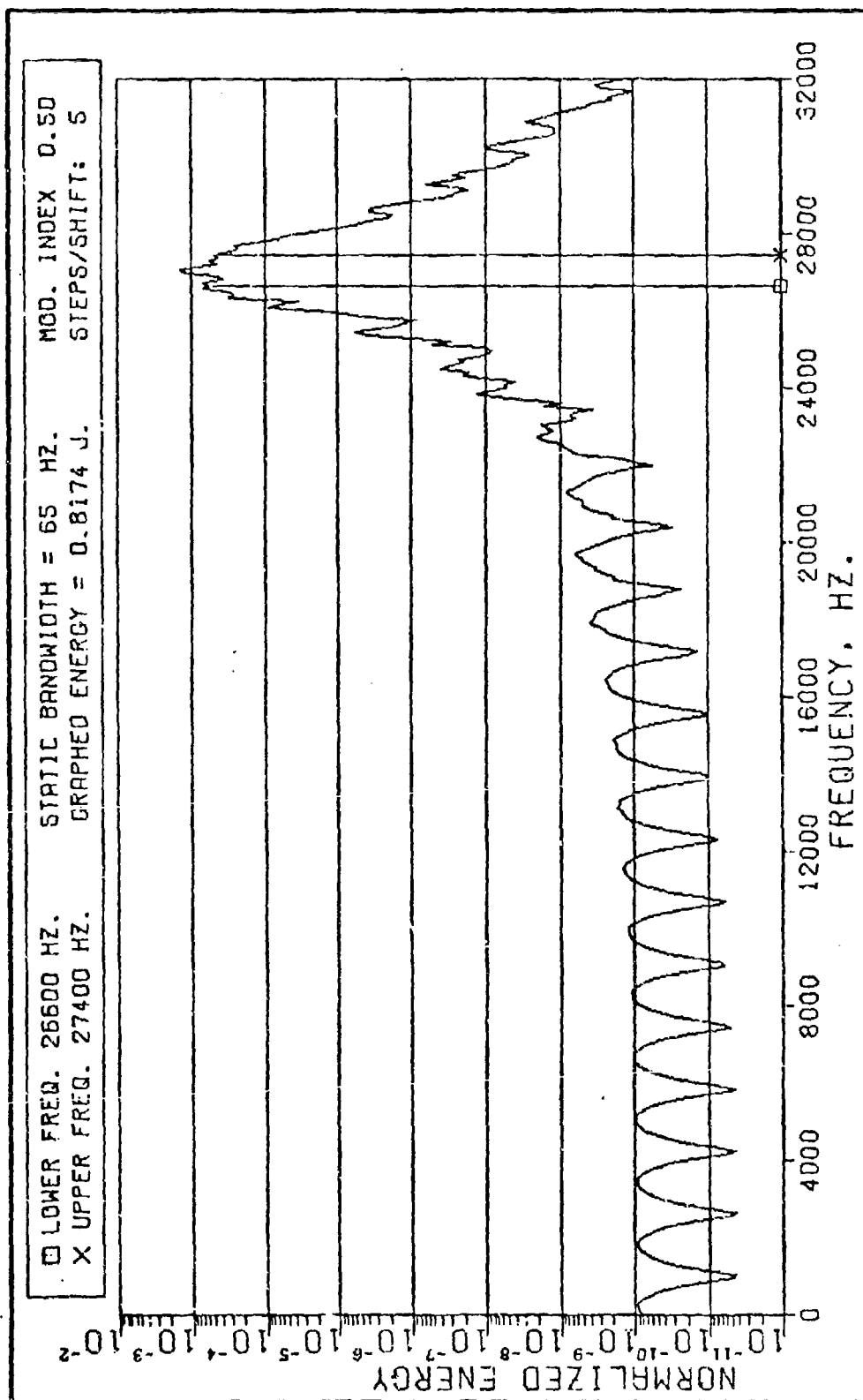


Fig. 20. Low-Band Spectra for Steps = 5.

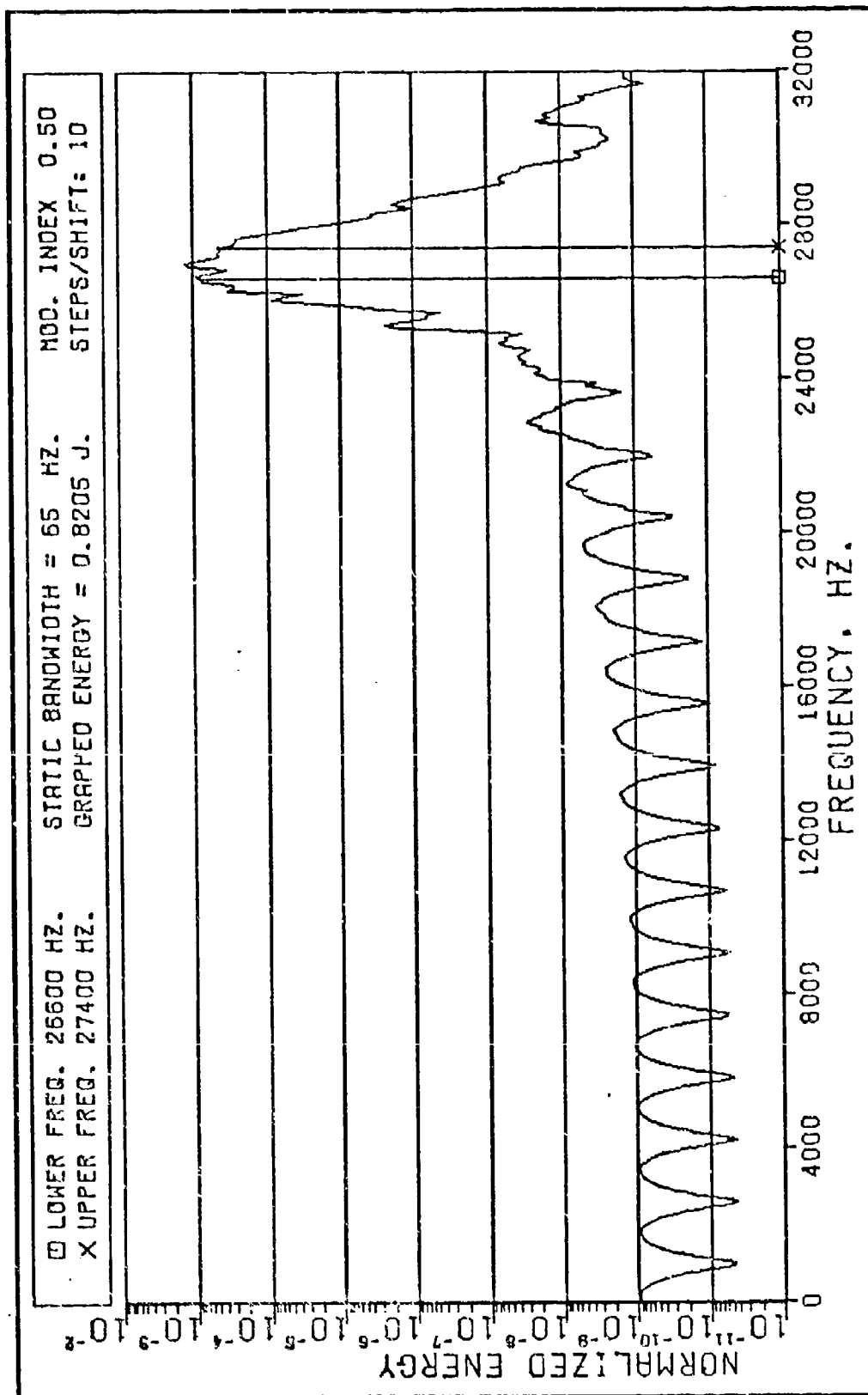


Fig. 21. Low-Band Spectra for Steps = 10.

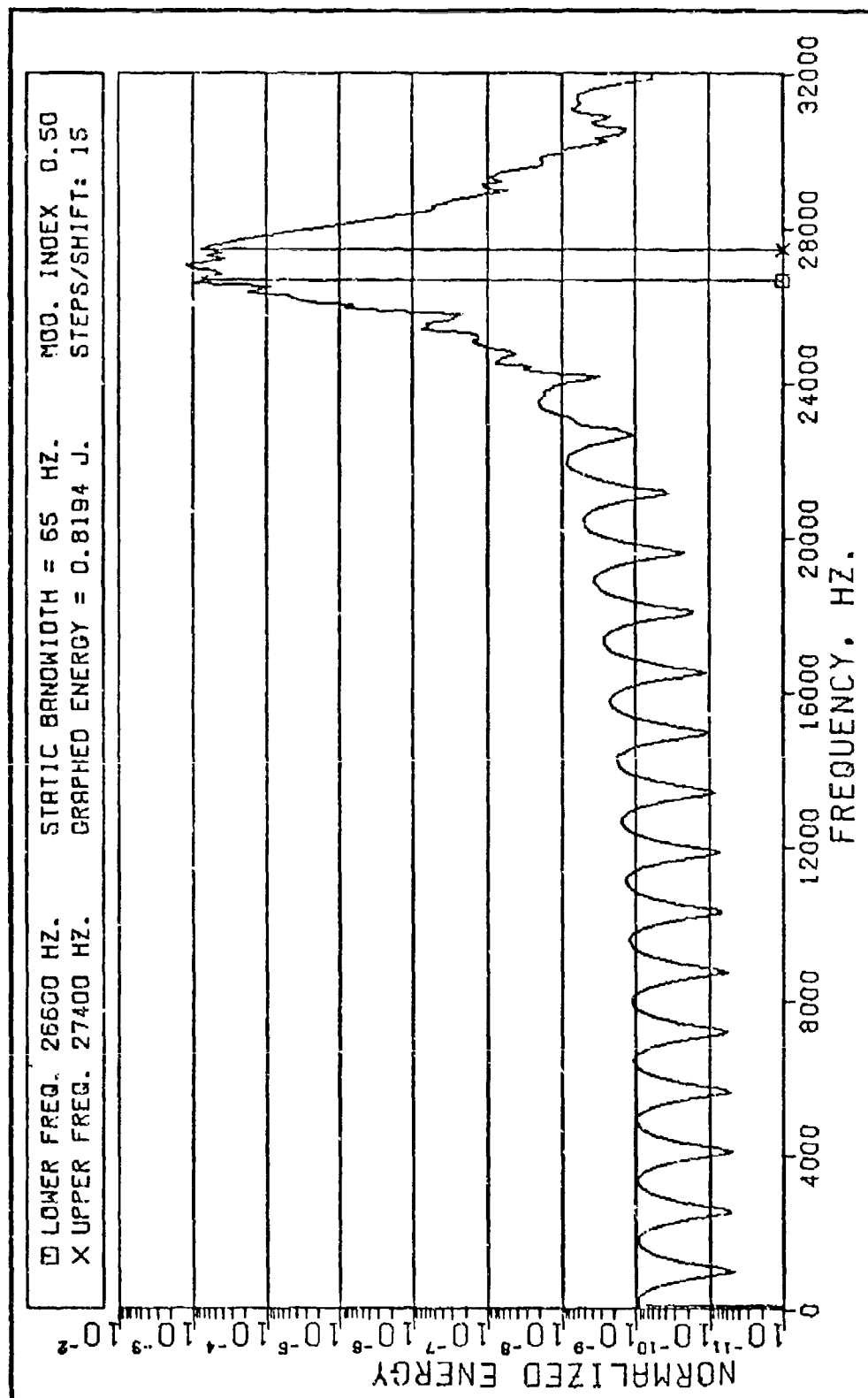


Fig. 22. Low-Band Spectra for Steps = 15.

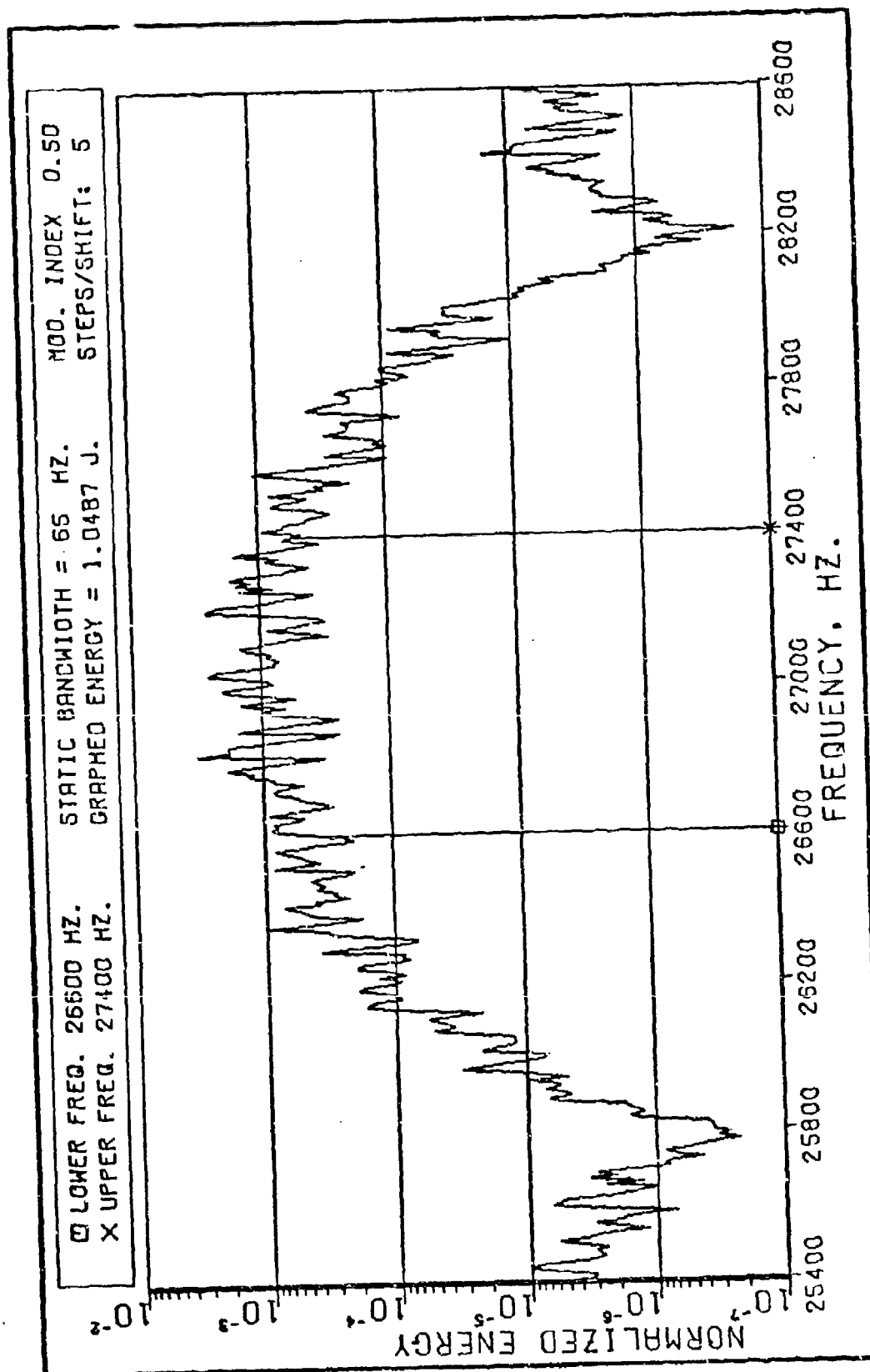


Fig. 23. Mid-Band Spectra for Steps = 5.

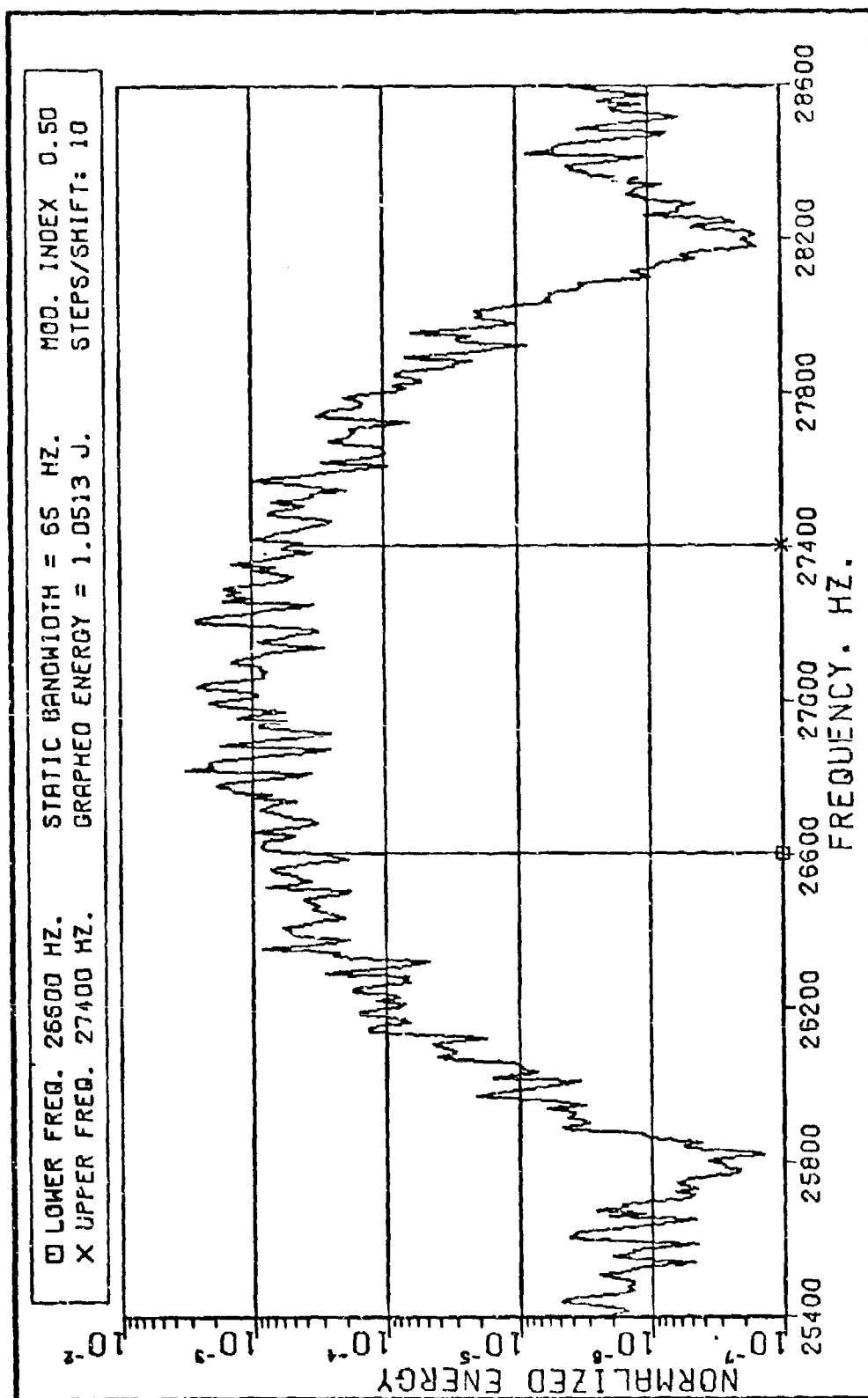
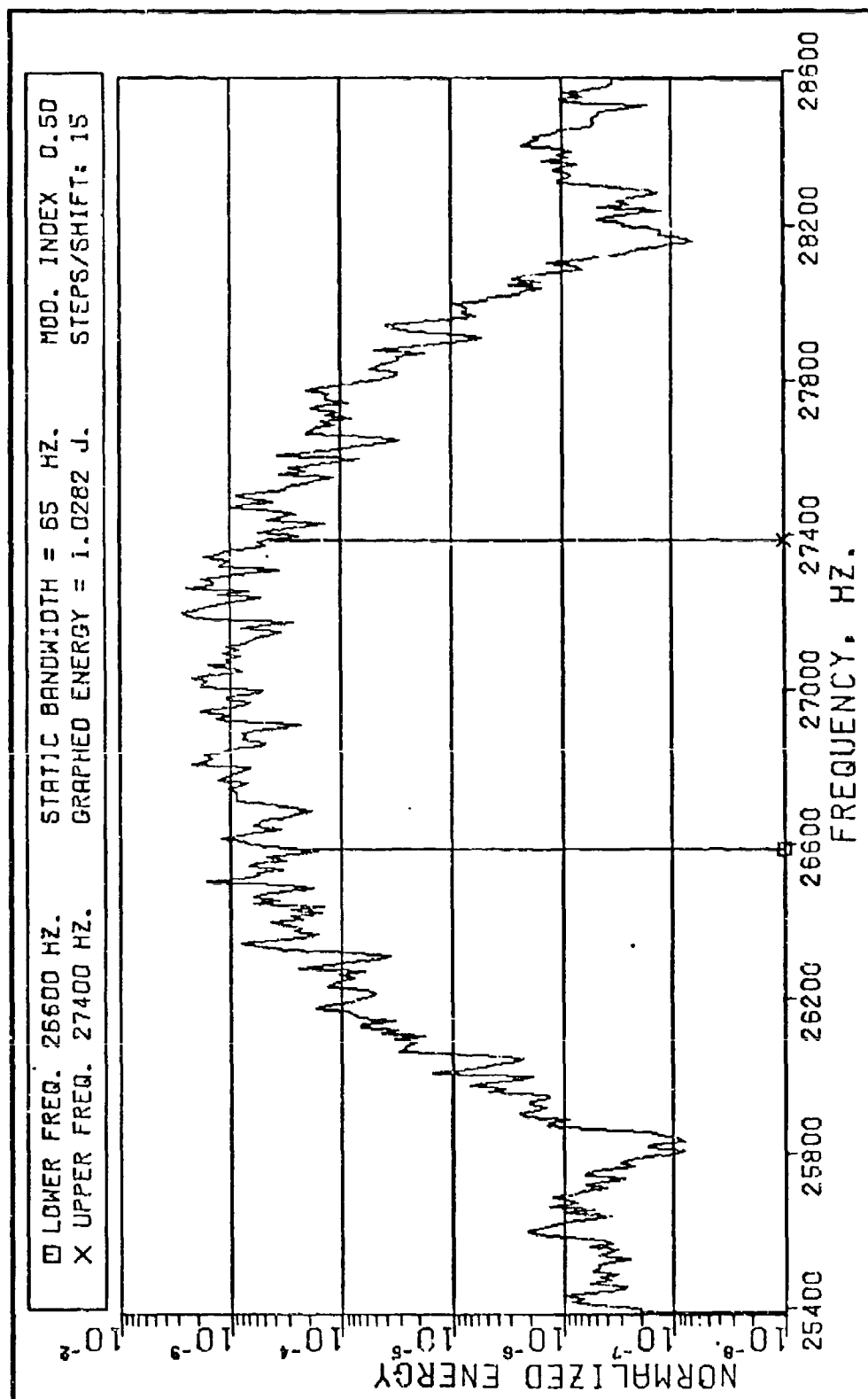


Fig. 24. Mid-Band Spectra for Steps = 10.



F 8. 25. Mid-Band Spectra for Steps = 15.

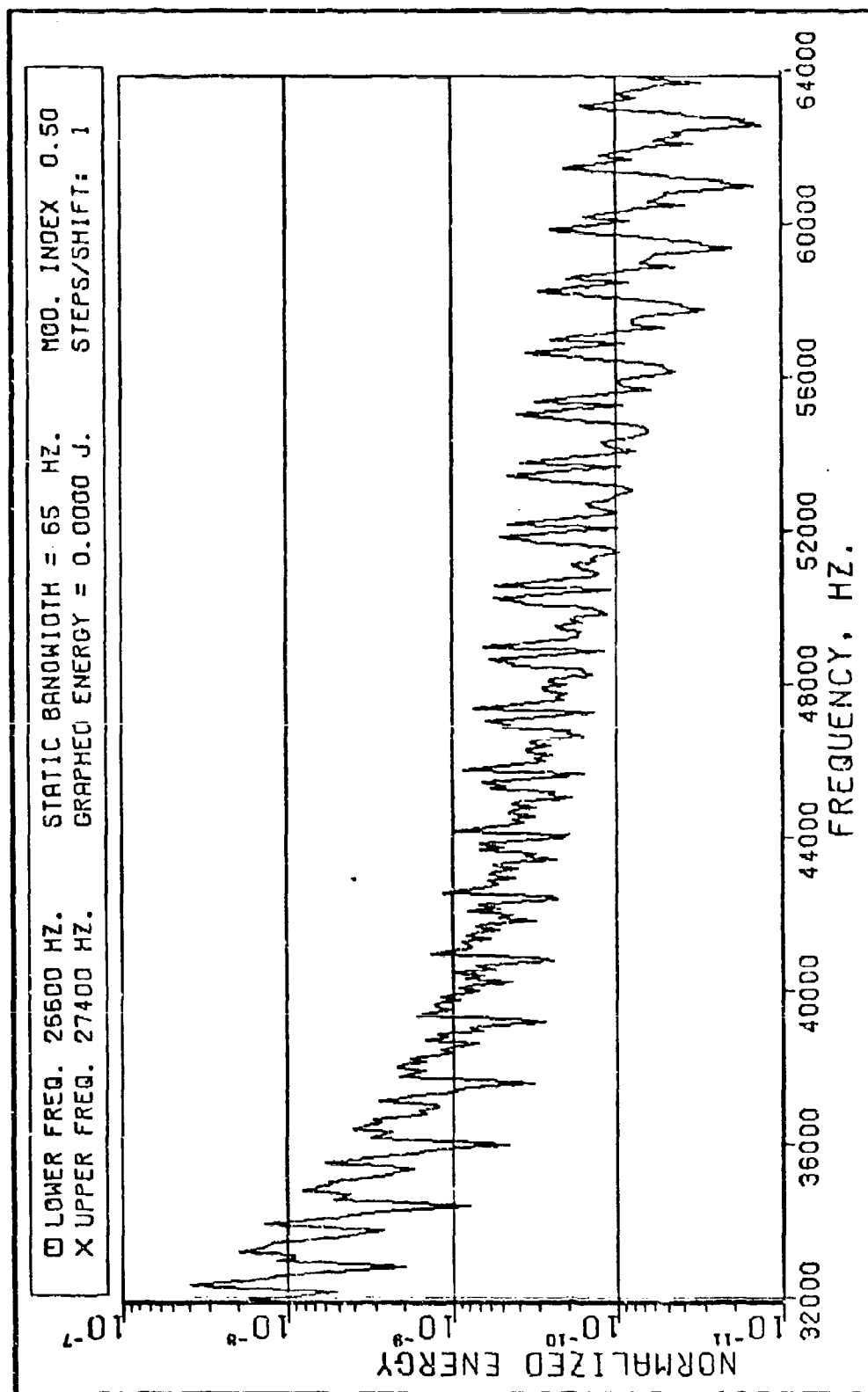


Fig. 26. High-Band Spectra for Steps = 1.

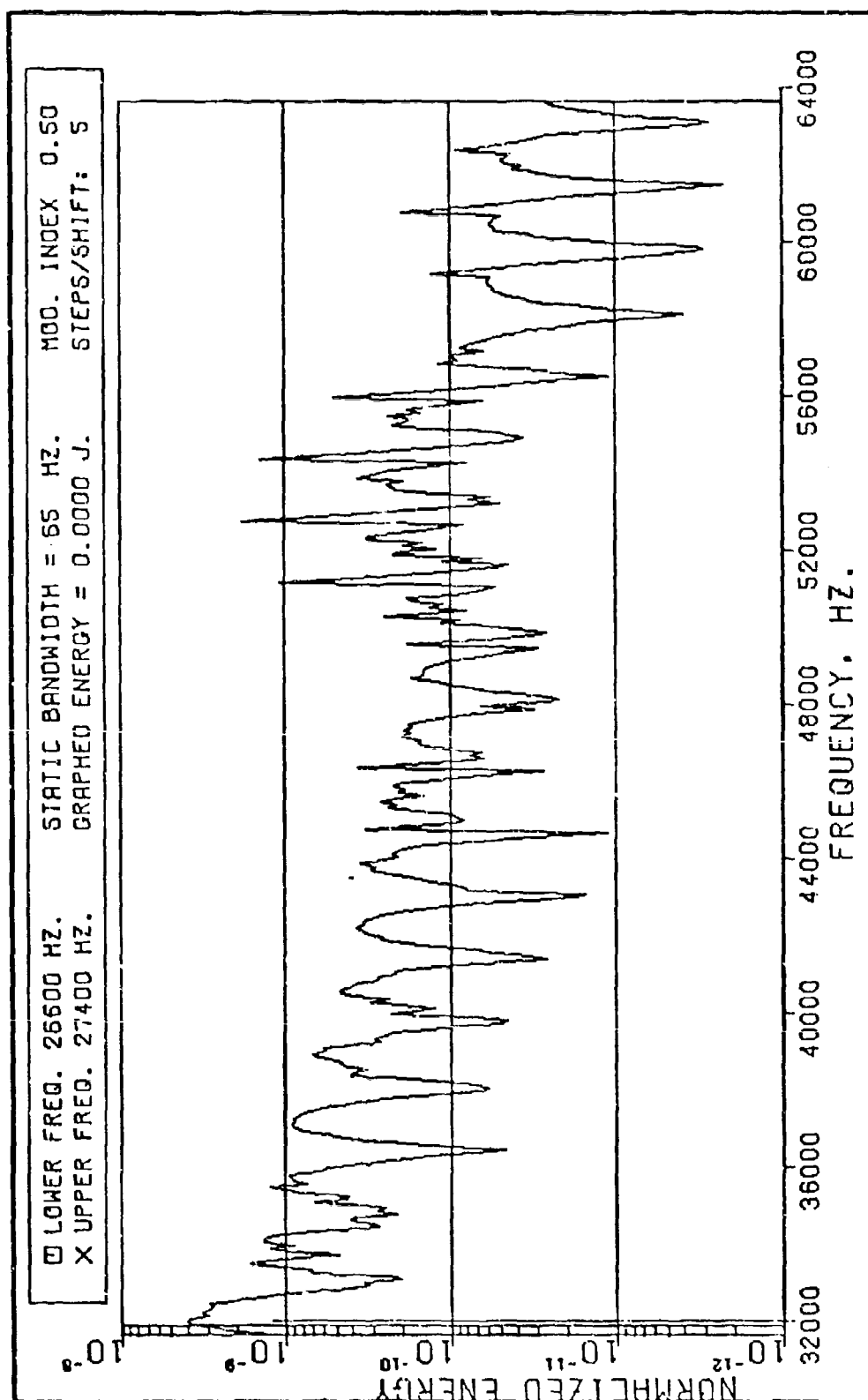


Fig. 27. High-Band Spectra for Steps = 5.

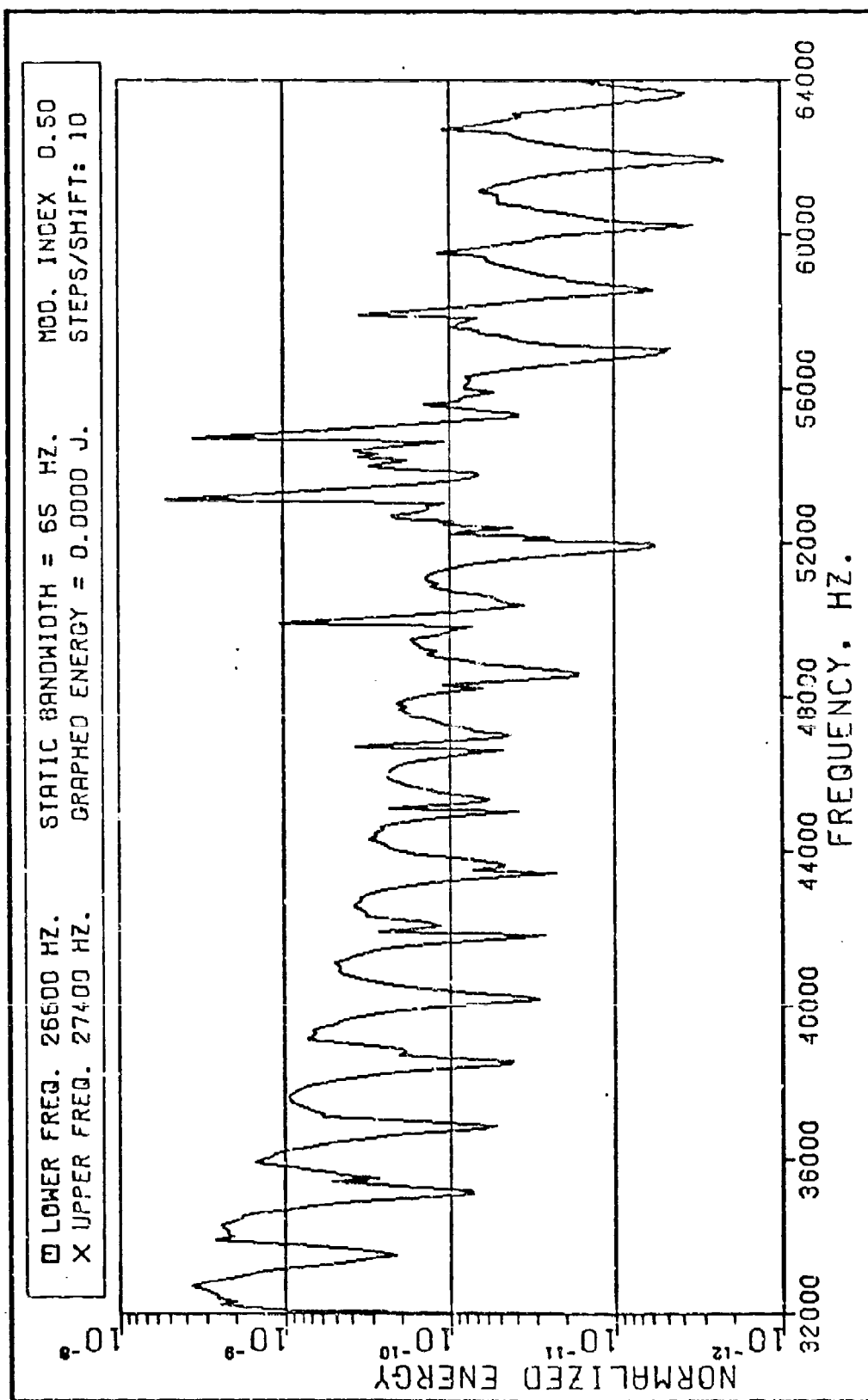


Fig. 28. High-Band Spectra for Steps = 10.

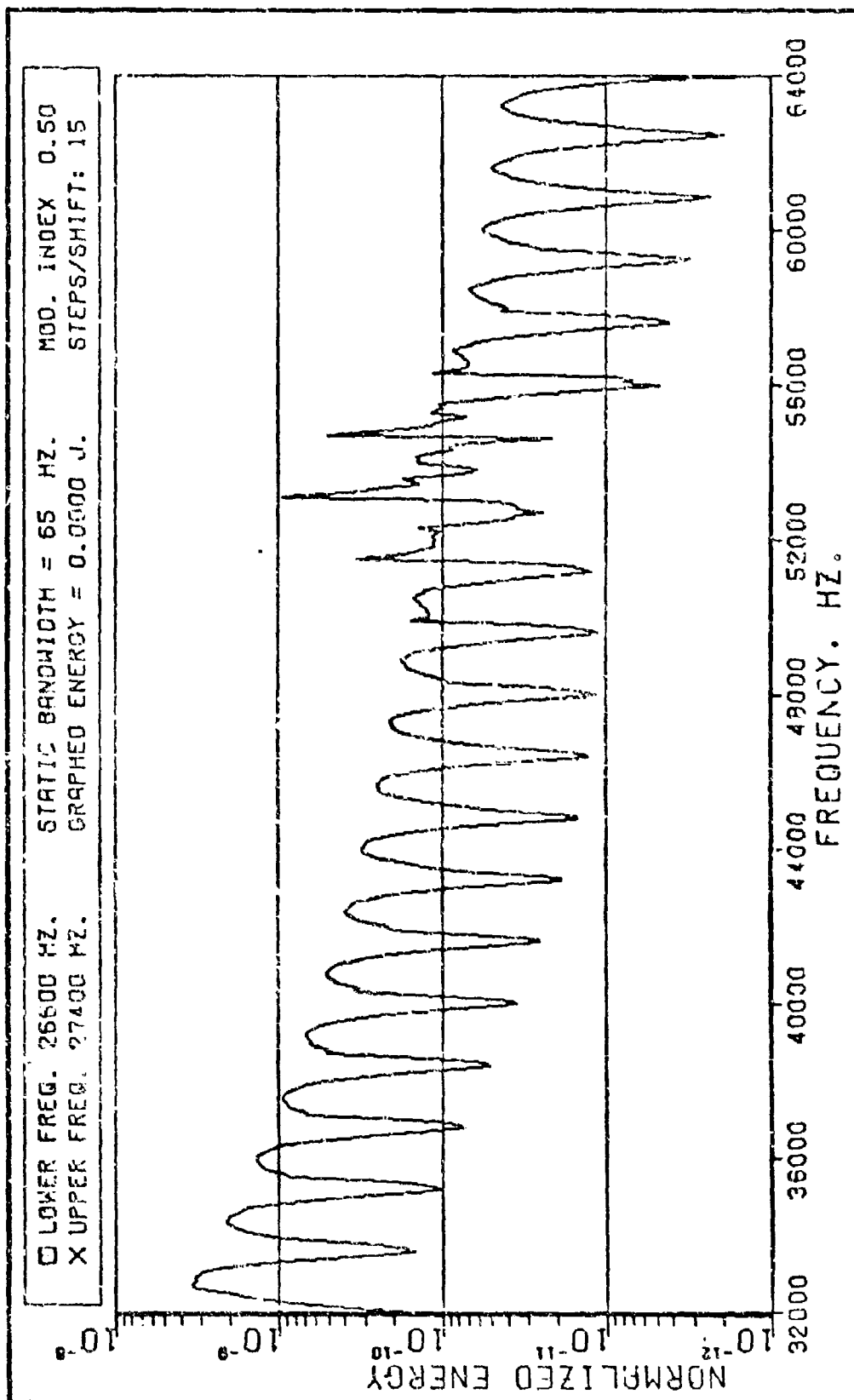


Fig. 29. High-Band Spectra for Steps = 15.

VI. Comparisons

The comparisons are divided into two sections which are the single-step cases and the multi-step cases.

The Single-Step Cases

Figs. 9 through 14 are plots of the spectra for FSK signals in which the baud rate is varied and the modulation index is held constant. Figs. 15 through 17 are plots of FSK spectra wherein the modulation index is varied and the baud rate is held constant. Comparison of the above listed plots with the equations and plots contained in Bennett and Rice's paper (Ref 1:2355-2385) reveals that their analytical expressions (even though for a slightly different FSK antenna current than that for the ETAM synchronous resonant circuit) are quite adequate to express the general characteristics of the spectra for the ETAM circuit for the cases where the frequency shift occurs in one step. Specifically, the main lobe width (for the cases where the modulation index is 0.5) is equal to 1.5 times the baud rate. For example, Fig. 14 is a spectrum plot for a baud rate of 1600, and the center lobe is between 25800 Hz and 28200 Hz. The main lobe width therefore is $2400 \text{ Hz} = (1600) \times (1.5) \text{ Hz}$. In addition, the side lobes each have a width equal to 0.5 times the baud rate; i.e., the sidelobes for the spectrum of Fig. 12 are 400 Hz wide while the baud rate is 800. For comparative

purposes, a plot of Bennett and Rice's equation for FSK spectra with a modulation index = 0.5 is shown in Appendix B.

Figs. 15 through 17 compare closely with Bennett and Rice's figures for modulation indices of 1.0, 2.0, and 3.0. The impulses on the spectra were very narrow in the unsmoothed data, and the smoothing routine caused a slight offset of the frequency marker on the figures in this thesis.

The Multi-Step Cases

In order to evaluate the plots of Figs. 19 through 29, an additional series of plots was prepared on which the differences of the spectra for two plots were compared in decibels. The spectrum for the dividend was the case for Steps = 1, and the divisor spectrum was one of the cases for Steps = 5, 10 or 15. At a specific frequency, if the spectra for the divisor was less than the spectra for the dividend, then the quotient expressed in dB was positive. Therefore, on Figs. 30 through 38, if the spectra ratio in dB is positive, then the value of the energy density spectrum for the multi-step case is lower. For example, Fig. 30 (the low-band (0 - 32000 Hz) comparison of the Steps = 1 case to the Steps = 5 case) shows that at 22000 Hz the Steps = 5 spectrum is approximately 12 dB lower than the Steps = 1 spectrum.

An evaluation of Figs. 30 through 38 with the FSK spectrum in Appendix B reveals four general trends for multi-step frequency switching. The first is that the main

lobe is essentially unchanged, except for the extreme edges where the stepped cases are as much as seven dB lower. Second, the first five sidelobes on each side of the main lobe are reduced between three and thirteen dB for the Steps = 5 case, between six and eighteen dB for the Steps = 10 case, and between nine and eighteen dB for the Steps = 15 case. Third, the sidelobes further removed from the center frequency than the first five sidelobes are, in general, reduced in magnitude by multi-step switching. However, not every sidelobe is reduced and some are actually increased. The increases are indicated by spectra ratios that are negative. Fourth, several sidelobes positioned around the second harmonic of the center frequency are actually increased by ten to eighteen dB through multi-step switching.

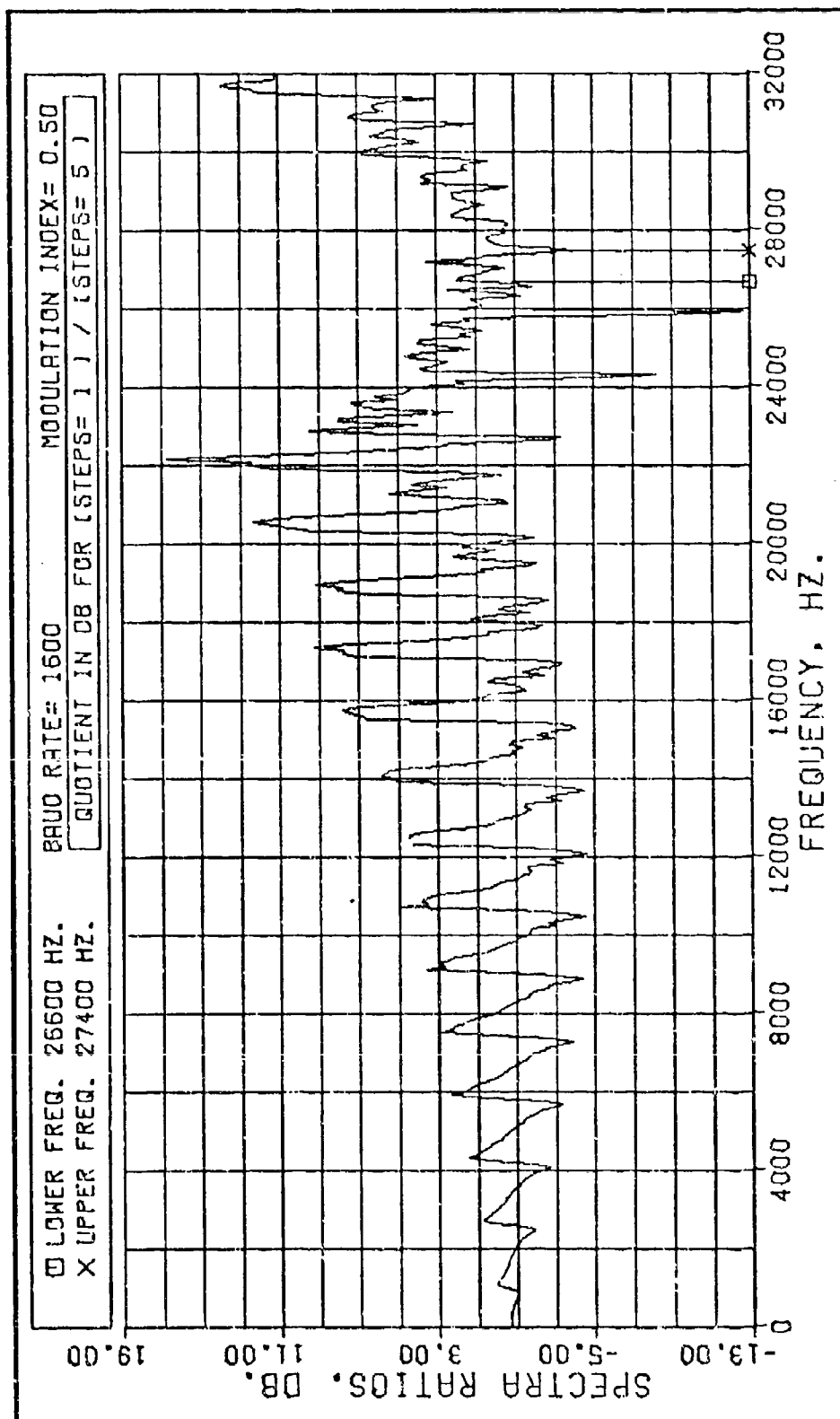


Fig. 30. Low-Band Comparison for Steps = 5.

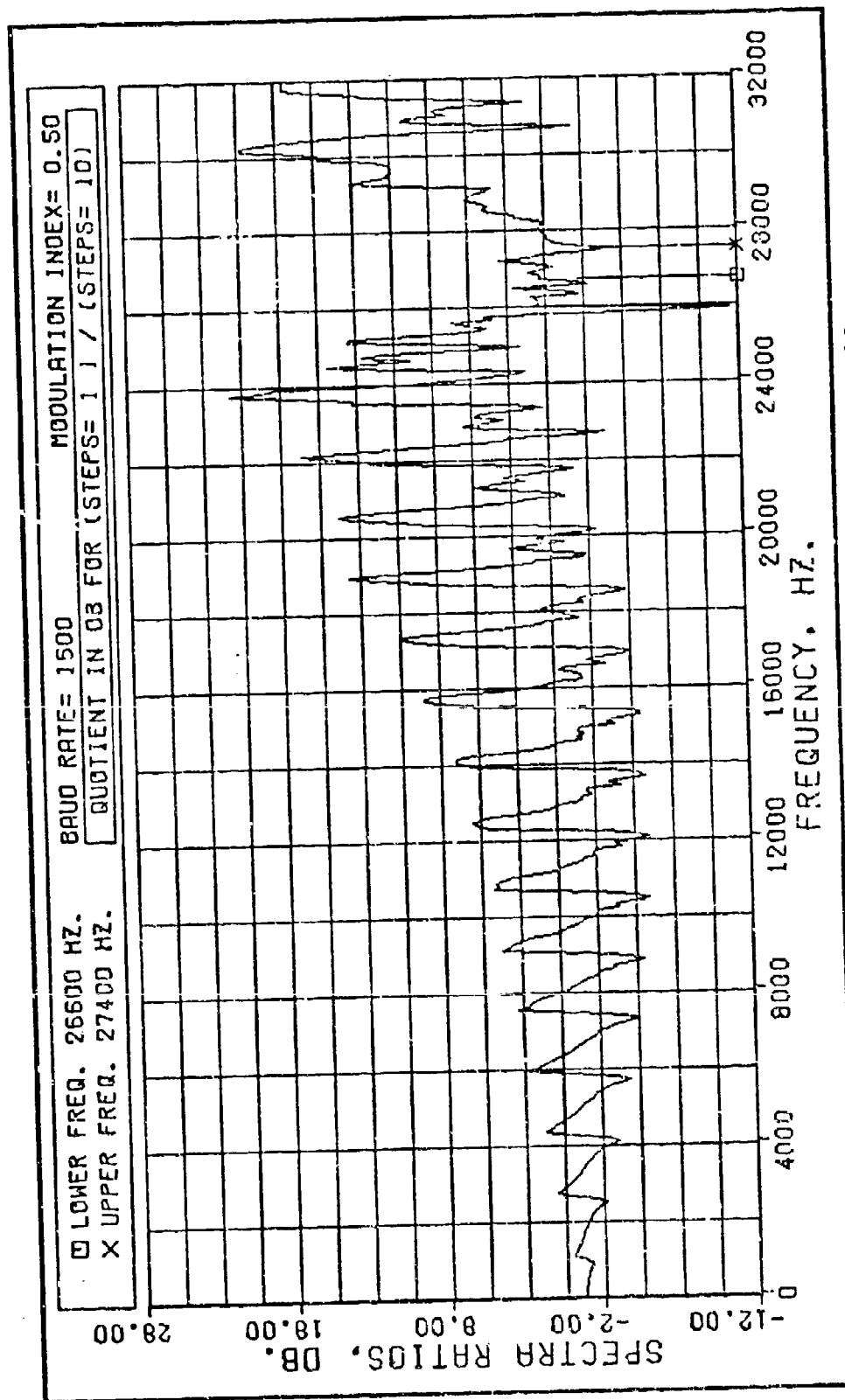


Fig. 31. Low-Band Comparison for Steps = 10.

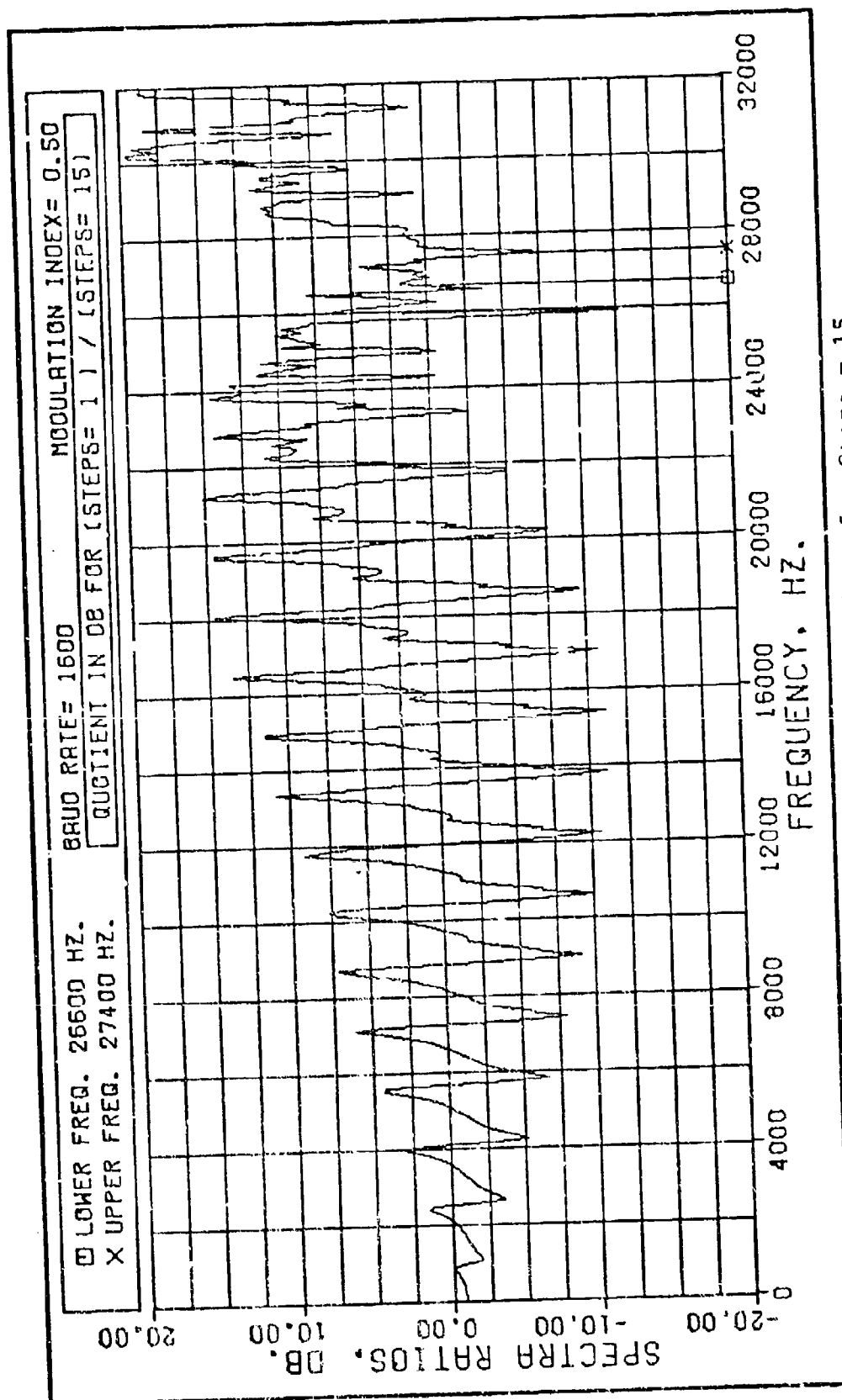


Fig. 32. Low-Band Comparison for Steps = 15.

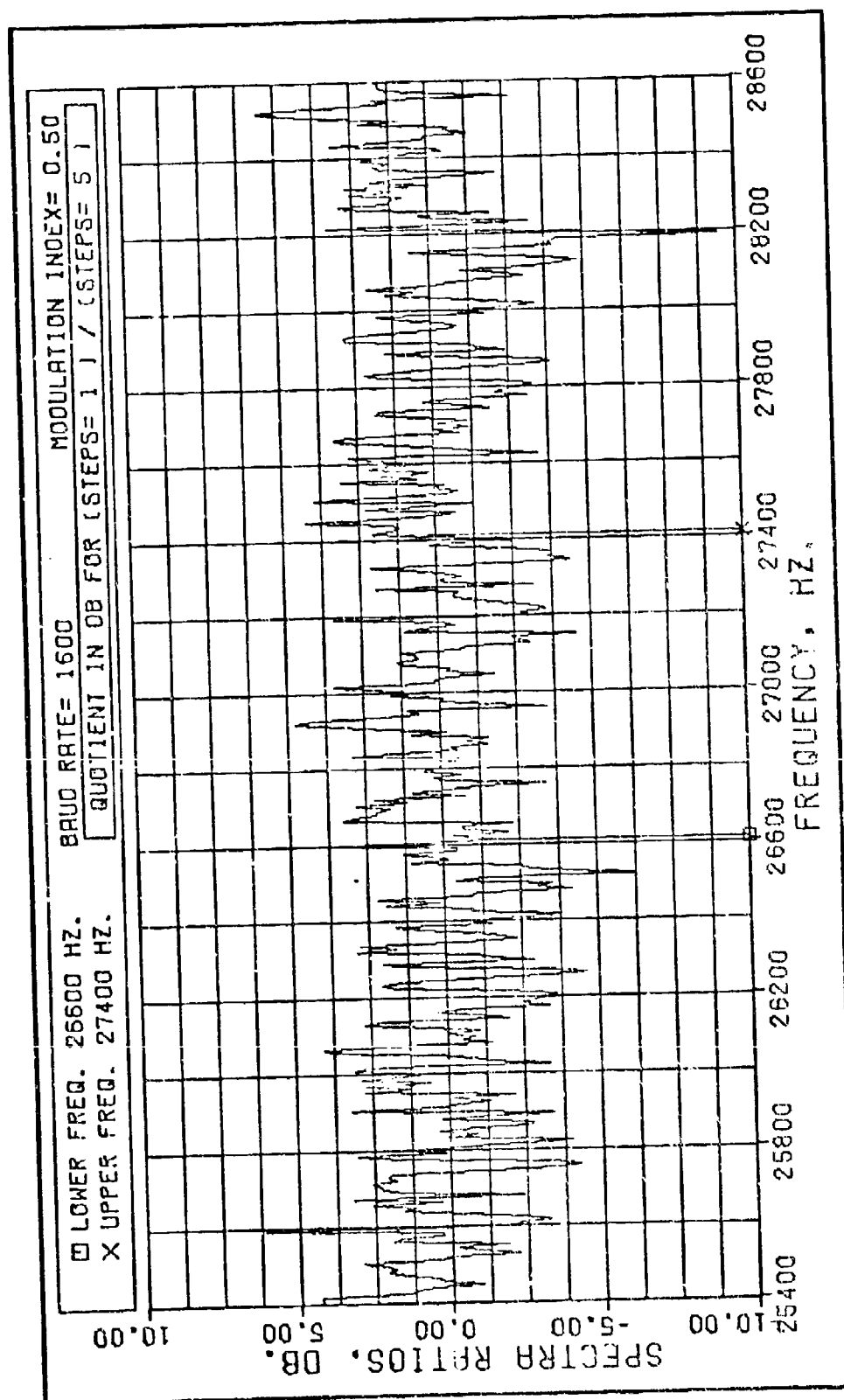


Fig. 33. Mid-Band Comparison for Steps = 5.

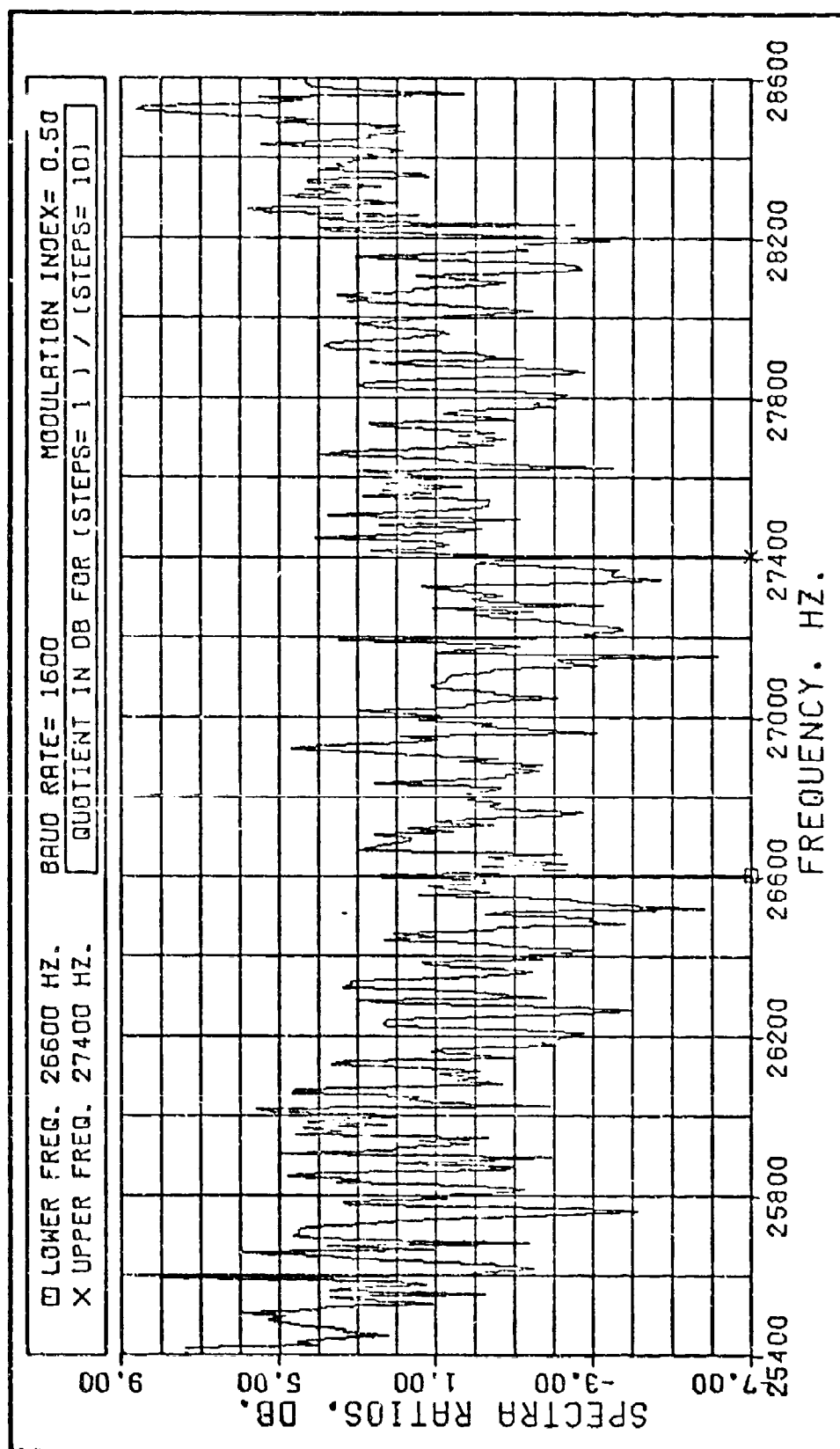


Fig. 34. Mid-Band Comparison for Steps = 10.

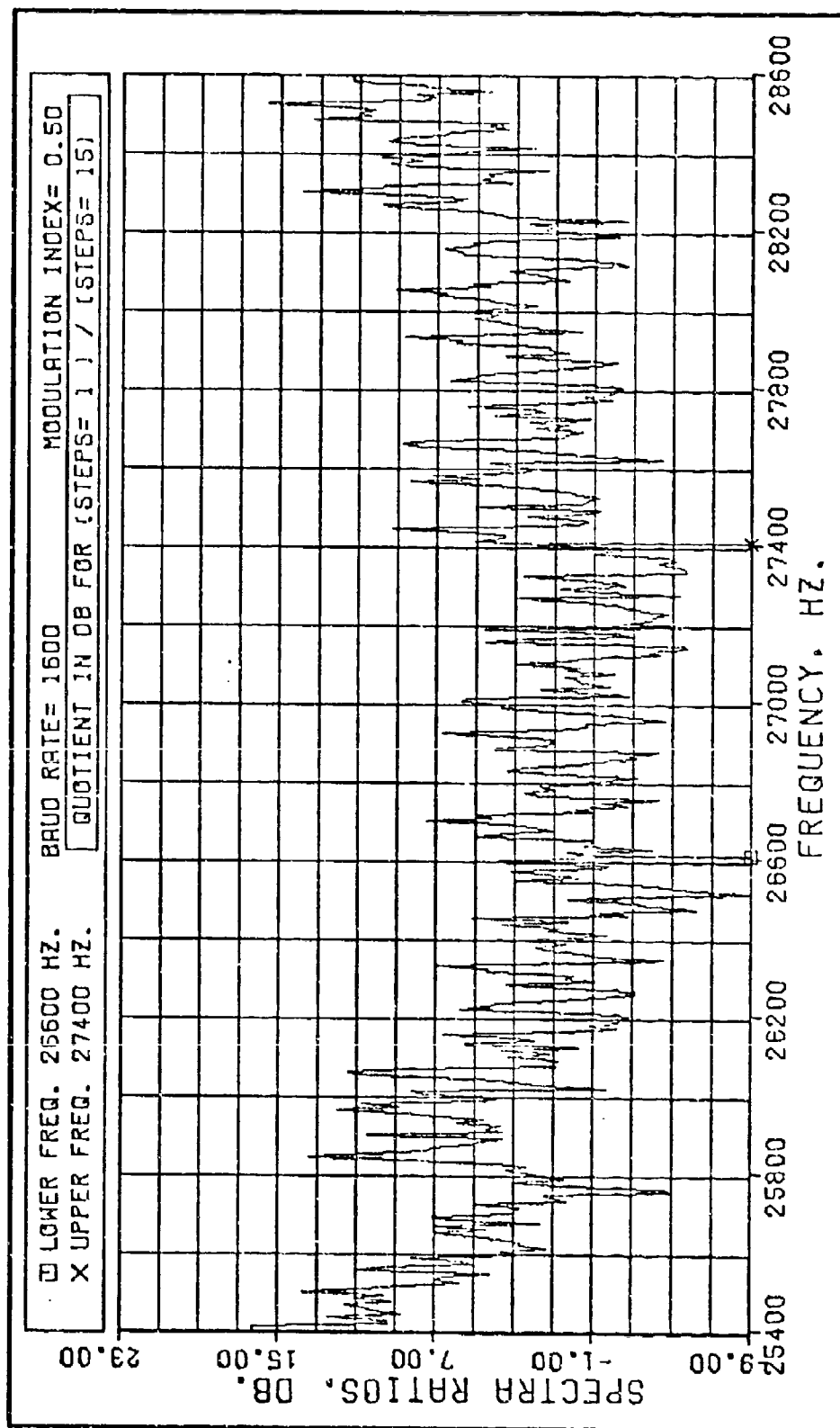


Fig. 35. Mid-Band Comparison for Steps = 15.

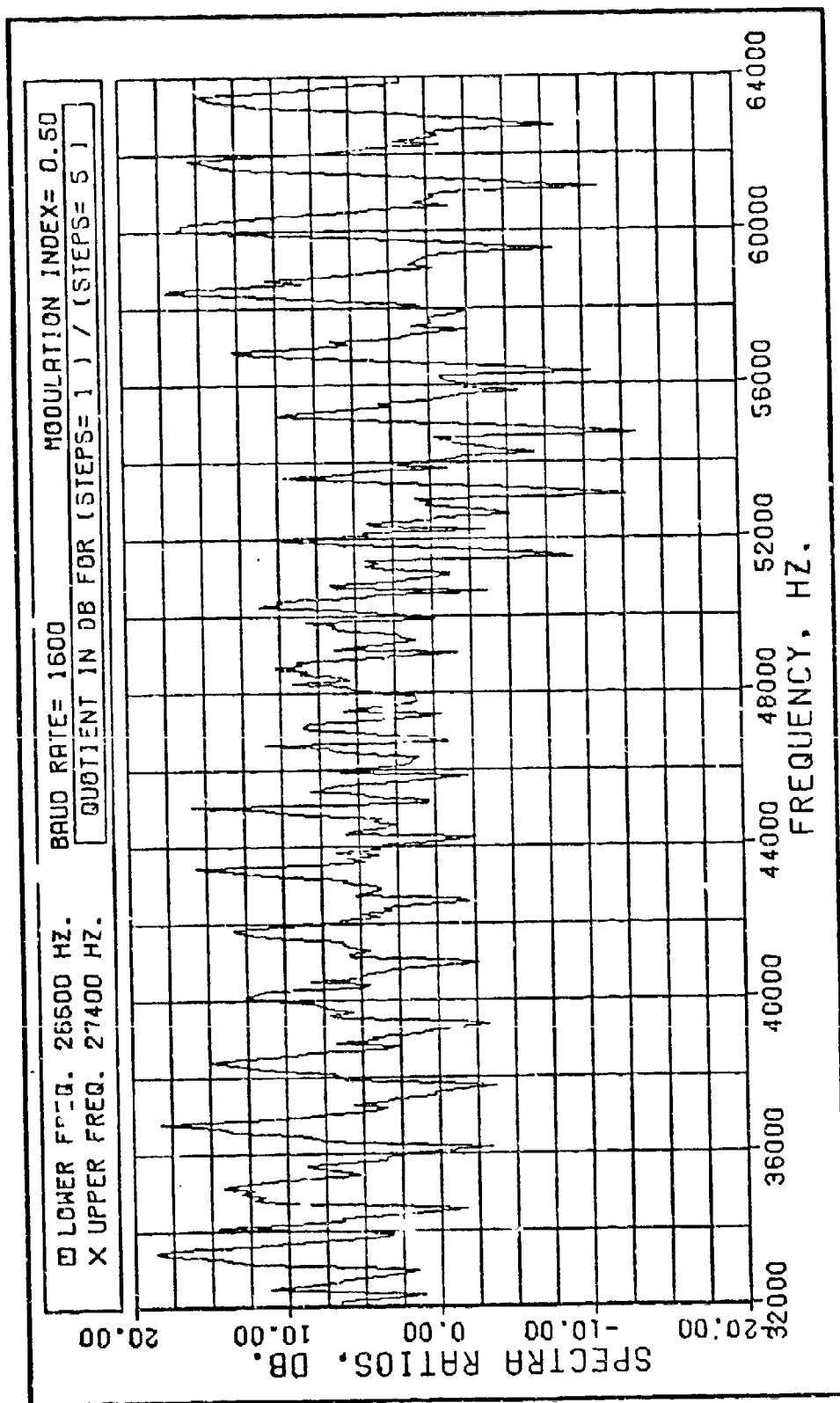


Fig. 36. High-Band Comparison for Steps = 5.

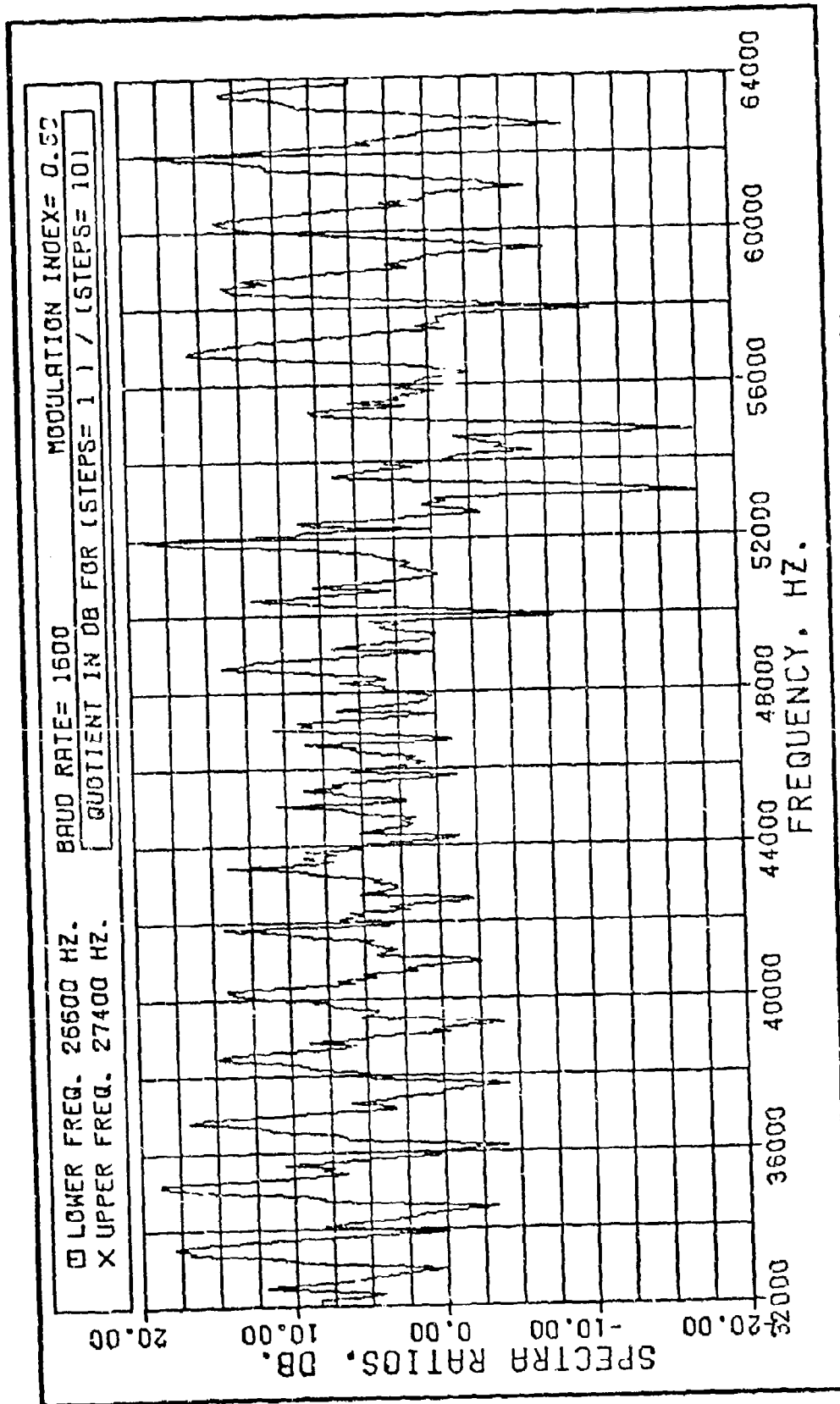


Fig. 37. High-Band Comparison for Steps = 10.

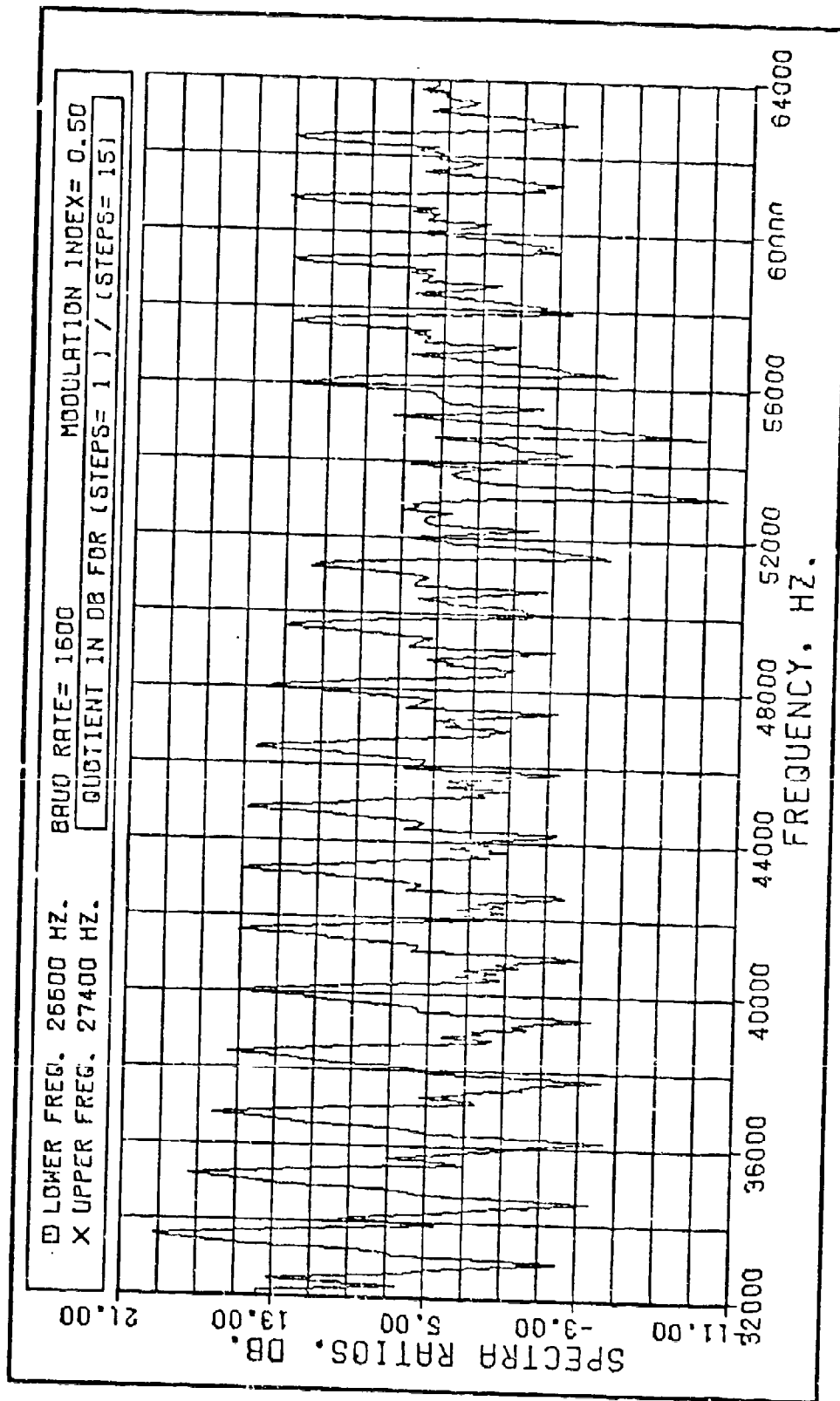


Fig. 38. High-Band Comparison for Steps = 15.

VII. Conclusions and Recommendations

Electronic broadbanding by means of synchronous retuning is the only practical method for transmitting high data rate, frequency shift key signals at very low frequencies. Efficient, high power, high data rate transmissions are not feasible in conventional VLF systems because of a severe transmitter/antenna impedance mismatch and because of prohibitive signal phase distortion. However, because the electronic broadbanding technique shifts the antenna system's resonant frequency in accordance with the transmitted signal, the bandwidth of the transmitted signal will be wider than the system bandwidth for an antenna that is not synchronously retuned. This thesis contains a computer program method for determining the energy spectrum for frequency shift keyed signals transmitted by synchronously resonated VLF antennas.

Conclusions

Single-Step Cases. The approximation for the energy density spectrum of an FSK signal with a modulation index of 0.5 that is transmitted by an electronically broadbanded antenna has shown that the width of the signal's main energy lobe is equal to 1.5 times the baud rate. In addition, the sidelobes each have a width equal to 0.5 times the baud rate. Those spectrum results were determined by an iterative method which used the specific stochastic process for the antenna

VII. Conclusions and Recommendations

Electronic broadbanding by means of synchronous retuning is the only practical method for transmitting high data rate, frequency shift key signals at very low frequencies. Efficient, high power, high data rate transmissions are not feasible in conventional VLF systems because of a severe transmitter/antenna impedance mismatch and because of prohibitive signal phase distortion. However, because the electronic broadbanding technique shifts the antenna system's resonant frequency in accordance with the transmitted signal, the bandwidth of the transmitted signal will be wider than the system bandwidth for an antenna that is not synchronously retuned. This thesis contains a computer program method for determining the energy spectrum for frequency shift keyed signals transmitted by synchronously resonated VLF antennas.

Conclusions

Single-Step Cases. The approximation for the energy density spectrum of an FSK signal with a modulation index of 0.5 that is transmitted by an electronically broadbanded antenna has shown that the width of the signal's main energy lobe is equal to 1.5 times the baud rate. In addition, the sidelobes each have a width equal to 0.5 times the baud rate. Those spectrum results were determined by an iterative method which used the specific stochastic process for the antenna

current of a synchronously resonated VLF antenna, in which a frequency shift could occur only at the instant of an antenna-current zero-crossing. Also, the algorithm included the effects of the current transients caused by an inherent initial condition mismatch.

Bennett and Rice (Ref 1:2384) found an analytic solution for the energy spectrum of a significantly different FSK signal. Their analysis did not include any time delays caused by the antenna-current zero-crossing criteria, nor did their work include the effects of the antenna current switching transients. However, Bennett and Rice's analytic solution gives the same width for the main and side lobes as does the iterative method, and the values of the two spectra are equal within one dB. Bennett and Rice's analytic solution, then, provides a close approximation to the iterative method used for this thesis.

Multi-Step Cases. All frequency shifts for the single-step cases were essentially instantaneous. The multi-step cases were devised to determine what spectrum changes would occur if the complete frequency shift occupied a finite time period. The program was modified to approximate a linear FM frequency shift by simulating the transmission of a series of single cycles at incrementally changing frequencies in order to reach a different FSK frequency. The frequency shift increment for each single cycle was the same, so that the frequency of the last incremental change was the terminal frequency for that shift. For example, a

Steps = 3 shift completed one cycle at the original frequency plus $1/3$ of the total shift, then one cycle was completed at the original frequency plus $2/3$ of the total shift, and then the final frequency was reached. The spectrum for a hypothetical 27000 Hz center frequency antenna which used synchronous retuning to transmit FSK data at 1600 baud was calculated for Steps = 5, 10, and 15. The results are that the main lobe is essentially unchanged, but the first five sidelobes on each side of the main lobe are reduced between three and thirteen dB for the Steps = 5 case, between six and eighteen dB for the Steps = 10 case, and between nine and eighteen dB for the Steps = 15 case. The other sidelobes are generally decreased by multi-step switching, although there is an increase in the spectra for all the multi-step cases near the second harmonic of the center frequency (54000 Hz). The first sidelobes on either side of 54000 Hz were increased between 13 and 20 dB.

Recommendations

Examination of the conclusions and criteria for this thesis brings forth two recommendations. The first is that the detectability of the signal for the multi-step cases should be investigated. Even though there are significant improvements in the transmitted spectrum for a multi-step case, the approximated linear FM in that signal may degrade its detectability by standard receivers. Second, the portion of the program which generates the linear frequency shifts could be modified to approximate a different shift

pattern so that further improvements in the energy density spectrum could be investigated. Specifically, the sidelobes near the second harmonic could possibly be reduced by a different FM pattern.

Bibliography

1. Bennett, W. R., and S. O. Rice. "Spectral Density and Autocorrelation Functions Associated with Binary Frequency-Shift Keying." The Bell System Technical Journal, 2355-2385 (September 1963).
2. Galejs, Janis. "Electronic Broadbanding of High-Q Tuned Circuits or Antennas." Archiv der Elektrischen Übertragung, 17, Part 8:375-380 (1963).
3. Gamble, John T. Wideband Coherent Communication at VLF with the Experimental Transmitting Antenna Modulator (ETAM). Unpublished Technical Report. Griffiss Air Force Base, New York: Rome Air Development Center, Laboratory Director's Fund Project # 01710108 (July 1973).
4. Hartley, H. F. "Electronic Broad Banding of VLF/LF Antennas for FSK Radio Communication." IEEE Transactions on Communication Technology, 19, #4:555-560 (August 1971).
5. Jones, Martin L., and Harry F. Hartley. Experimental Transmitting Antenna Modulator. RADC-TR-72-212. Griffiss Air Force Base, New York: Rome Air Development Center, Air Force Systems Command.
6. Lathi, B. P. Communication Systems. New York: John Wiley & Sons, Inc. (1968).
7. Ramo, S., J. R. Whinnery, and T. Van Duzer. Fields and Waves in Communications Electronics. New York: John Wiley and Sons, Inc. (1965).
8. Watt, A. D. VLF Radio Engineering. New York: Pergamon (1967).

Appendix A

Computer Programs

The main computer program written for this thesis is listed on the following pages. The program is written in Extended FORTRAN for the CDC 6600 computer, hence, some of the Input/Output format statements may not work on all machines capable of compiling a FORTRAN program. The type of data cards required are defined on Comment cards within the listing. An example set of data cards is shown at the end of this Appendix.

The product of this program is two arrays, one for a set of frequency points and one for the corresponding set of energy density spectrum values for the data stream fed in as data, or as generated from a random number function. The author did not include an output format, but the place to insert a standard textbook variety format was noted in the listing. The author used an array only for testing of the routine, then later, he used a Call statement to a subroutine for creating a machine plot from these arrays.

The main portion of the smoothing routine for the plotting program is included before the data card examples. The spectrum array points are very jagged and a smoothing routine is necessary for a machine plot or for a set of points which can be manually plotted. The data cards shown for the program contain the parameters for the smoothing

routine, hence, the parameters are available for the smoothing routine whether it is used in the main program or in a plotting subroutine.

```

PROGRAM POINTS (INPUT,OUTPUT,TAPE5=INPUT,TAPE6=OUTPUT,
1FLCT,PUNCH,TAPE3,TAPE4)

C
C   ARRAYS REA, CLX, JOULES, AND RATIO MUST HAVE THE SAME LENGTH
C   IN THIS PROGRAM AND IN THE SUBROUTINE SPECTRA.
C
COMMON REA(2003), CLX(2003), ENERGY
DIMENSION JOULES(2003), RATIO(2003)
DIMENSION GAM1(1), GA10(1), STREAM(1000)
EQUIVALENCE (REA(1), JOULES(1)), (CLX(1), RATIO(1))

C
INTEGER BIT,ZERCES,CNES,BITO,STREAM
REAL JOULES
PI2 = 2.*3.1415926535

C
C   INITIALIZE INTERNAL VALUES BEFORE PARAMETER CARD IS READ
608 J = 0
   ETIME = 0.
   TELLAY = 0
   LAST2 = 0
   LAST3 = 0
   ZERCES = 0
   CNES = 0
   J1 = 0
   K = 1
   ENERGY = 0.

C
READ 200, FHIGH, FLOW, AMARK, ASPACE, EALC, FMIN, FMAX, GAMMA,
1RMARK, RSPACE, A, STEPS, PLOT, PRIN, SMOOTH, DEL, ERROR, RANDOM,
2SMCTOP

C
C   THE PARAMETERS ARE DEFINED BELOW.
C
C   FHIGH IS THE HIGHER TRANSMITTED FREQUENCY
C   FLOW IS THE LOWER TRANSMITTED FREQUENCY
C   AMARK IS THE ALPHA PARAMETER FOR THE HIGHER FREQUENCY
C   WHICH IS ARBITRARILY CHOSEN TO BE TRANSMITTED WHEN A
C   BINARY ONE IS READ IN THE BIT STREAM.
C
C   ASPLC IS THE ALPHA PARAMETER FOR THE LOWER FREQUENCY.
C   EALC IS THE PAUL RATE.
C   FMIN IS THE LOWER EDGE FREQUENCY OF THE SPECTRUM WINDOW.
C   FMAX IS THE UPPER EDGE FREQUENCY OF THE SPECTRUM WINDOW.
C
C   GAMMA IS THE INITIAL ERROR FRACTION.
C   RMARK IS THE TOTAL RESISTANCE FOR THE HIGHER FREQUENCY.
C   RSPACE IS THE TOTAL RESISTANCE FOR THE LOWER FREQUENCY.
C   A IS THE TRANSMITTER VOLTAGE AMPLITUDE, USUALLY 1.0
C
C   STEPS IS THE NUMBER OF FREQUENCY CHANGES TO COMPLETE A
C   SWITCH BETWEEN FHIGH AND FLOW.
C   PLOT = 1 ENABLES A PLOTTING SUBROUTINE, PLOT = 0 SKIPS IT.
C   PRIN = 1 ENABLES PRINTING OF PARAMETERS FOR SUBROUTINE
C   SPECTRA ON EACH CALL TO IT. BE AWARE OF THE

```

```

C      VOLUME OF DATA WHICH MAY BE PRINTED.  IF PRIN = 0,
C      THEN THE PRINTED OUTPUT IS OMITTED.
C
C      SMOOTH = 1 ENABLES SMOOTHING IN THE PLOTTING ROUTINE.
C      DEL INVERSE IS THE LENGTH OF THE SMOOTHING BAR.
C      FRCF = 1 ENABLES ERROR FRACTION CALCULATION FOR EACH
C      CALL TO SPECTRA.  ERROR = 0 SETS GAMMA TO ZERO.
C
C      RANDOM = 1 ENABLES GENERATION OF A RANDOM BIT STREAM BY
C      CALLS TO THE RANDOM NUMBER GENERATOR.  RANDOM = 0
C      CAUSES THE BIT STREAM TO BE READ FROM CARDS.
C      SPECTOP = 1 CAUSES THE SMOOTHING ROUTINE TO WORK ON ALL
C      THE SPECTRAL DATA.  SPECTOP = 0 CAUSES THE SMOOTHING
C      ROUTINE TO SMOOTH THE VALLIES AND IGNORE THE PEAKS.
C
C      * * * * *
C
C      THE END-OF-FILE FLAG FOR TAPE (5) IS SET TO ONE IF THERE IS
C      NO DATA IN THE INPUT FILE.
C      IF (EOF(5).NE.0) STOP
C
C      READ 201, L,LS
C
C      L IS THE NUMBER OF POINTS BETWEEN FMIN AND FMAX AT
C      WHICH THE SPECTRUM IS CALCULATED.  L MUST NOT BE LARGER
C      THAN THE DIMENSION OF THE ARRAY PEA.
C      LS IS THE LENGTH OF THE BIT STREAM.  LS MUST NOT BE GREATER
C      THAN THE DIMENSION OF THE ARRAY STREAM.
C
200  FORMAT(F15.0)
201  FORMAT(I5)
C
C      ESTABLISHES Radian AND FREQUENCY PARAMETER SET.
C      WMARK = PI2*FHIGH
C      WSPACE = PI2*FLOW
C      WMEAN = (WMARK + WSPACE)/2.
C      RMIN = (FMIN/WMEAN)*PI2
C      RMAX = (FMAX/WMEAN)*PI2
C      WMIN = RMIN*WMEAN
C      WMAX = RMAX*WMEAN
C      WDELTA = (WMAX-WMIN) / (L-1)
C      FMEAN = WMEAN/PI2
C      FMIN = WMIN/PI2
C      FMAX = WMAX / PI2
C      FDELTA = WDELTA / PI2
C
C      RMARK AND AMARK ARE CALCULATED INSTEAD OF FIXED BY WHAT
C      WAS READ IN PREVIOUSLY.
C      RMARK=RSRACE*(1.+(FHIGH-LOW)/(2.*ASPACE/PI2)*.015)
C      AMARK=(PI2/2.)*((WMARK**2)*RMARK*(2*ASPACE/PI2))/(WSPACE
1**2)*RSRACE)
C
C      CLEARS ARRAYS PEA AND CLX
C      DO 502 M=1,L

```

```

      FEA(MM) = 0.
502  CLY(MM) = 0.
C
C      PRINTS OUT THE PARAMETERS THAT WERE READ IN.
      PRINT 406
406  FORMAT(141)
      PRINT 402, FHIGH, AMARK, RMARK, FLOW, ASFACE, RSFACE,
1EALC, FMAX, GAMMA, A, L, FMIN, WMIN, WMAX, WDELTA
402  FORMAT(14, T20, *THE PARAMETERS READ IN WERE*//
1T20, *FHIGH*, T40, *AMARK*, T60, *RMARK*/
2T19, 3(1PE13.6, 7X), //
3T20, *FLOW*, T40, *ASFACE*, T60, *RSFACE*/
4T19, 3(1PE13.6, 7X), //
5T20, *BAUD*, T40, *FMAX*, T60, *GAMMA*/
6T19, 3(1PE13.6, 7X), //
7T20, *AMPLITUDE*, T40, *ARRAY LENGTH*, T60, *FMIN*/
8T19, 1PE13.6, T39, I5, T59, 1PE13.6//
9T20, *WMIN*, T40, *WMAX*, T60, *WDELTA*/
AT19, 3(1PE13.6, 7X)////)
C
C      THIS FILLS THE ARRAY STREAM
622  IF (RANDOM.EQ.0.) GO TO 641
      LSM = LS - 1
      DO 507 IA=1, LSM
        FIA = IA
        FCA = RANF(PIA)
        FAN = RANF(POA)
        STREAM(IA) = 1
        IF (RAN.LE.0.5) STREAM(IA) = 0
507  CONTINUE
      STREAM(LS) = 3
      GO TO 642
C
641  FEAD 202, (STREAM(IK), IK = 1, LS)
202  FORMAT (72I1)
      IF (EOF(5).NE.0) STOP
C
642  IF (FPIV.EQ.0.) GO TO 507
      PRINT 403
403  FORMAT(140, T5, *STEPS*, T15, *IS*, T25, *WN*,
1T35, *RN*, T45, *AN*, T55, *WX*,
2T65, *RX*, T75, *AX*, T85, *TDELAY*,
3T95, *GNEW*, T105, *ENERGY*, /)
C
C      BEGIN READING AND PROCESSING THE STORED EIT STREAM.
C
C      THE EXAMINATION OF THE STREAM ARRAY.
607  FIT = STREAM(K)
      K = K+1
      IF (FIT.EQ.1) GO TO 610
      IF (FIT.EQ.0) GO TO 613
      IF (FIT.EQ.2) GO TO 606
      IF (FIT.EQ.3) GO TO 603
      GO TO 603

```

```

C
610 CNES = ONES + 1
600 IF (J.EQ.1) GO TO 603
    J = 1
    FITC = BIT
    GO TO 607

C
613 ZERCEES = ZEROES + 1
    GO TO 600

C
603 IF (FIT.EQ.BITC) GO TO 607
    GO TO 604

C
606 LAST2 = 1
    GO TO 604

C
609 LAST3 = 1

C
C      (NEW) VARIABLES ARE FOR SERIES JUST READ IN FROM STREAM
C      (OLD) VARIABLES ARE FOR PREVIOUS SERIES OR FOR SERIES
C      TO BE READ FROM STREAM NEXT.
C
604 IF (FITC.EQ.1) GO TO 611
    FITC = BIT
    FITTIME = ZEROES/BAUD + BITTIME
    ZERCEES = 0
    WNEW = WSPACE
    ANEW = ASPACE
    FNEW = RSPACE
    ACLC = AMARK
    WCLC = WMARK
    FCLC = RMARK
    GO TO 605

C
611 FITTIME = ONES/BAUD + FITTIME
    FITC = BIT
    CNES = 0
    WNEW = WMARK
    ANEW = AMARK
    FNEW = RMARK
    ACLC = ASPACE
    WCLC = WSPACE
    FCLC = RSPACE
    GO TO 605

C
C      J1 = 0 IF THIS IS THE FIRST SERIES TO BE READ FROM STREAM.
C
605 IF (J1.NE.0) GO TO 614
    IF (ERROR.NE.1.) GNEW = 0.
    GO TO 623

614 CNES = GAMMA
    IF (ERROR.NE.1.) GNEW = 0.
    J1 = 1
    GO TO 623

C

```

```

C      BRANCH POINT FOR MULTI-STEP SWITCHING.
623  IF (STEPS.EQ.1) GO TO 633
      ISTEP = STEPS - 1.
      WN = WOLD
      RN = ROLD
      AN = AOLD

C
C      DO 530 IS = 1, ISTEP
C
C      CALCULATE FREQUENCY AND PARAMETERS FOR THIS SINGLE CYCLE AND
C      FOR NEXT SINGLE CYCLE.
C      THIS LOOP INCREMENTS THE PARAMETERS THROUGH
C      (STEPS-1.) CALLS TO SPECTRA FOR THE SINGLE CYCLES.
C
C      THE PARAMETERS FOR THIS SINGLE CYCLE.
      WN = WN + (WNEW-WOLD)/STEPS
      RN = RN + (RNEW-ROLD)/STEPS
      AN = AN + (ANEW-AOLD)/STEPS
C
C      THE PARAMETERS FOR THE NEXT SINGLE CYCLE.
      WX = WN + (WNEW-WOLD)/STEPS
      RX = RN + (RNEW-ROLD)/STEPS
      AX = AN + (ANEW-AOLD)/STEPS
C
C      CALL SPECTRA(AN,WN,1,GNEW,L,TDelay,WMIN,WDELTA,A,RN)
      IF (FRIN.EQ.0.) GO TO 421
      PRINT 410,STEPS,IS,WN,RN,AN,WX,RX,AX,TDelay,GNEW,ENERGY
410  FORMAT(14, 'T3,1PE10.2,2X,I3,5X,1PE10.2)
C
C      CALCULATES GAMMA FOR THE NEXT FREQUENCY.
421  GNEW = ((PX*WX)/(RN*WN)) * (1.+GNEW*EXP((-PI2*AN)/WN)) - 1.
      IF (ERFOR.NE.1.) GNEW = 0.
      TDELAY = TDELAY + PI2/WN
530  CONTINUE
C
C      DETERMINE NUMBER OF CYCLES TO MOVE TDELAY PAST BITTIME.
633  N = 1
      CYCLE = PI2/WNEW
616  IF (N*CYCLE+TDELAY.GE.BITTIME) GO TO 612
      N = N+1
      GO TO 616
C
C      CALCULATION OF LONG SERIES OF CYCLES.
612  IF (STEPS.EQ.1.) GO TO 632
C
C      CALCULATE INCREMENTAL (N) VALUES AND KEEP SAME (X) VALUES.
      WN = WX
      RN = RX
      AN = RX
C
C      THE PARAMETERS THAT WILL BE NEEDED FOR THE NEXT SINGLE CYCLE.
      WX = WNEW-(WNEW-WOLD)/STEPS
      RX = ANEW-(ANEW-AOLD)/STEPS

```

```

      FX = RNEW - (RNEW-RCLO)/STEPS
      GO TO 634
C
632  RX = WOLD
      RY = ROLD
      AX = AOLD
      WY = WNEW
      RN = RNEW
      AN = ANEW
      IS = 0
C
634  CALL SPECTRA(AN,WY,N,GNEW,L,TDELAY,WPIN,WDELTA,A,RN)
      IF (FRIN.EQ.0.) GO TO 635
      PRINT 410,STEPS,IS,WY,RN,AN,WX,RX,AX,TDELAY,GNEW,ENERGY
      IF (STEPS.EQ.1.) GO TO 635
      PRINT 420
420  FORMAT(1H )
635  GNEW = ((RX*WX)/(RN*WY)) * (1.+GNEW*EXP((-PI2*N*AN)/WY)) -1.
      IF (ERROR.NE.1.) GNEW = 0.
      TDELAY = TDELAY + N*PI2/WNEW
C
      IF (LAST2.EQ.1) GO TO 619
      IF (LAST3.EQ.1) GO TO 619
      GO TO 607
C
C      JOULES CONTAINS A NORMALIZED ONE-SIDED ENERGY SPECTRUM
C      THAT IS NORMALIZED TO ONE JOULE UNDER THE CURVE OF
C      JOULES PER UNIT FREQUENCY.
C
619  PRINT 411,ENERGY
411  FORMAT(//,T5,*TOTAL STREAM ENERGY = *,1PE12.4,2X,*
1JOULES.*//)
      DO 504 IJ = 1, L
504  JOULES(IJ) = ((RFA(IJ)**2+CLX(IJ)**2)/ENERGY)**2.
C
C      INTEGRATE THE NORMALIZED ENERGY SPECTRUM.
      AREA = 0.
      LM = L-1
      DO 506 IE = 1,LM
506  AREA = (((JOULES(IE+1)+JOULES(IE))/2.)*WDELTA)/PI2 + AREA
C
      PRINT 412,AREA
412  FORMAT(1H ,T5,*THE ENERGY IN THE NORMALIZED ENERGY BAND
1 IS *,1PE12.4,2X,*JOULES.*//)
C
C      JOULES IS SAVED FOR POSSIBLE PERMANENT STORAGE.
C      THIS STORAGE DEVICE COULD BE A MAGNETIC TAPE OR AN
C      OPERATING-SYSTEM-CONTROLLED PERMANENT DISC FILE.
      EN=2.*ASPACE/PI2
      WRITE(3) L,FLCH,FHIGH,FMEAN,STEPS,LAUC,FMIN,FMAX,
1SPCOTH,DEL,ERROR,LS,GW,SPOTOP,AREA
      WRITE(3) (JOULES(IT), IT = 1,L)
C
      IF (RANDOM1.EQ.0.) GO TO 643

```

```

C      FLUNCHES A SET OF CARDS SO THE RANDOM STREAM CAN BE
C      USED AGAIN.
C
C      FLNCH 422, (STREAM(IC), IC = 1,LS)
422  FORMAT(72I1)
643  KC = K-1
      PRINT 403, (STREAM(IZ), IZ=1,K0)
403  FORMAT(14 , T5, *THE BIT STREAM FOR THIS POWER SPECTRUM *,
1*WAS*// (T5,72I1))
      PRINT 413
413  FORMAT(14-)
C
C      IF (FICT.EQ.0.) GO TO 640
C      THIS FILLS THE ARRAY RATIO WITH FREQUENCY VALUES.
C      DO 505 IL = 1,L
505  RATIO(IL) = (IL-1.)*FOELYA + FMIN
C
C      THIS IS THE PLACE AN ARRAY PRINTING ROUTINE SHOULD
C      BE LOCATED FOR PRINTING THE CONTENTS OF THE ARRAYS
C      COULES AND RATIO ( THE SPECTRUM AND THE FREQUENCY
C      VALUES) THE AUTHOR ALWAYS USED A PLOTTING ROUTINE
C      SO AN ARRAY PLOTTER IS NOT SHOWN, THEY ARE
C      EASILY FOUND IN FORTRAN TEXT BOOKS.
C
C      THIS IS THE CALL TO THE PLOTTING ROUTINE.
      ENERGY = AREA
      CALL PICTURE(L,FLCH,FHIGH,FMEAN,STEPS,BAUC,FMIN,FMAX,SMOOTH,
1CEL,ERROR,LS,PA)
C
C      CLEARS REA AND CLX ARRAYS
640  DO 503 MN = 1,L
      REA(MN) = 0.
503  CLX(MN) = 0.
C
C      RESET INTERNAL VALUES PRIOR TO PROCESSING A NEW STREAM.
      ETIME = 0.
      ENERGY = 0.
      TDELAY = 0
      J1 = 0
      J = 0
      ZERGES = 0
      CNES = 0
      K = 1
C
C      IF THE LAST BIT IN THE STREAM IS A TWO, THEN THE
C      PROGRAM LOOKS FOR ANOTHER BIT STREAM ON CARDS.
C      IF THE LAST BIT IN THE STREAM IS A THREE, THEN THE
C      PROGRAM LOOKS FOR ANOTHER SET OF PARAMETER CARDS AND
C      ANOTHER SET OF BIT STREAM CARDS.
C      IF THERE ARE NO CARDS, THE PROGRAM STOPS.
      IF (LAST2.EQ.1) GO TO 620
      LAST3 = 0
      GO TO 603
620  LAST2 = 0
      GO TO 622

```



```

SUBROUTINE SPECTRA(ANEW,WNEW,N,GOLD,L,TDELAY,
1WMIN,WDELTA,A,FNEW)
COMMON REA(2003), CLX(2003), ENERGY
REAL IM
PI2 = 2.*3.1415926535
A1 = A
F = A1/WNEW
A = EXP((-PI2*N*ANEW)/WNEW)

C
DO 500 I = 1,L
W = WMIN + (I-1)*WDELTA
P = ANEW**2 + WNEW**2 - W**2
C = 2.*ANEW*W
D = (PI2*N*W)/WNEW
E = WNEW**2 - W**2
F = COS(I)
G = SIN(I)

C
CUT = WNEW-(1.E-7)*WNEW
LCUT = WNEW + (1.E-7)*WNEW
IF(W.GE.CUT.AND.W.LE.UCUT) GO TO 500
RE = (((1.-F)*WNEW)/E+(GOLD*WNEW*(B-A*B+F+A*C*G))/(B**2
1+C**2))*4
IM = ((WNEW*G)/E+(GOLD*WNEW*(A*C*F-C+A*B*G))/(E**2+C**2))*4
GO TO 601

C
C THIS IS THE LIMIT FUNCTION WHEN W = WNEW.
C
600 RE = H*((GOLD*WNEW*(ANEW**2*(1.-A)))/
1(ANEW**2*(ANEW**2+4.*WNEW**2)))
IM = (-PI2*N*F)/(2.*WNEW) +
1(GOLD*WNEW*H*(-C*(1.-A)))/(ANEW**2
2(ANEW**2 + 4.*WNEW**2))
GO TO 601

C
601 Y = COS(W*TDELAY)
Z = SIN(W*TDELAY)

C
REA(I) = (P*Y + IM*Z) + REA(I)
CLX(I) = (IM*Y - P*Z) + CLX(I)

C
C 500 CONTINUE
C
C CALCULATION OF THE ENERGY IN THIS SERIES OF MARKS OR SPACES.
C
C = (PI2*N)/(WNEW**2.)
F = (4.*GOLD*WNEW**2)/(ANEW**3 + 4.*ANEW*WNEW**2)
C = EXP((-PI2*N*ANEW)/(WNEW)) - 1.
B = ((GOLD*WNEW)*(GOLD*WNEW))/(4.*ANEW**3.+4.*ANEW*WNEW**2.)
S = EXP((-2.*PI2*ANEW*N)/(WNEW)) - 1.
ENERGY = ENERGY + (F**2) * (O-F*Q-R*S)
A = A1
RETURN

```

```

C      SMOOTHING ROUTINE
C
C      IF (SMCOTH.NE.1.) GO TO 651
C      ARRAY LI(10) CONTAINS IX WORDS FROM REA(L)
C      ARRAY LT(10) CONTAINS A LINEAR APPROXIMATION TO LI(10).
C      IX IS THE NUMBER OF ARRAY WORDS IN THE SMOOTHING ROUTINES
C
C      CC 523 M3 = 1,2
C      IF (MP.EQ.1) GO TO 654
C      IX = L/(3.*DEL)
C      IF (IX.LT.4) GO TO 655
C      IF (IX.GT.50) GO TO 655
C      IL = 1
C      IH = IX
C      GO TO 659
654  JX = 3
C      IL = 1
C      IH = IX
C
C      LOAD ARRAY LI(10).
650  CC 520 MX=1,IX
520  LI(MX) = REA(IL-1+MX)
C      LI(IX) = LI(IX)
C      LT(1) = LI(1)
C
C      CALCULATE MIDDLE LINEAR VALUES FOR LT(10) AND TEST AGAINST
C      MIDDLE VALUES OF LI(10).
C      M2 = IX-2
C      CC 521 MY = 1,M2
C      MS = MY + 1
C      LT(MS) = LI(1) + ((LI(IX) - LI(1))) / (IX-1) * MY
C      IF (SMOTOP.EQ.1.) GO TO 521
C      IF (LI(MS).GT.LT(MS)) GO TO 652
521  CONTINUE
C
C      INCREASE MIDDLE REA() VALUES TO EQUAL MIDDLE LT() VALUES.
C      CC 522 M4 = 1,M7
C      MT = MA + IL
C      MC = MA + 1
C      REA(MT) = LT(MC)
522  CONTINUE
C
C      INCREMENT THE PCINTERS AND TEST FOR END OF REA().
652  IL = IL+1
C      IH = IH+1
C      IF (IH.LE.L) GO TO 650
523  CONTINUE
655  CONTINUE

```

* * * * * PARAMETER CARDS * * * * *

PARAMETER CARDS FOR A TYPICAL RUN ARE SHOWN BELOW. AMARK AND RMARK ARE DUMMY CARDS ONLY IF THOSE TWO VALUES ARE NOT CALCULATED WITHIN THE PROGRAM. NOTE THAT L AND LS ARE INTEGER VALUES. THE BIT STREAM CONTAINS 999 RANDOM BITS WHICH ARE ENDED BY A (3) TO CAUSE A NEW PARAMETER SET AND A NEW BIT STREAM TO BE READ IN. IF LESS THAN LS BITS ARE IN YOUR PARTICULAR BIT STREAM ON CARDS, YOU MUST STILL PROVIDE ENOUGH BLANK CARDS OR BLANK BITS TO FILL LS WORDS OF THE ARRAY STREAM.

27400.	FHIGH
20600.	FLOW
250.	AMARK DUMMY
204.1	ASPACE
1600.	EALC
25400.	FMIN
20600.	FMAX
0.	GAMMA
2.	RMARK DUMMY
.28	RSPACE
1.	A AMPLITUDE
1.	STEPS
0.	PICT
0.	PSIN
1.	SMOOTH
25.	CEL
1.	ERRCR
0.	RANDCM
1.	SMOTOP
401	L CARD
1000	LS STREAM LENGTH

column #1

column #72

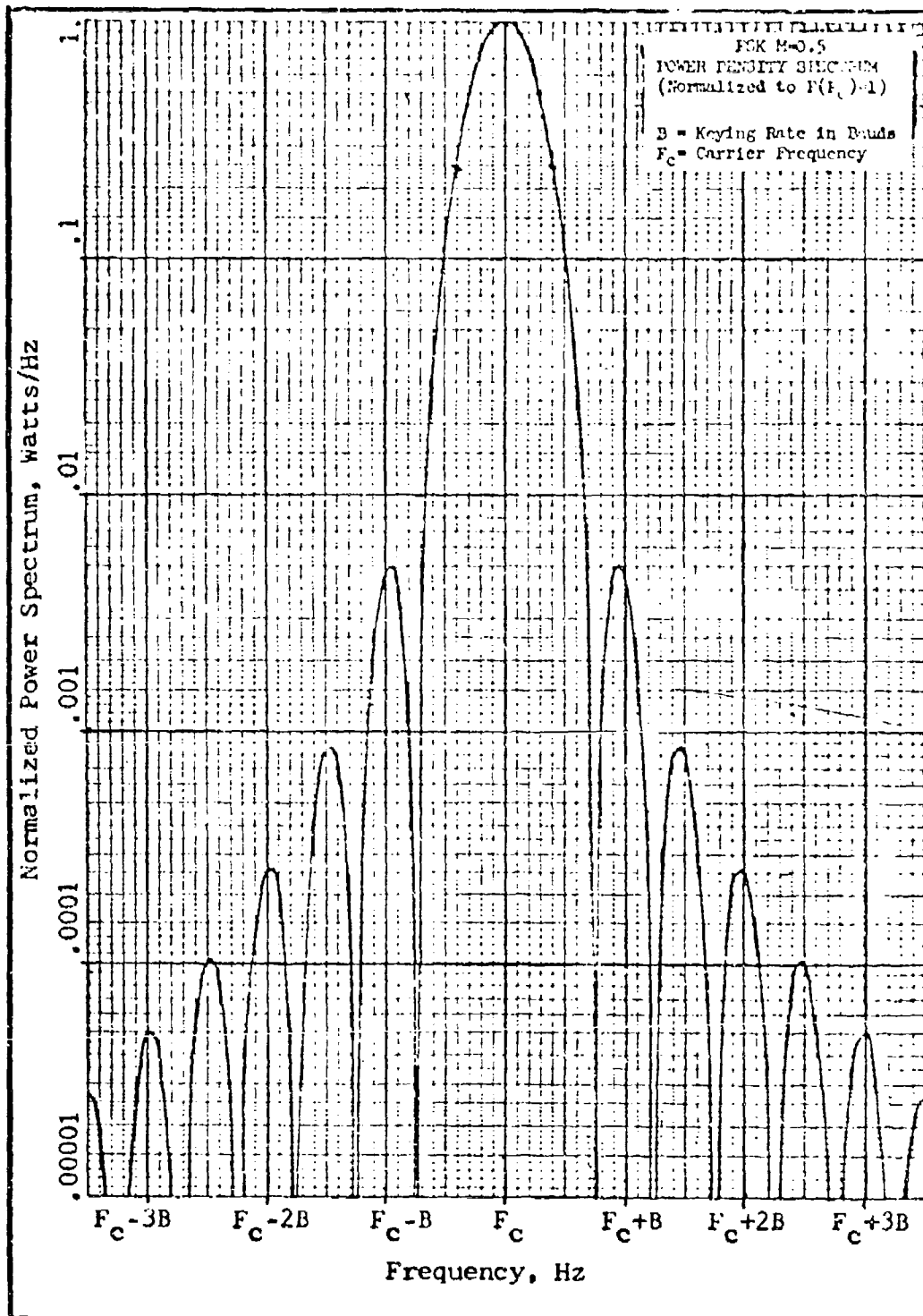
1101001110101110111110000	10111001010110010111
000110000100110111100100	111100010011100101001
11101110000010011111111	000010111000111011000
1111011110101111100111	10111101011011111101001
110100010010011100000	11010001011000010011111
010000110100111010001	11010101110100110000001
111011001010110100001	01011010110001110010010
110100000111001010000	01010110101100110111011
011011111000100011000	11010001000111011101111
00101110101010111101	000111011011100000000100
0111001010111101101	110100111011000111001011
110001011010110001	111000001001110000010110
11010011001000110	110110111011001001100011
0001101111010000	00101010101110111110003

Appendix B

Ideal Spectra for $M = 1/2$

The plot of Fig. B-1 is a normalized power spectrum for a constant amplitude frequency shift key signal with a modulation index of $1/2$. The plot was provided by John Gamble, the sponsor for this thesis. The analytic expression for the spectrum is referenced as Bennett and Rice's work (Ref 1:2384).

The plot is normalized to a value of one watt per unit frequency at the center frequency, F_c . That normalization technique is different than that used for the plots in the body of this thesis; they were normalized to one joule under the entire spectrum of joules/unit frequency. The change from joules to watts makes no difference, however, because unit power is the integral of unit energy for one second; i.e., the normalized spectrum is the same regardless of whether joules/unit frequency or watts/unit frequency is plotted on the ordinate. The important information conveyed by Fig. B-1 is that the main power density or energy density lobe width is 1.5 times the baud rate (B), and that the side lobe widths are 0.5 times the baud rate.

Fig. B-1. Power Density Spectrum for FSK ($M = .5$)

VITA

Tee Roy Hadley III was born on 18 September 1945 in Beeville, Texas. He graduated from high school in Odessa, Texas, in 1963; and attended Texas Technological College from which he received the degree of Bachelor of Science in Electrical Engineering in 1968. He attended Officer Training School and received a commission in 1969. He served as a Spacetrack and Missile Warning System, Staff Maintenance Officer at Headquarters Aerospace Defense Command. He attended the Air Force Institute of Technology where he received the degree of Master of Science in Electrical Engineering in 1973 and was elected to Eta Kappa Nu.

Permanent address: 1502 Alpine Street
Odessa, Texas 79762

This thesis was typed by Mrs. Donna M. Hadley